Characterizing novel Rho GTPase effectors and signalling pathways by BioID-proteomics

Halil Bagci

Department of Anatomy & Cell Biology
McGill University, Montréal, Québec, Canada

Submitted December, 2018
A thesis submitted to McGill University in partial fulfillment of the requirements of the degree of

Doctor of Philosophy

© Halil Bagci, 2018

Dedication

I dedicate this thesis to my mother, Ümmühan Bağcı (1950-2017), who passed away from cancer. She will never be forgotten. I will always honor and remember her. May her soul rest in eternal peace.

Ruhun sonsuza dek huzur bulsun anne. Yeniden görüşmek üzere.

Oğlun, Halil

Acknowledgements

There are many people whom I should thank for their help and assistance. First, I would like to thank Dr. Jean-François Côté for all challenges he endured in supervising me during my PhD studies, especially in the last two years. I express my sincere gratitude to my supervisor for his patience and trust. He helped me a lot to achieve my objectives.

I would like to thank Dr. Mélanie Laurin for her help. She teached me how to do western blots, GST pulldowns, immunohistochemistry and immunofluorescence assays. I am sincerely grateful for her attention and support during my master's internship and in the first year of my PhD. I would like to thank Viviane Tran for her unfailing support as a colleague. She was there for me when I needed encouragement and motivation. I would like to thank Michelle El-Khoury for her kindness and sincerity as a colleague. I am grateful to Catherine Julien, Vilayphone Luangrath, Ariane Pelletier and Marie-Pier Thibault for their help and technical assistance. I express my sincere thanks to Rebecca Cusseddu and Carine Delliaux for their assistance.

I would like to give my sincere respect to Islam Elkholi for his friendship and hardwork on the SLK project. He is a very motivated researcher and I am sure he will achieve a great success in his career. I would like to thank Marie-Anne Goyette for her technical assistance on cell tracking assays, being a good listener and a sincere colleague. I would also like to thank Afnan Abu-Thuraia and Noumeira Hamoud for their assistance and support throughout my PhD studies.

I would like to express my sincere thanks to Dr. Jonathan Boulais for his assistance on protein interactome and network analyses. I am sincerely grateful to Dr. Anne-Claude Gingras and her team for their collaboration on my project. I would like to thank the members of the IRCM Proteomics Discovery Research Platform, Marguerite Boulos, Sylvain Tessier, Josée Champagne, Christian Poitras and Dr. Denis Faubert for their technical assistance and support. I am grateful to Dr. David R. Hipfner and Neera Sriskandarajah for collaborating with us on the SLK project.

I would like to thank to the Department of Anatomy and Cell Biology and the Faculty of Medicine of McGill University for the Graduate Excellence Award, J.P. Collip Fellowship in Medical Research and giving me the opportunity to study here. I am thankful to the Fonds de recherche en santé du Québec (FRSQ) for the doctoral scholarship. I would like to thank to the IRCM for the Michel-Bélanger Internal Scholarship. Also, I would like to thank to Keystone Symposia and the São Paulo Research Foundation (FAPESP) for the travel award. I am grateful to the Natural Sciences and Engineering Research Council of Canada (NSERC) for supporting this project with a Discovery grant.

I would also like to thank to the members of my advisory committee, friends from my department and friends from the IRCM.

Finally, this hard work would not have been possible without the support of my family. I am sincerely grateful to my mother, Ümmühan Bağcı, my father, İbrahim Bağcı and my sister, Meltem Bağcı for all their essential, continuous and unforgettable support throughout my life. I would also like to thank my all colleagues and friends who I haven't mentioned for their support and their sincere friendship.

Abstract

Cell migration is an essential process that is involved in cancer metastasis, embryonic development, wound healing and regeneration. Rho GTPases are central regulators of the actin cytoskeleton. They play an important role for the reorganization of cytoskeletal dynamics and cell migration. Most studies to date were focused on a single Rho GTPase-effector/GEF/GAP signaling. The Rho GTPases signaling networks and effectors are largely unexplored. How GEFs and GAPs achieve specific engagement of Rho-effector signaling remains to be elucidated. Using BioID-proteomics as a powerful approach, we globally explored the Rho GTPase signaling networks. We identified well-known Rho GTPase effector complexes, but also many new interactions. In addition, we mapped Rho-GEF/GAP interactions providing new insights into GEF/GAP specificity for Rho GTPases. We characterized the SLK serine/threonine kinase a novel RhoA effector that is required for RhoA-mediated ERM proteins phosphorylation. Also, we uncovered KIAA0355 as a potential Rac1 effector that is involved in membrane ruffling and migration. Furthermore, we conducted a functional siRNA screen for RhoG and identified potential RhoG effectors that are essential for membrane ruffling. Our work provides an unprecedented resource for Rho GTPase signaling networks and dynamics, paving the way for understanding of biological functions of these proteins.

Résumé

La migration cellulaire est un processus essentiel qui est impliquée dans la formation de métastases durant la progression du cancer, le développement embryonnaire, la cicatrisation des plaies and la régénération. Les Rho GTPases sont des régulateurs centraux du cytosquelette d'actine. Elles jouent un rôle important dans la dynamique du cytosquelette et la migration cellulaire. La plupart des études jusqu'à présent se sont concentrées sur une seule signalisation Rho GTPase-effecteur/GEF/GAP. Les réseaux de signalisation et les effecteurs des Rho GTPases sont largement inexplorés. De plus, comment les GEF et les GAP médient le recrutement spécifique de la signalisation Rho-effecteur reste à élucider. En utilisant la protéomique BioID comme approche puissante, nous avons globalement exploré les réseaux de signalisation des Rho GTPases. Nous avons identifié des complexes d'effecteurs de Rho GTPases bien connus, mais aussi de nombreuses interactions inconnues. De plus, nous avons cartographié les interactions Rho-GEF/GAP, fournissant de nouveaux aperçus sur la spécificité des GEF/GAP pour les Rho GTPases. Nous avons caractérisé la kinase sérine/thréonine SLK comme un nouvel effecteur de RhoA qui est requis pour la phosphorylation des protéines ERM médiée par RhoA. Aussi, nous avons découvert KIAA0355 comme un effecteur potentiel de Rac1 qui est impliqué dans la protubérance membranaire et la migration. De plus, nous avons conduit un criblage fonctionnel par ARNi et nous avons identifié des effecteurs de RhoG qui sont essentiels pour la protubérance membranaire. Notre étude fournit une ressource sans précédent pour les réseaux et la dynamique de la signalisation des Rho GTPases, ouvrant la voie à la compréhension des fonctions biologiques de ces protéines.

List of Figures

Chapter 1

Fig. 1 | Rho GTPases

Fig. 2 | A typical Rho GTPase domain structure

Fig. 3 | Structural organization of the Rho GTPases

Fig. 4 | Rho GTPase regulation by GEFs, GAPs, GDIs or at transcriptional level or by PTMs

Fig. 5 | Dbl family of RhoGEFs

Fig. 6 | Dock family of RhoGEFs

Fig. 7 | Major Rho GAPs and their domain organization

Fig. 8 | Lamellipodia and filopodia stimulation

Fig. 9 | Overview of protein identification by AP-MS

Fig. 10 | Protein microarray

Fig. 11 | Overview of the peptide phage display method

Fig. 12 | Overview of FRET and BRET assays

Fig. 13 | Comparison between the BioID and traditional AP-MS methods

Chapter 3

Fig. 14 | a, Immunoblotting of lysates from Flp-In T-REx HEK293 cells expressing the indicated constructs **b**, Immunoblotting of lysates from Flp-In T-REx HeLa cells expressing the indicated constructs **c**. Representative IF images of BirA*-Flag-tagged Rho GTPases

Fig. 15 | Schematic illustration of the experimental pipeline and expected outcome of Rho GTPase BioID screens

Fig. 16 | BioID recovers major Rho GTPase effector complexes that regulate lamellipodia, focal adhesion, filopodia and stress fiber formation downstream of active Rac1, Cdc42 and RhoA subfamilies

Fig. 17 | Significantly enriched cellular components and biological processes of GO terms identified in BioID screens of classical Rho GTPases

Fig. 18 | Significantly enriched cellular components and biological processes of GO terms identified in BioID screens of atypical Rho GTPases

Fig. 19 | RhoA/Rac1/Cdc42-GEF interactions in Flp-In T-REx HEK293 and Flp-In T-REx HeLa cells

Fig. 20 | a, RhoA/Rac1/Cdc42-GAP interactions in Flp-In T-REx HEK293 and Flp-In T-REx HeLacells

Fig. 21 | a, Dotplot showing BioID interactions between SLK and Rho GTPases in Flp-In T-REx HEK293 cells **b**, Validation of SLK-RhoA^{G14V} interaction by GST pulldown **c**, SLK interacts with active RhoA but not with wild-type (WT) RhoA

Fig. 22 | Active RhoA induces ERM proteins phosphorylation

Fig. 23 | SLK is as essential kinase in RhoA-induced ERM proteins phosphorylation

Fig. 24 | Active RhoA enhances SLK kinase activity

Fig. 25 | Active RhoA increases SLK autophosphorylation on T183

Fig. 26 | The ATH domain, but not the kinase or coiled-coil domains, of SLK mediates active RhoA binding *in vitro*

Fig. 27 | Amino acids at the C-terminal part of the SLK ATH domain integrates the signal from active RhoA to promote SLK kinase activity

Fig. 28 | KIAA0355 is a novel binding partner of active Rac1

Fig. 29 | KIAA0355, an essential Rac1 effector, is involved in membrane ruffling

Fig. 30 | KIAA0355 expression enhances cell migration

Fig. 31 | KIAA0355, a novel Rac1 effector, integrates the Rac1 signaling pathway for cell migration

Fig. 32 | a, Schematic illustration of the functional siRNA screening for RhoG. **b**, Dotplot showing top BioID interactors identified in $RhoG^{WT}$ and $RhoG^{G12V}$ in Flp-In T-REx HeLa cells.

Fig. 33 | A functional siRNA screening for RhoG reveals potential effectors that are essential for membrane ruffling

List of Tables

Chapter 1

Table 1 | Post-translational modifications of Rho GTPases

Chapter 2

Table 2 | Expression vectors used for functional assays

Abbreviations

ABR	Active BCR-related
AD	Activation domain
AKT	AKT serine/threonine kinase
APEX	Ascorbate peroxidase
AP-MS	Affinity purification-mass spectrometry
Arf	ADP ribosylation factor
ArhGAP	Rho GTPase-activating protein
Arp2/3	Actin-related 2 and 3 complexes
ATP	Adenosine triphosphate
BAIAP2	BAI1 associated protein 2
BCR	Breakpoint cluster region protein
BH	BCR homology
BioAMP	Biotinoyl-5'-AMP
BioID	Proximity-dependent biotin identification
BirA	Biotin ligase
βPIX	Rho guanine nucleotide exchange factor 7
BRET	Bioluminescence resonance energy transfer
CAAX	C, Cys; A, Aliphatic amino acid; and X, any amino acid
Cas9	CRISPR associated protein 9
CCND1	Cyclin D1
Cdc42	Cell division cycle protein 42
CHP	Cdc42-like GTPase 2

Co-IP	Co-immunoprecipitation
COPS2	Cullin3 and COP9 signalosome subunit 2
CRIB	Cdc42 and Rac interactive binding
CRISPR	Clustered regularly interspaced short palindromic repeats
Crk	Crk proto-oncogene, adaptor protein
DAD	Diaphanous autoinhibitory domain
DAPI	4', 6-diamidino-2-phenylindole
DBC2	Deleted in breast cancer 2
DBD	DNA binding domain
Dbl	Diffuse B-cell lymphoma
DH	Dbl homology
DHR	Dock homology region
DIAPH	Diaphanous homolog
DMEM	Dulbecco's modified Eagle's medium
DNA	Deoxyribonucleic acid
Dock	Dedicator of cytokinesis
ECM	Extracellular matrix
EDTA	Ethylenediaminetetraacetic acid
Elmo	Engulfment and cell motility
ER	Endoplasmic reticulum
ERM	Ezrin/Radixin/Moesin
F-actin	Filamentous-actin
FAK	Focal adhesion kinase

F-BAR	Fes-Cip4 homology Bin/Amphiphysin/Rvs
FBS	Fetal bovine serum
FH2	Formin homology 2
FILIP	FLNa-interacting protein
FKBP	FK506-binding protein
FLN	Filamin
FMNL	Formin like
FRB	FKBP-rapamycin-binding domain
FRET	Fluorescence resonance energy transfer
GAP	GTPase-activating protein
GBD	GTPase binding domain
GDI	Guanine nucleotide dissociation inhibitor
GDP	Guanosine diphosphate
GEF	Guanine nucleotide exchange factor
GIT	G Protein-coupled receptor kinase interacting ArfGAP
GPCR	G-Protein coupled receptor
Grb2	Growth factor receptor bound protein-2
GRD	GAP-related domain
GST	Glutathione-S-transferase
GTP	Guanosine triphosphate
GTPase	Guanisone triphosphate hydrolase
HA	Hemagglutinin
HACE1	HECT domain and ankyrin repeat containing E3 ubiquitin ligase 1

HCET	Human corneal epithelial
HER2	Erb-B2 receptor tyrosine kinase 2
HPC	Hematopoietic progenitor cells
HRas	HRas proto-oncogene, GTPase
HRP	Horseradish peroxidase
HSV	Herpes simplex virus
I-BAR	Bin/Amphiphysin/Rvs
IQGAP	IQ motif containing GTPase activating protein
IRES	Internal Ribosome Entry Site
IRSp53	Insulin receptor substrate P53
ITAM	Immunoreceptor tyrosine-based activation motif
LaA	Lamin A
LIMK	LIM kinase
LOK	Serine/threonine kinase 10
LPA	Lysophosphatidic acid
LRR	Leucine rich repeat
mDIA	Diaphanous related formin
miRISC	miRNA-induced silencing complex
miRNA	microRNA
MLC	Myosin light chain
MLCP	Myosin light chain phosphatase
MRLC	Myosin Regulatory light chain
MYPT	Myosin phosphatase

NFκB	Nuclear factor-kappa B
NLS	Nuclear localization signal
NMR	Nuclear magnetic resonance
NPC	Nuclear pore complex
NPF	Nucleation promoting factor
N-WASP	Neuronal-WASP
P3	Gene-3 minor coat protein
P8	Gene-8 major coat protein
PACSIN2	Protein Kinase C and casein kinase substrate in neurons 2
PAGE	Polyacrylamide gel electrophoresis
PAK	P21 activated kinase
PBS	Phosphate-buffered saline
PCR	Polymerase chain reaction
PDGF	Platelet-derived growth factor
PH	Pleckstrin homology
PI3K	Phosphatidylinositol 3-kinase
PI5K	Phosphatidylinositol-4-phosphate 5-kinase
PIAS3	Protein inhibitor of activated STAT3
PIP2	Phosphatidylinositol (4,5)-biphosphate
PIP3	Phosphatidylinositol (3,4,5)-triphosphate
PKA	Protein Kinase A
P-loop	Phosphate-binding loop
PPARγ	Peroxisome proliferator-activated receptor γ

PPI	Protein-protein interaction
Prex	PIP3-dependent Rac exchange factor
PTB	Phosphotyrosine binding
PTEN	Phosphatase and tensin homolog deleted on chromosome 10
PTM	Post-translational modification
Pxxp	Proline-rich
Rab	Ras-related in brain
Rac	Ras-related C3 botulinum toxin substrate
Ran	Ras-related nuclear
Ras	Rat sarcoma
RB	RhoA-GTP binding
Rho	Ras homologous
RhoA	Ras homolog family member A
RhoB	Ras homolog family member B
RhoBTB1	Rho related BTB domain containing 1
RhoBTB2	Rho related BTB domain containing 2
RhoC	Ras homolog family member C
RhoD	Ras homolog family member D
RhoE	Rho related GTP-binding protein RhoE
RhoF	Ras homolog family member F, filopodia associated
RhoG	Ras homolog family member G
RhoGDI	Rho GDP dissociation inhibitor
RhoH	Ras homolog family member H

RhoJ	Ras homolog family member J
RhoQ	Ras homolog family member Q
RhoU	Ras homolog family member U
RhoV	Ras homolog family member V
RIF	Rho family GTPase Rif
RNA	Ribonucleic acid
Rnd1	Rho family GTPase 1
Rnd2	Rho family GTPase 2
Rnd3	Rho family GTPase 3
Rock	Rho-associated protein kinase
ROS	Reactive oxygen species
RTK	Receptor tyrosine kinase
SCAR	Suppressor of cAMP receptor
SDS	Sodium dodecyl sulfate
SENP	SUMO specific protease
SH2	Src homology 2
SH3	Src homology 3
siRNA	Small interfering RNA
SLAP75	Soluble lamina-associated protein of 75 KD
SLK	Ste20-like kinase
Slug	Snail family transcriptional repressor 2
Sox9	SRY-Box 9
Src	Proto-oncogene tyrosine-protein kinase Src

srGAP	Slit-Robo GTPase activating protein
SUMO	Small ubiquitin-related modifier
TC10	Ras-like protein TC10
TCL	TC10-like GTP-binding protein
TCR	T cell receptor
Trio	Triple functional domain protein
Twist	Twist family BHLH transcription factor
VCA	Verprolin, cofilin homology and acidic region
VEGF	Vascular endothelial growth factor
WASP	Wiskott-Aldrich syndrome protein
WAVE	WASP-family verprolin-homologous protein
WHAMM	WASP homolog associated with actin Golgi membranes and microtubules
WRC	SCAR/Wave regulatory complex
WRCH1	Wnt-1 responsive Cdc42 homolog
WRP	WAVE-associated Rac GTPase-activating protein
Y2H	Yeast two-hybrid
Zap70	Zeta chain of TCR associated protein kinase 70

Original Contribution to Knowledge

Work presented in Chapter 3 represents an unprecedented resource for the Rho GTPase family of proteins that can be used for understanding their molecular basis and functions. These results include BioID analyses of all human Rho GTPases in HEK293 and HeLa cells. We also provided identification and functional characterization of different Rho GTPase interacting-proteins or effectors such as SLK, KIAA0355 and potential RhoG interactors.

Moreover, our work provides a global protein interactome for Rho GTPase-GEF/GAP interactions and specificity. These findings can be further used to decipher the molecular mechanisms of Rho GTPase networks and will contribute to the advancement of cancer and development research.

Preface

I hereby declare that I prepared this Ph.D. thesis entitled “Characterizing novel Rho GTPase effectors and signalling pathways by BioID-proteomics” on my own. I did not receive outside aid, other than those cited below. The data presented in this thesis will be prepared as a manuscript for submission to scientific journals.

Contribution of Authors

Chapter 3:

BioID-MS and protein network analysis: Cloning of BirA*-Flag tagged Rho GTPases and generation of stable Flp-In T-REx HEK293 and Flp-In T-REx HeLa cells were performed by Halil Bagci. Cloning of other constructs were also carried out by Halil Bagci (constructs shown in Table 2). Majority of the BioID-MS experiments in Flp-In T-REx HEK293 cells were carried by Zhen Yuan-Lin in the laboratory of Dr. Anne-Claude Gingras (Lunenfeld-Tanenbaum Research Institute, Toronto). MS injections of these samples were performed by Zhen Yuan-Lin. All other BioIDs assays in Flp-In T-REx HEK293 and Flp-In T-REx HeLa cells were performed by Halil Bagci and Viviane Tran at the IRCM. Injection of these samples were carried out by Marguerite Boulos, Sylvain Tessier and Dr. Denis Faubert at the IRCM Proteomics Discovery Research Platform. ProHits software, which was developped by the laboratory of Dr. Anne-Claude Gingras, was installed on IRCM servers by Christian Poitras. Protein identification and data search in ProHits was performed by Halil Bagci. Dr. Nadia Dubé carried out preliminary protein interaction analyses. Dr. Jonathan Boulais (experiments in figures 17, 18 and 16 excluding the Venn Diagram analysis) performed Cytoscape interactome and GO term SAFE analyses. Halil Bagci performed dotplots and other protein network analyses.

SLK and RhoA experiments: Halil Bagci (experiments in figures 21, 23a, 24, 26 and 27) and Islam Elkholi (figures 22, 23b, 23c, 23d and 25) performed all SLK and RhoA experiments.

KIAA0355 experiments: Halil Bagci (experiments in figures 28, 29, 30a, 31a, 31b and 31c) and Marie-Anne Goyette (figures 30b and 31d) performed all KIAA0355 experiments. Dr. Jean-François Côté generated KIAA0355-null cell lines by CRISPR/Cas9.

siRNA screen of RhoG interactors: Halil Bagci (experiments in figures 32 and 33) performed all siRNA screen experiments for RhoG interactors. Ariane Pelletier provided technical assistance for cell culture and siRNA transfection.

Project design: Dr. Jean-François Côté designed the project.

List of Publications

The following list includes peer-reviewed publications that are not part of this thesis.

Bagci, H., M. Laurin, J. Huber, W. J. Muller and J. F. Cote (2014). "Impaired cell death and mammary gland involution in the absence of Dock1 and Rac1 signaling." Cell Death Dis **5**: e1375.

Methot, S. P., L. C. Litzler, P. G. Subramani, A. K. Eranki, H. Fifield, A. M. Patenaude, J. C. Gilmore, G. E. Santiago, **H. Bagci**, J. F. Cote, M. Larijani, R. E. Verdun and J. M. Di Noia (2018). "A licensing step links AID to transcription elongation for mutagenesis in B cells." Nat Commun **9**(1): 1248.

Youn, J. Y., W. H. Dunham, S. J. Hong, J. D. R. Knight, M. Bashkurov, G. I. Chen, **H. Bagci**, B. Rathod, G. MacLeod, S. W. M. Eng, S. Angers, Q. Morris, M. Fabian, J. F. Cote and A. C. Gingras (2018). "High-Density Proximity Mapping Reveals the Subcellular Organization of mRNA-Associated Granules and Bodies." Mol Cell **69**(3): 517-532 e511.

Table of Contents

Dedication……...I

Acknowledgements……..II

Abstract……IV

Résumé……..V

List of Figures……..VI

List of Tables……IX

Abbreviations……X

Original Contribution to Knowledge……XVIII

Preface……..…….…..XIX

List of Publications……XXI

CHAPTER 1: INTRODUCTION AND LITERATURE REVIEW……1

1.0. General Introduction……2

1.1. Overview of the Rho GTPases……...3

1.1.1. Rho GTPase structure……..5

1.1.2. Rho GTPase regulation……7

1.1.2.1. Rho Guanine Nucleotide Exchange Factors (RhoGEFs)……...9

1.1.2.2. Rho GTPase activating Proteins (RhoGAPs)……13

1.1.2.3. Rho guanine Nucleotide Dissociation Inhibitors (RhoGDIs)……16

1.1.2.4. Regulation by post-translational modifications (PTMs)……17

1.1.2.4.1. Lipids modifications……19

1.1.2.4.2. Phosphorylation……..20

1.1.2.4.3. Ubiquitination……..21

1.1.2.4.4. Sumoylation……22

1.2. Rho GTPase effectors and signalling pathways……23

1.2.1. Classical Rho GTPases……..24

1.2.1.1. Rac subfamily……..24

1.2.1.2. Cdc42 subfamily……..29
1.2.1.3. RhoA subfamily……...32
1.2.1.4. RhoD and RhoF subfamily……34
1.2.2. Atypical Rho GTPases……35
1.3. Characterization of the Rho GTPase signaling networks……38
1.3.1. Traditional PPI methods……38
1.3.2. BioID: a proximity-based and powerpul PPI method……49
1.3.2.1. Overview of the BioID method…….....49
1.3.2.2. Exploitation of BioID for PPI……..52
1.4. Rationale and objectives……55

CHAPTER 2: MATERIALS AND METHODS……57

2.1. Antibodies……...58
2.2. Plasmids……..59
2.3. Generation of KIAA0355-null cell lines by CRISPR/Cas9……61
2.4. Cell culture and generation of stable cell lines……..63
2.5. BioID and MS data analysis……..64
2.6. Protein network and interactome analysis……..66
2.7. Coimmunoprecipitation or GST pulldown……...66
2.8. Immunofluorescence and microscopy analysis……68
2.9. In vitro kinase assays……70
2.10. Cell migration assays……71
2.11. High-content imaging and microscopy analysis for siRNA screening of active RhoG.....72
2.12. Statistics……...73

CHAPTER 3: DECIPHERING RHO GTPASES EFFECTORS AND RHO GTPASE/GEF-GAP INTERACTIONS BY BIOID-PROTEOMICS…….74

3.1. A systematic BioID analysis to uncover new effectors and map Rho GTPase-GEF/GAP interactions……..75
3.2. BioID recovers known Rho GTPase effector complexes and biologically-relevant GO term profiles……80

3.3. BioID reveals Rho GTPase-GEF/GAP interactions and specificity……88
3.4. Identification of SLK as a novel RhoA effector……..95
3.5. SLK regulates ERM phosphorylation downstream of active RhoA……97
3.6. KIAA0355, an uncharacterized Rac1 effector, is involved in cell migration…...111
3.7. A functional siRNA screen of RhoG interacting proteins defines essential interactors for membrane ruffling……...120

CHAPTER 4: GENERAL DISCUSSION AND CONCLUSIONS……127

4.1. BioID-Proteomics reveals well-known, but also many novel Rho GTPase effectors……128
4.2. Rho/GEF-GAP interactions and specificity revealed by BioID……..128
4.2.1. Rho-GEF interactions……...129
4.2.2. Rho-GAP interactions……...131
4.3. SLK, a novel RhoA effector, is involved in RhoA-mediated ERM phosphorylation……..131
4.4. KIAA0355, a novel Rac1 effector, is involved in membrane ruffling and migration……...133
4.5. A functional siRNA screening of RhoG BioID candidates reveals potential interactors that are essential for membrane ruffling……134
4.6. Conclusion……134

CHAPTER 5: REFERENCES……136

CHAPTER 1: INTRODUCTION AND LITERATURE REVIEW

1.0. General Introduction

Spatiotemporal organization of a cell is essential for interacting with other cells and the microenvironment. A migration of a cell involves morphological changes that requires the remodeling of various internal constituents. Cytoskeleton, which gives the body support to a cell, is one of the major components of eukaryotic or prokaryotic cells. It is composed of internal constituents such as microtubules, actin filaments and intermediate filaments[1]. Each of these cytoskeletal protein filaments controls different cellular processes that allow cells to change their shape, regulate their mechanical strength and migrate. Proper functioning of these cytoskeletal filaments is essential for cellular polarity, motility and adhesion.

Over the last decades, studies on cell migration paved the way for the better understanding of how different cytoskeleton components mediate tissue formation and vascularization during embryogenesis[2], wound healing[3], leukocyte invasion of tissues in the immune response[4], tumor formation and metastasis[5]. Of those, actin filaments are long helical filaments composed of actin proteins[1]. In vertebrates, there are six actin isoforms and they display a similar identity in their amino acid sequences[6]. Each of the actin genes has been shown to play different biological functions[7, 8]. Reorganization of actin filaments after polymerization can lead to morphological changes that result in the formation of lamellipodia, filopodia or stress fibers[9]. Small Rho GTPases are viewed as central regulators of these cellular morphological changes.

1.1. Overview of the Rho GTPases

Rho GTPases are master regulators of the actin cytoskeleton. They are part of the Ras superfamily of proteins, which also contains the Arf, Rab, Ran and Ras families[10]. They are found in all eukaryotic cells[11]. Rho GTPases cycle between the GDP-bound inactive and the GTP-bound active states. Their activation is tightly controlled by three major regulatory proteins: Guanine nucleotide exchange factors (GEFs), GTPase activating proteins (GAPs) and guanine nucleotide dissociation inhibitors (GDIs). In mammals, the Rho GTPase family of proteins include 20 members based on the alignment of their amino acid sequences (**Fig. 1**). They are divided into 8 subfamilies; Rac subfamily (Rac1, Rac2, Rac3 and RhoG), Cdc42 subfamily (Cdc42, RhoQ/TC10 and RhoJ/TCL), RhoA subfamily (RhoA, RhoB and RhoC), a subfamily that includes RhoV/CHP and RhoU/WRCH1, RhoBTB subfamily (RhoBTB1 and RhoBTB2), RND subfamily (RND1, RND2 and RND3/RhoE), another subfamily that comprises RhoD and RhoF/RIF and finally, RhoH which is considered a subfamily on its own[12].

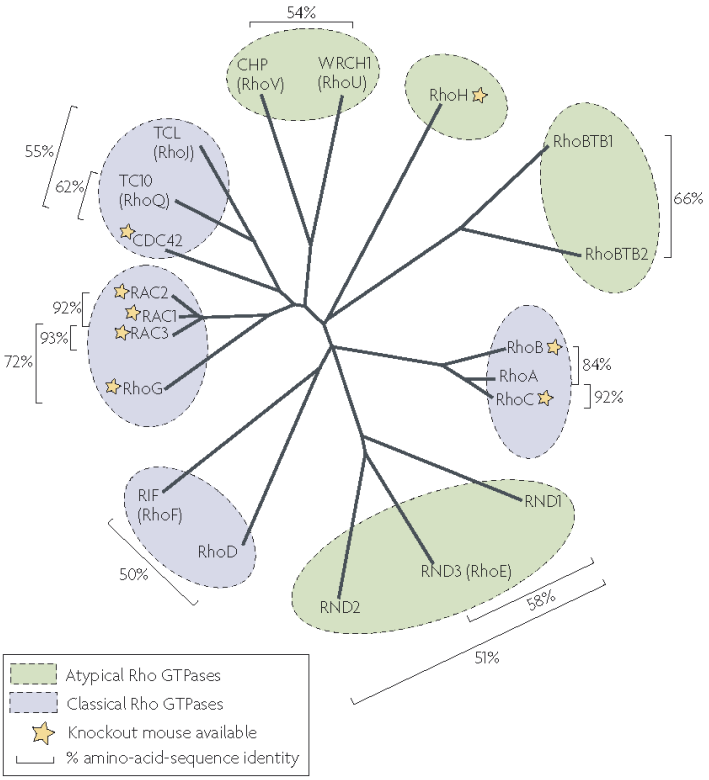

Fig. 1 | Rho GTPases. The Rho GTPase family of proteins comprise 8 subfamilies based on the alignment of their amino acid sequences. Rac, Cdc42, RhoA and RhoF and RhoD subfamilies are considered as classical Rho GTPases since they can cycle between the GDP-bound inactive and the GTP-bound active states. Other Rho GTPases, such as RND, RhoBTB, RhoH and RhoU and RhoV are considered as atypical Rho GTPases since they are always GTP-bound and their regulation can be dependent on other mechanisms such as protein levels and phosphorylation.

Reprinted by permission from [Springer]: [Nature]: [Nature Reviews Molecular Cell Biology]: [Mammalian Rho GTPases: new insights into their functions from in vivo studies, Sarah J. Heasman, Anne J. Ridley]: [Springer Nature: All rights reserved]: (2008)

Once GTP-loaded and activated, Rho GTPases can recruit a plethora of effector proteins that are involved in various biological processes such as cell division, adhesion, migration, vesicular transport, membrane trafficking, microtubule dynamics, neuronal development, regulation of gene expression[12].

1.1.1. Rho GTPase structure

Since the structural determination of HRas by X-ray crystallography[13, 14], understanding of the GDP-bound and GTP-bound forms of small GTPases enabled the characterization of Switch I and II regions and revealed that the on and off states of Switch regions upon nucleotide binding result in conformational changes[15]. Like other small GTPases which belong to the Ras superfamily, members of the Rho family are small monomeric proteins with molecular weight of ~21 kDa, except RhoBTB1 and RhoBTB2 with ~70 or ~80 kDa. A typical Rho GTPase structure includes the conserved G domain with Switch I and II regions, an insert region and a hypervariable motif that is located at the C-terminus[16] (**Fig. 2**).

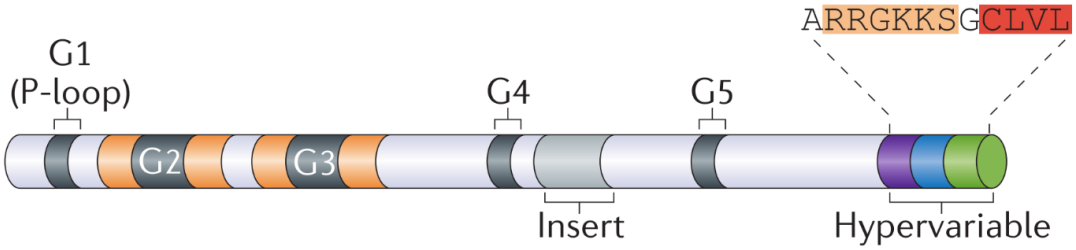

Fig. 2 | A typical Rho GTPase domain structure. It includes the conserved G domain, an insert motif and a hypervariable motif at the C-terminus.

Adapted by permission from [Springer]: [Nature]: [Nature Reviews Molecular Cell Biology]: [Regulating RhoGTPases and their regulators, Richard G. Hodge, Anne J. Ridley]: [Springer Nature: All rights reserved]: (2016)

The highly conserved G domain includes the conserved sequence motifs G1-G5. The G1 motif, also known as the P-loop (phosphate-binding loop), coordinates the binding of the β-phosphate of the guanine nucleotide and the Mg^{2+} ion which is indispensable for nucleotide binding[16]. The G2 and G3 domains, that comprise the Switch I and Switch II regions, mediate GDP and GTP binding, which in turn regulates conformational changes[16]. The G4 and G5 domains mediate the binding of guanine base[16]. The insert motif, which is found between the G4 and G5 domains, is responsible for GEF binding as well as binding and activation of some effectors such as Rock, IQGAP and mDIA[16]. It has been shown that the insert region of Rho GTPases contains additional ~10-15 amino acids compared to that of the Ras family of GTPases, forming a pair of α helices[15, 17]. It is therefore possible that the presence of these additional amino acids in the insert motif may confer Rho GTPases an ability to interact with GEFs or recruit effectors that are specific to the Rho family. The C-terminus includes the hypervariable region which serves as protein binding site and partially determines specific interaction with effectors or regulatory proteins. It also contains the CAAX motif (in red) which coordinates post-translational lipid modifications that are required for membrane targeting[18]. In addition, some Rho GTPases include a polybasic region (in orange) in the C-terminus which precedes the CAAX motif, mostly composed of Lys and Arg residues, creating a positively charged interface for membrane binding[18].

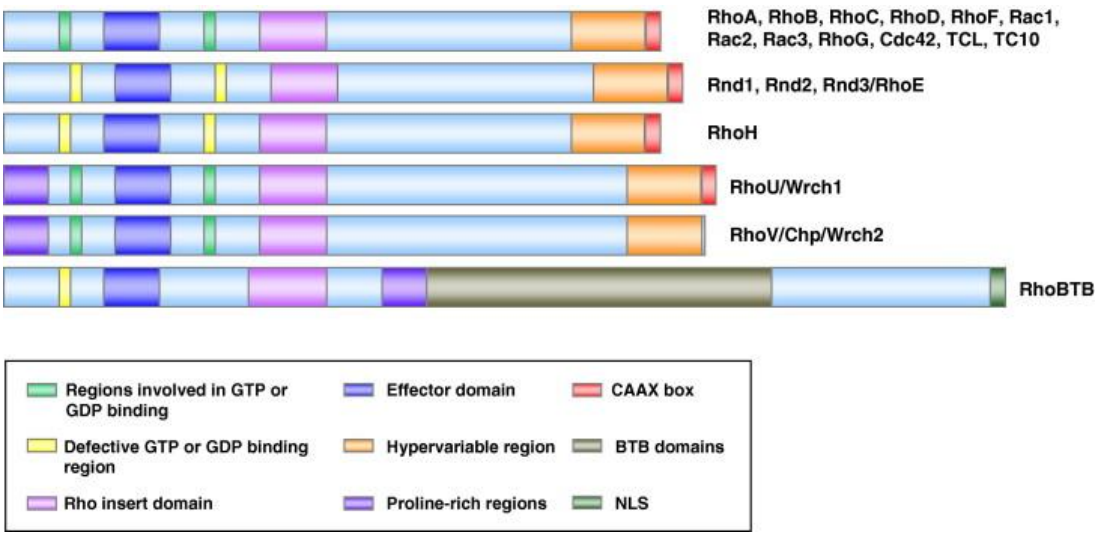

Fig. 3 | Structural organization of the Rho GTPases. Rac, Ccd42, Rho and RhoF subfamilies have similar domain architecture.

Reprinted by permission from: [FEBS PRESS]: [FEBS Letters]: [Rho GTPases in cancer cell biology, Francisco M. Vega, Anne J. Ridley]: [John Wiley and Sons: All rights reserved]: (2008)

Rac, Cdc42, Rho and RhoF subfamilies share a high similary in terms of domain architecture (**Fig. 3**). The Rnd subfamily and RhoH lack GTPase activity due to amino acid modifications in the GTP/GDP binding region[10]. Unlike other Rho GTPases, RhoU and RhoV are featured by the presence of a N-terminal Proline-rich region[10]. The RhoBTB subfamily is distinguished by the presence of a BTB domain and a nuclear localization signal (NLS) at the C-terminus[10].

1.1.2. Rho GTPase regulation

Rho GTPases are tightly regulated by GEFs, GAPs and GDIs, but also at transcription level or by post-translational modifications (PTMs) (**Fig. 4**). There are so

many GEFs and GAPs and this can be explained by the fact that some GEFs and GAPs display tissue-specific expression and functions. In addition, GEFs and GAPs can exhibit compartment-specific activity due to their localization.

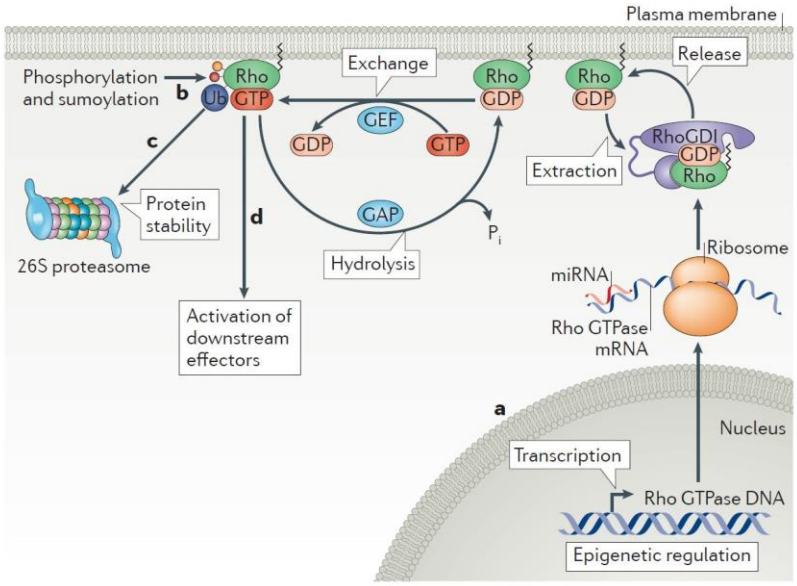

Fig. 4 | Rho GTPase regulation by GEFs, GAPs, GDIs or at transcriptional level or by PTMs.

Reprinted by permission from [Springer]: [Nature]: [Nature Reviews Molecular Cell Biology]: [Regulating RhoGTPases and their regulators, Richard G. Hodge, Anne J. Ridley]: [Springer Nature: All rights reserved]: (2016)

1.1.2.1. Rho Guanine Nucleotide Exchange Factors (RhoGEFs)

GEFs induce the release of bound GDP, which, in turn, results in a formation of a nucleotide-free GTPase-GEF complex. Because the GTP concentration in the cell is higher than that of GDP, the nucleotide-free GTPase will be reloaded with GTP to undergo a conformational change that leads to Rho GTPase activation[16, 19].

So far, more than 80 different RhoGEFs have been revealed[16, 20, 21]. GEFs are known to bind to both Switch regions of Rho GTPases. There are two families of GEFs, based on sequence similiarity: Diffuse B-cell lymphoma (Dbl) and Dedicator of cytokinesis (Dock). There are approximately 70 human Dbl GEFs (**Fig. 5**). They contain a ~200 amino-acid catalytic Dbl Homology (DH) domain, which is often flanked by an adjacent, regulatory ~100 amino-acid Pleckstrin Homology (PH) domain[16, 18, 22, 23]. While the DH domain is known to stimulate guanine nucleotide exchange, different roles have been shown for the PH domain, such as phospholipid binding, which promotes membrane targeting of the GEF in the proximity of a membrane-bound Rho GTPase[22]. The DH and PH domains are also known to promote the formation of the nucleotide-free/GEF complex and further nucleotide binding[24].

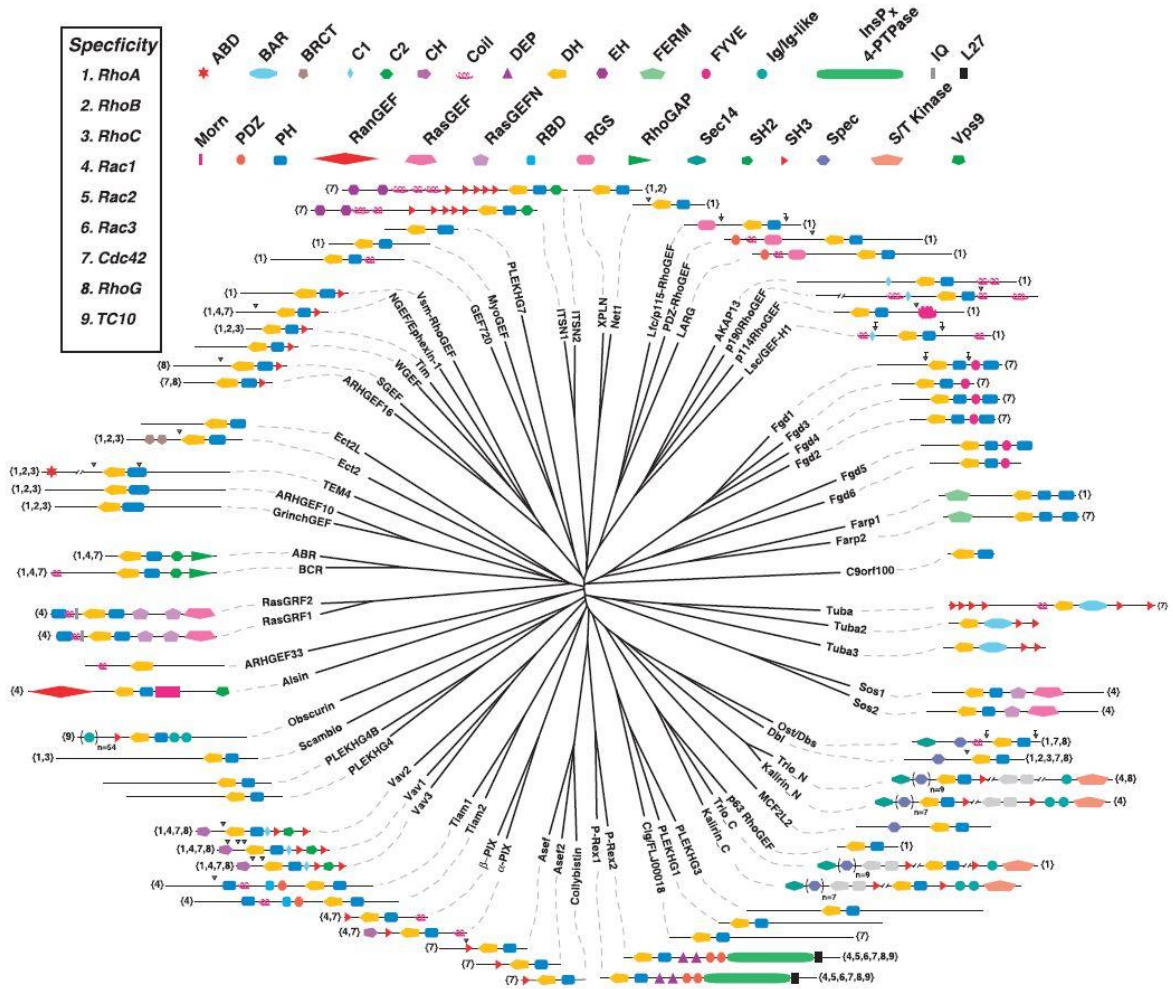

Fig. 5 | Dbl family of RhoGEFs. The protein domain organization for each Dbl GEF are shown. Numbers in braces next to each Dbl GEF designates the reported Rho GTPase specificity.

Reprinted by permission from [Springer]: [Nature]: [Oncogene]: [Rho guanine nucleotide exchange factors: regulators of Rho GTPase activity in development and disease, D R Cook, K L Rossman, C J Der]: [Springer Nature: All rights reserved]: (2013)

There are 11 human Dock GEFs (**Fig. 6**). Unlike Dbl GEFs, they are characterized by the absence of a DH domain and the presence of two evolutionarily conserved domains: a ~200 amino-acid Dock homology region-1 (DHR-1), which regulates

phospholipid binding and membrane localization and ~450 amino-acid catalytic Dock homology region-2 (DHR-2), which is responsible for the GEF activity[23, 25-27]. Dock GEFs are classified into four subgroups, based on domain architecture and sequence similarity. The Dock-A subgroup includes Dock1 (also known as Dock180), Dock2, Dock5. The Dock-B subgroup contains Dock3 and Dock4. Dock-A and Dock-B subgroups includes an N-terminal SH3 domain that mediates the interaction with Elmo (Engulfment and Motility) scaffold proteins and a C-terminal proline rich motif (PxxP) which binds to SH3-domain containing adaptors, such as Crk[21, 27]. The Dock-C subgroup comprises Dock6, Dock7 and Dock8. The Dock-D subgroup contains Dock9, Dock10 and Dock11, which are defined by the presence of an N-terminal PH domain that is involved in phosphoinositide binding for membrane targeting[21, 27].

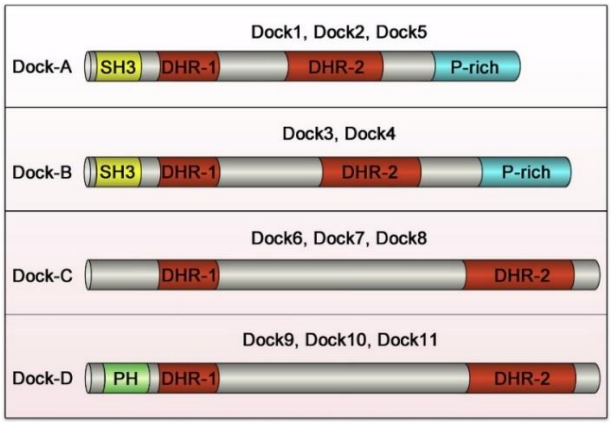

Fig. 6 | Dock family of RhoGEFs. Dock GEFs are classified into four different subgroups: Dock-A, Dock-B, Dock-C and Dock-D.

Reprinted by permission from [Elsevier]: [Progress in Retinal and Eye Research]: [Dock GEFs and their therapeutic potential: Neuroprotection and axon regeneration, Kazuhiko Namekata, Atsuko Kimura, Kazuto Kawamura, Chikako Harada, Takayuki Harada]: [Elsevier: All rights reserved]: (2014)

Dock-A and Dock-B subgroups exhibit GEF activity for Rac, Dock-D for Cdc42, while the Dock-C subgroup of RhoGEFs are thought to activate both Rac1 and Cdc42, but this is still controversial[21]. The molecular basis of how Dock GEFs are activated through their catalytic DHR2 domain and recognize specific Rho GTPases have been revealed by X-ray crystallography studies. Barford and colleagues revealed the crystal structure of the Dock9^{DHR2}-Cdc42 complex, showing that a nucleotide sensor in the DHR2 domain is involved in the release of GDP and then the discharge of GTP-bound Cdc42[28]. In addition, they compared the crystal structure of Dock2^{DHR} in complex with Rac1 to the Dock9^{DHR2}-Cdc42 complex and uncovered multiple structural differences that allow selectivity towards Rac1 and Cdc42[29]. They identified two important sites that confer GTPase specificity: Residues 56 and 27. Rac-specific Dock GEFs prefer Trp at residue 56, but it can also accommodate Phe. By replacing Trp for Phe at residue 56, they showed that Rac1^{W56F} can also be activated by Dock9^{DHR2} in addition to Dock2^{DHR2}. Moreover, an Ala or Lys at the residue 27 of Switch I allows conformational differences to determine Dock specificity between Rac1 and Cdc42[29].

Still, GEF-Rho GTPase interactions have not been mapped in detail. Furthermore, how each GEFs engage specific Rho GTPase-effector couples has not been elucidated.

1.1.2.2. Rho GTPase Activating Proteins (RhoGAPs)

RhoGAPs are negative regulators of Rho GTPases. They include a ~170 amino acid RhoGAP domain, which allows RhoGAPs to bind GTP-loaded Rho proteins and stimulate the slow intrinsic GTP hydrolysis of Rho GTPases that leads to inactivation[16, 18, 30]. In humans, there are around 80 members of the RhoGAP family[18] (**Fig. 7**). RhoGAPs are less studied compared to RhoGEFs and only a few RhoGAPs have been characterized to display specificity for major Rho GTPases such as Rac1, Cdc42 and RhoA[30]. Some RhoGAPs such as Slit-Robo GTPase-activating proteins (srGAPs) contain an N-terminal Fes-Cip4 homology Bin/Amphiphysin/Rvs (F-BAR) domain that induces membrane curvatures leading to the formation of protrusions[31]. Others, such as α2 and β2-chimaerins, include a Src homology 2 (SH2) or Src homology 3 (SH3) domains which are involved the signal transduction downstream of receptor tyrosine kinases (RTKs)[30].

Each GAP can specifically target a Rho GTPase. srGAP1 has been shown to specifically downregulate RhoA and Cdc42, whereas srGAP3 inactivate Rac1. srGAP3, also known as WAVE-associated Rac GTPase-activating protein (WRP) directly interacts with WAVE1, inhibiting Rac1-mediate neurite outgrowth[32]. In addition, it has been shown that some Rho GTPases can antagonize the function of other Rho GTPases by recruiting their target GAPs. For example, Rnd proteins can interact with ArhGAP35/p190RhoGAP by increasing its GAP activity towards GTP-bound RhoA[33]. RhoA inactivation by p190RhoGAP can then positively regulate spreading and migration by controlling cell protrusion and polarity[34]. Similar to GEF-Rho interactions, GAP-Rho interactions have not been fully investigated. How GAPs inactivate particular Rho GTPase-effector signaling

pathways has not been uncovered.

Breakpoint cluster region protein (BCR) and Active BCR-related (ABR) exhibit GAP activity toward Rac1[30]. BCR and ABR are considered as GAPs, but also GEFs, since they contain a DH domain and a GAP domain. It has been shown that both BCR and ABR display GEF activity toward Rac1, Cdc42 and RhoA[30]. It has been suggested that the GAP and GEF domains of these proteins might interact with Rho GTPases in a non-competitive manner and regulate them in response to different cellular signals[30].

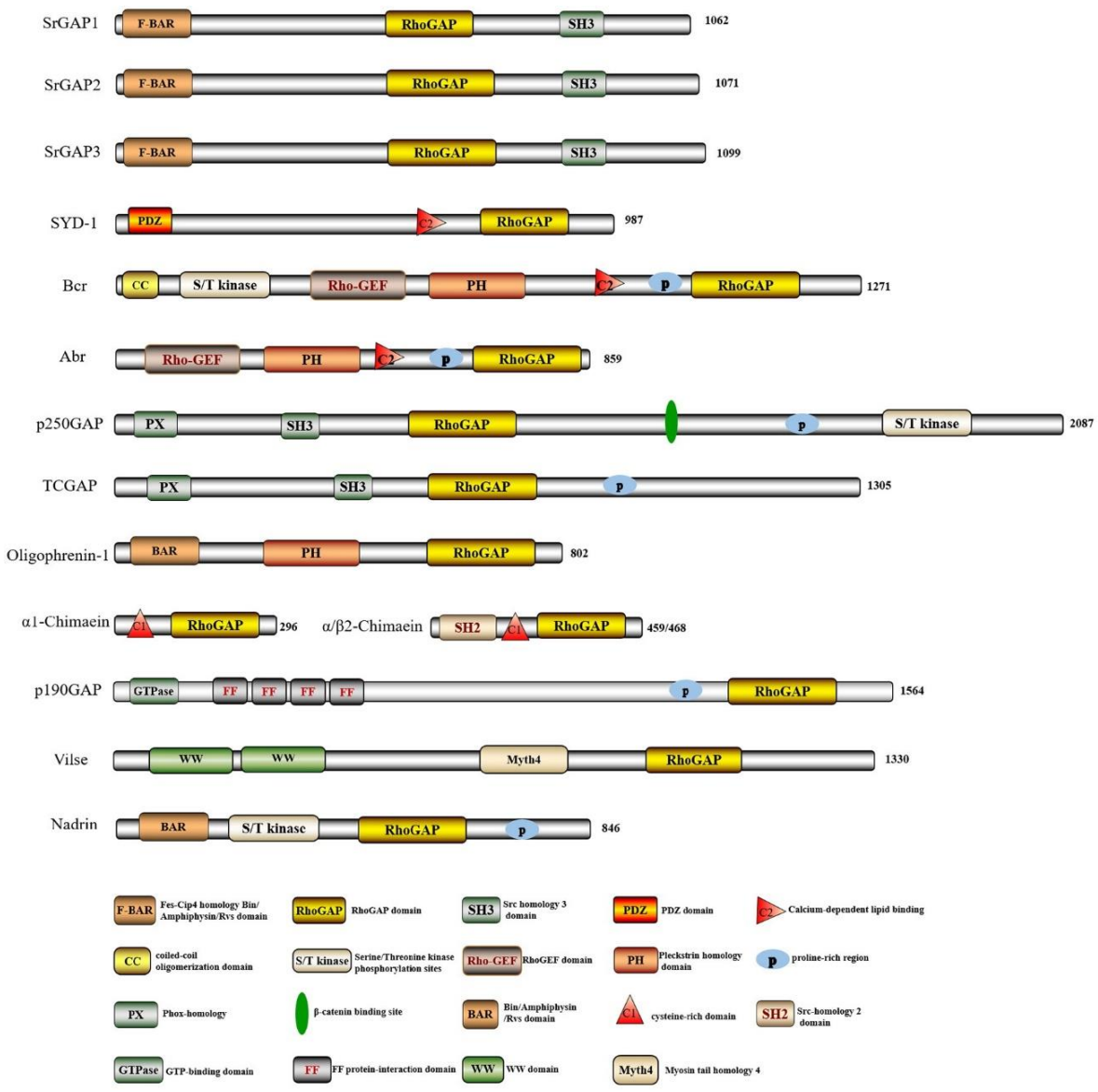

Fig. 7 | Major Rho GAPs and their domain organization.

Reprinted by permission from [Elsevier]: [Molecular and Cellular Neuroscience]: [Rho GTPase-activating proteins: Regulators of Rho GTPase activity in neuronal development and CNS diseases, Guo-Hui Huang, Zhao-Liang Sun, Hong-Jiang Li, Dong-Fu Feng]: [Elsevier: All rights reserved]: (2017)

1.1.2.3. Rho guanine Nucleotide Dissociation Inhibitors (RhoGDIs)

RhoGDIs are cytosolic proteins without enzymatic activity. They retain Rho GTPases in an inactive, GDP-bound state, sequester them from the cell membrane, thus preventing them from proteolytic degradation or effector interaction[16]. Interestingly, not all small Ras GTPases have GDIs. The Ras family does not have any GDIs, while the Rho and Rab small GTPases have been described to bind GDIs[35]. In mammals, the RhoGDI family contains three members: RhoGDI1/ARHGDIG/RhoGDIα, RhoGDI2/RhoGDIβ and RhoGDI3/RhoGDIγ. RhoGDI1 is ubiquitously expressed in most cell lines, while RhoGDI2 has been shown to be expressed in haematopoietic cells and upregulated in some tumors[35, 36]. RhoGDI3 is mostly expressed in the brain[35, 36]. The N-terminal regulatory domain of RhoGDIs mediates the interaction with the Switch I and II regions of Rho GTPases[16, 18]. This interaction prevents the exchange between the GDP- and GTP-bound states[18]. The hydrophobic pocket that is located on the C-terminal domain allows RhoGDIs to binds to the isoprenyl moiety of Rho GTPases, extracting Rho GTPases from the cell membrane[18, 36]. It has been shown that RhoGDI1 promotes degradation and inactivation of the cytosolic Rho GTPases while activating the membrane-bound Rho GTPases[37]. In addition, RhoGDI-Rho GTPase interaction has been shown to be regulated by several mechanisms such as phosphorylation which diminishes the RhoGDI affinity for Rho GTPases, favouring Rho GEF-Rho GTPase complex and subsequent Rho GTPase activation or by binding to 14-3-3 proteins, preventing RhoGDI-Rho GTPase association[18, 38].

1.1.2.4. Regulation by post-translational modifications (PTMs)

In addition to their regulation by GEFs, GAPs and GDIs, Rho GTPases are also regulated by PTMs such as phosphorylation, lipid modifications, sumoylation or ubiquitination[39] (**Table 1**).

Rho GTPase	Phosphorylation	Ubiquitylation	Sumoylation
CDC42	• SRC → Y64 — enhancement of RhoGDI interaction[137] • PKA → S185 — translocation to the cytosol by increasing interaction with RhoGDI[25]	—	—
RhoQ	• CDK5 → T197 — maintains RhoQ in lipid raft compartments, thereby disrupting cortical actin[138] • ‡aPKC → T197 — might regulate RhoQ role in coordinating actin remodelling during the fusion/docking of GLUT4 vesicles in response to insulin stimulation[138]	—	—
RAC1	• ERK → T108 — targets RAC1 for translocation to the nucleus[32] • FAK → Y64 — negative regulator of RAC1 activity and cell spreading[30] • SRC → Y64 — negative regulator of RAC1 activity and cell spreading[30] • AKT → S71 — inhibits GTP binding and decreases RAC1 activity[31]	• XIAP and cIAP1 → K147 — polyubiquitylation and proteasomal degradation, regulates plasticity of cell migration[59] • HACE1 → K147 — preferentially targets GTP-bound, active RAC1 for degradation, to control RAC1 activity[61,62,64] • §SCF^{FBXL19} → K166 — proteasomal degradation in a AKT-dependent manner[65]	‖PIAS3 → K183, K184, K186, K188 — results in increased GTP binding and RAC1 activation. Does not seem to be important in RAC1 localization[67]
RAC3	—	SCF^{FBXL19} → K166 — targets RAC3 for proteasomal degradation and results in E-cadherin downregulation[66]	—
RhoA	• ¶PKA → S188 — translocation to the cytosol by increasing interaction with RhoGDI[21–23] • Decreases binding and inhibits activity of ROCK effector[26] • Protects GTP-bound RhoA from proteasome-mediated degradation • PKG → S188 — translocation to the cytosol. • Protects RhoA, particularly GTP-bound form, from proteasome-mediated degradation[24] • PKC → T127 and S188 — translocation to the plasma membrane. Protects GTP-bound RhoA from proteasome-mediated degradation[128] • ERK2 — required for FBXL19-dependent RhoA degradation[47] • SLK → S188 — might inhibit RhoA activity[139]	• #SMURF1 → K6, K7 and K51 — proteasomal degradation[48,49,51,140] • §SCF^{FBXL19} → K135 — proteasomal degradation in an ERK-dependent manner[47] • $CUL3^{BACURD}$ — proteasomal degradation of GDP-bound inactive RhoA[52] • SCF^{FBXW7} — proteasomal degradation[141]	—
RhoB	CK1 → S185 — increases GDP-bound inactive form[142]	• $CUL2^{RBX1}$ — proteasomal degradation leading to liver carcinogenesis[143] • SMURF1 → K6 and K7 — degradation as part of DNA damage response pathway. RhoB abundance controls cell fate in response to DNA damage[56]	—
RhoC	AKT → S73 — required for downstream signalling and mediates increased breast cancer cell invasiveness[144]	—	—
RND1	? → S228 — regulates 14-3-3 protein binding[38]	—	—
RND2	? → S223 — regulates 14-3-3 protein binding[38]	—	—
RND3	• ROCK1 → S240 and S218 — regulates binding to 14-3-3 proteins, where RND3 is translocated to the cytosol[38] • PKC → S210 — regulates 14-3-3 binding[38]	SCF^{SKP2} → K235 — proteasome-mediated degradation to control cell cycle progression[145]	—
RhoU	SRC → Y254 — translocation from the plasma membrane to endosomes[39]	$CUL5^{RAB40A}$ → K177, K248 — protein degradation, RhoU protected by PAK4 binding to promote focal adhesion turnover[133]	—
RhoBTB2	—	CUL3 ubiquitin ligase complex — proteasome-mediated degradation[58]	—
RhoH	‡LCK? → Y73, Y83 — Tyr phosphorylation of ITAMs might modulate interaction of RhoH with ZAP70 in T cells[41]	—	—

Table 1 | Post-translational modifications of Rho GTPases: Phosphorylation, ubiquitylation and sumoylation.

Reprinted by permission from [Springer]: [Nature]: [Nature Reviews Molecular Cell Biology]: [Regulating RhoGTPases and their regulators, Richard G. Hodge, Anne J. Ridley]: [Springer Nature: All rights reserved]: (2016)

1.1.2.4.1. Lipid modifications

Lipid modifications are essential for controlling subcellular localization of Rho GTPases. The C-terminal CAAX motifs plays a major role in lipid modifications[39]. This cysteine residue of the CAAX motif is prenylated, which implicates the addition of either a farnesyl or geranyl-geranyl isoprenoid lipid. This prenylation process is mediated by farnesyltransferase and geranyl-geranyltransferase. Prenylation is then succeeded by proteolysis of the 3 C-terminal (AAX) amino acids and carboxymethylation of the prenylated cysteine residue[18, 39]. Prenylation is crucially important for plasma membrane or endomembrane targeting of Rho GTPases.

Some of the atypical Rho GTPases, such as RhoU and RhoV do not possess a CAAX motif, but they have a C-terminal CFV motif that undergoes palmitoylation[18, 40]. However, it has been shown that palmitoylation alone is not sufficient to target RhoV to the plasma membrane[40]. Basic amino acids in the carboxy terminal residues have been demonstrated to be important for RhoV translocation to the plasma membrane or endomembranes[40]. Palmitoylation and membrane targeting of RhoV facilitates its interaction with PAK serine/threonine kinases, which are also common effectors for Rac1 and Cdc42[41].

Classical Rho GTPases can undergo both prenylation and palmitoylation. For example, Rac1 is palmitoylated at Cys178 which is located on the CAAX motif, but only after prenylation at Cys189[42]. It has been shown that palmitoylated Rac1 shows increased GTP loading and higher association with detergent-resistant membranes. This promotes

the formation of Rac1-effector complexes in the plasma membrane and subsequent signalling cascades that lead to actin polymerization[18, 42]. Cells that express palmitoylation-deficient form of Rac1 exhibited migration defects[43].

1.1.2.4.2. Phosphorylation

Phosphorylation is another posttranslational modification for Rho GTPases, which regulates their activity and localization. Rho GTPases can be negatively regulated by phosphorylation. For example, RhoA phosphorylation on Ser188 by Protein Kinase A (PKA) triggers GDI binding, which results in RhoA translocation from the plasma membrane to the cytosol[44]. GDI-bound RhoA is protected from proteolytic degradation, however this also prevents RhoA to interact with downstream effectors such as Rho-associated protein kinase (Rock)[44-46]. It has been demonstrated that this results in a decreased Myosin Regulatory Light Chain (MRLC) phosphorylation by Myosin Light Chain Phosphatase (MLCP) since the Myosin- binding subunit of Myosin Phosphatase (MYPT1) remains activated following Rock inactivation in C2C12 cells in response to compressive stress[47, 48]. Interestingly, this Ser188 residue is not found in other members of the RhoA subfamily, RhoB or RhoC, suggesting that it is RhoA-specific regulation to control RhoA activity and downstream signaling pathways[16].

Rac1 phosphorylation on Tyr64 or Ser71 has been reported to have major consequences on Rac1-mediated actin polymerization and cell adhesion[18, 49]. Proto-oncogene tyrosine-protein kinase Src (Src) or Focal adhesion kinase (FAK) induce Rac1

phosphorylation on Tyr64, which resulted in altered spreading of HUVEC cells on fibronectin[49]. Abrogation of Src- or FAK-mediated Rac1 phosphorylation on Tyr64 by using a mutant form of Rac1, Rac1^{Y64F}, resulted in increased GTP-binding and cell spreading[49]. In addition, Rac1 phosphorylation on Ser71 by Rac-alpha serine/threonine-protein kinase (AKT) has been reported to show decreased GTP-binding[50].

1.1.2.4.3. Ubiquitination

Ubiquitination (also called ubiquitylation) is a posttranslation modification that involves the attachement of ubiquitin peptides to lysine residues of target proteins. It requires the involvement of three enzymes: Ubiquitin-activating (E1), ubiquitin-conjugating (E2) and ubiquitin-ligase (E3) enyzmes. Monoubiquitination or polyubiquitination can regulate proteasome-mediated degradation as well as localization of target proteins to different cellular compartments[18].

Although several Rho GTPases have been described to undergo ubiquitination, mechanisms underlying how RhoA is ubiquinated have been better elucidated compared to other Rho GTPases[18, 39]. Nucleotiode-free and GDP-loaded forms of RhoA have been reported to be ubiquitinated by the Smurf1 E3 ubiquitin ligase[51], while both GDP- and GTP-loaded forms of RhoA are ubiquitinated by the SCFFBXL19 E3 ubiquitin ligase[52]. Ubiqutination of RhoA by these two E3 ligases lead to proteosomal degradation, helping RhoA to maintain its protein expression levels and turnover. It has been shown that an increased SMURF1 expression is associated with decreased RhoA expression levels and

cell adhesion, which resulted in an increase in migration and invasion of MCF-7 breast cancer cells[53]. RhoA ubiquitination by SCFFBXL-19 has been reported to decrease the phosphorylation levels of Myosin light chain (MLC) in MLE12 lung epithelial cells[52].

Interestingly, Rac1 has been reported to be ubiquitinated only when it is GTP-loaded[54-56]. Rac1 is ubiquitinated by a variety of E3 ligases such as SCFFBXL-19[57] and HACE1[56, 58-60]. Abrogating HACE1 expression increased total Rac1 expression levels and Rac1-induced membrane ruffling[59]. It is known that overexpression of HER2 promotes Rac1 activation and is associated with cell proliferation, survival, migration and invasion[60, 61]. Neither HER2 overexpression nor HACE1 knockdown alone in MCF12A cells were able form tumors when implanted into mammary fat pads of immunodeficient NOD-SCID mice[60]. However, a combinatorial HER2 overexpression and HACE knockdown resulted in tumor formation in NOD-SCID mice, which is driven by Rac1 overactivation[60]. These studies highlighted the regulation of Rac1 activity by ubiquitination in cancer.

1.1.2.4.4. Sumoylation

Sumoylation is another posttranslational modification that regulates Rho GTPase activity[18]. It requires the involvement of small ubiquitin-related modifiers (SUMO) such as the activating SUMO1, the conjugating SUMO2, the SUMO3 E3 ligase and the lately discovered SUMO4, which is expressed in the human placenta and whose function remained largely unexplored[18, 62]. SUMO attachment to target proteins is very similar to that of ubiquitin enzymes, with few differences. Prior to activation and conjugation, the C-

terminal peptides of SUMO proteins need to be cleaved by the SUMO specific protease (SENP). Following conjugation, E3 SUMO ligases can transfer the SUMO group to a lysine residue of the target protein. Unlike ubiquitination, sumoylation does not lead to protein degradation. It primarily affects biological processes such as transcriptional regulation or nuclear transport[18, 63].

Surprisingly, Rac1 is the only Rho GTPase that has been shown to be regulated by sumoylation[18, 39, 64]. Sumoylation is not required for Rac1 activation but helps to keep Rac1 in a GTP-loaded, activated form[64]. Interaction of Rac1 with Protein inhibitor of activated STAT3 (PIAS3), a E3 SUMO ligase, is essential for increased Rac1 activity and cell migration[64]. It has been demonstrated that PIAS3-induced Rac1 sumoylation maintains GTP-bound levels of Rac1, controlling its capability to promote lamellipodia, migration and invasion[64]. In addition, sumoylation of RhoGDI at Lys138 provides RhoGDI a higher binding affinity to small GTPases such as RhoA, Rac1 and Cdc42 and has been shown to be essential for inhibiting actin polymerization and motility of HTC116 colon cancer cells[65].

1.2. Rho GTPase effectors and signalling pathways

Most studies in the Rho GTPase field focused on the characterization of effectors and signaling pathways of the three Rho GTPases: Rac1, Cdc42 and RhoA. The subfamilies belong to these three major Rho GTPases and the RhoD/RhoF subfamily have been described as classical Rho GTPases. The remaining subfamilies, which

comprise the Rnd subfamily, the RhoBTB subfamily, the RhoU/RhoV subfamily and RhoH are considered as atypical Rho GTPases as they are constitutively GTP-loaded. Their protein levels, activity and localization are mostly regulated by mechanisms such as ubiquitination or phosphorylation.

So far, studies on Rho GTPases identified a considerable number of effectors and signaling pathways. However, there are most likely other effectors and signaling cascades to be identified.

1.2.1. Classical Rho GTPases

1.2.1.1. Rac subfamily

Rac1 is one of the three major Rho GTPases and is the prototype member of the Rac subfamily. Rac1 and Rac3 are widely expressed, however Rac2 expression is mostly limited to hematopoietic cells. The first function of Rac1 has been described in 1992 by Alan Hall and his colleagues, who showed that Rac1 induces lamellipodia formation and membrane ruffling upon Plateled-derived growth factor (PDGF) stimulation[66]. Lamellipodia are thin sheet-like extensions that are formed at the front of migrating cells[39]. The formation of these transient membrane trusions is driven by the polymerization of actin filaments and the establishment of adhesions with the extracellular matrix (ECM)[67]. Membrane ruffles are described as wave-like membrane extensions that move upside towards the main cell body[68]. It has been demonstrated that membrane ruffles are formed

due to inefficient ligand-integrin interaction, such as integrin α5β1 and fibronectin interaction, at the leading edge of lamellipodia and regulated by both Rac1 and RhoA[68]. Membrane ruffles are stabilized by actin filament cross-linker proteins such as Filamin or Ezrin, that signal downstream of Rac1 and RhoA, respectively[68-70]. It has been suggested that the formation of membrane ruffles depends on an increase in the activity of Phospholipase D2 (PLD2) upon Growth factor Receptor Bound protein-2 (Grb2) binding and Rac overexpression[71].

Active Rac1 stimulates lamellipodia formation via direct binding to Sra1/Cyfip1, one of the members of the SCAR/Wave Regulatory Complex (WRC). The binding of GTP-loaded Rac1 with Sra1 is followed by a conformational change that releases the verprolin homology, cofilin homology and acidic region (VCA) motif that is located on WAVE1, which results in the activation of the Arp2/3 complex and assembly of actin filaments[72-76], leading to lamellipodia formation and membrane ruffling[77] (**Fig. 8**). Later, studies also revealed that WAVE includes another direct effector for Rac proteins, IRSp53/BAIAP2, which directly binds to and connects active Rac1 with the proline-rich motif of WAVE[77, 78]. It has been revealed that active Rac1 binds to the inverse Bin/Amphiphysin/Rvs (I-BAR) domain of IRSp53, promotes protrusion formation by causing outward membrane curvature[79]. This enhances Arp2/3-driven actin polymerization, lamellipodia formation and membrane ruffling[79].

Like IRSp53, Rac1 binds to other BAR-domain containing proteins to regulate membrane deformation. For example, PACSIN2, an F-BAR domain containing protein that promotes membrane tubulation and endocytosis, has been shown to directly bind to active Rac1. Active Rac1 triggered a loss of PACSIN2-positive intracellular tubules, while

inhibition of Rac1 resulted in accumulation of PACSIN2-positive tubules. Overexpression of PACSIN2 decreased the levels of Rac1-GTP while siRNA-mediated knockdown of PACSIN2 increased the levels of Rac1-GTP, enhancing cell spreading and migration[80].

Focal adhesions are molecular complexes that links the cytoskeleton to the ECM. They contain integrins, transmembrane receptors and integrin-associated cytosolic proteins that connect integrins between the ECM and actin stress fibers[67]. The formation of focal adhesion is a pre-requisite step for lamellipodia and membrane ruffling stimulation[67]. The involvement of GIT-βPIX-PAK complex is essential for focal adhesion disassembly[81]. This complex activates Rac1 and promotes cell migration via GIT-Paxillin interaction and PAK-dependent phosphorylation of Paxillin at Ser273[9, 22, 81-83]. This acts as a positive feedback and increases adhesion turnover at the leading edge of migrating cells. GIT acts as a GAP for the ARF small GTPases, suggesting that the GIT-driven Rac activation is correlated with ARF inactivation, which plays an important role in cell migration[22, 84]. β-PIX is a Rac-specific GEF that connects PAK, a serine/threonine kinase that is a Rac effector, with Rac1, showing that GEFs can directly interact with Rho GTPase effectors and link them to their corresponding GTPases[22]. The engagement of GEFs in Rho GTPase-effector complexes may determine the effector specificity of Rho GTPases to promote distinct signaling pathways and biological functions. PAK, which are activated by Rac GTPases, phosphorylate and induce LIMK kinase (LIMK) activation. LIMK activation results in Cofilin phosphorylation and inactivation[85]. Since Cofilins are actin-binding proteins that are involved in the disassembly of actin filaments, inactivation of these proteins leads to actin polymerization[39, 85].

Lipid kinases are another group of effectors that are involved downstream of Rho

GTPases. Active Rac proteins can activate Phosphatidylinositol-4,5-biphosphate 3-kinase (PI3K) which produces phosphorylated lipids that are important for cell polarization[86]. In humans, there are three classes of the PI3K family: Class I, Class II and Class III. The class I of PI3Ks are the best characterized among the PI3K family and can produce phosphatidylinositol (3,4,5)-triphosphate (called PtdIns(3,4,5)P_3 or PIP3) from phosphatidylinositol (4,5)-biphosphate (called PtdIns(4,5)P_2 or PIP2). There is a crosstalk between the PI3K signaling cascade and Rac activation[87]. G-protein coupled receptors (GPCRs) can induce the PI3K activity to promote Rac activation through Prex1. Co-expression of both G protein beta/gamma subunit and PI3K has been reported to recruit Prex1 to the plasma membrane, which positively regulates Rac1 activation[88]. This translocation of Prex from cytosol to the plasma membrane is mediated by the lipid second messenger PIP_3, which recruits proteins comprising the PH domain such as some members of the GEF proteins such as Prex. It has been shown that Prex2 can inhibit phosphatase and tensin homolog deleted on chromosome 10 (PTEN), a phosphatase that blocks the PI3K pathway by the dephosphorylation of PIP3, through its PH domain, which interacts with the PTEN catalytic region[89]. Although these studies provided evidence that PI3K leads to Rac activation, some others showed that Rac GTPases induce PI3K activation as well. PI3K binds to GTP-loaded form of Rac1 and Cdc42 via its p85 regulatory subunit, indicating that it is an effector for these two Rho GTPases[90]. Moreover, it has been reported that Rac directly binds to the BCR homology (BH) domain of the PI3K p85 regulatory subunit and this binding is dependent upon Rac being GTP-loaded form, suggesting that PI3K is a Rac effector[86, 90, 91]. The crosstalk between Rac and PI3K is a perfect example of positive feedbacks of small GTPases with their effectors.

Another example of how Rho GEFs can directly connect their Rho GTPases to their effectors is Prex1-mediated flightless-1 homolog (FLII) binding of Rac1[92, 93]. FLII has been identified as a novel Rac1 effector and promotes fibroblast migration[92]. Prex1, not only activates Rac1, but also acts as a scaffold to induce active Rac1 binding to the leucine rich repeats (LRR) domain of FLII[92, 93].

Rac proteins are involved in defense against pathogens[94]. Leukocytes can phagocytose pathogenic bacteria[94]. The NADPH oxidase complex is implicated in the production of toxic oxygen radicals produced in phagocytic cells that kill internalized bacteria[94]. The activation of the multimolecular NADPH oxidase complex at the membrane requires the assembly of cytosolic components such as $p47^{Phox}$ and $p67^{Phox}$. It has been shown that both GTP-loaded Rac1 and GTP-loaded Rac2 bind directly to $p67^{Phox}$ in neutrophils[95-97], leading to reactive oxygen species (ROS) production.

RhoG is the neglected member of the Rac subfamily. The functions of RhoG are not as well characterized as three other Rac proteins at present. RhoG is best known to activate Rac1 by directly interacting with Engulfment and Cell Motility (Elmo), a direct binding partner of Dock[98]. RhoG-mediated Elmo/Dock activation of Rac1 promotes cytoskeletal dynamics such as lamellipodia or membrane ruffling[99]. It has been shown that the RBD domain of Elmo mediates RhoG-binding, which, in turns, reliefs Elmo from its autoinhibited state[100]. This leads to a conformational change that favors Elmo/Dock interaction and the subsequent Rac activation[99]. In addition, RhoG is also known to activate Kinectin, an endoplasmic reticulum (ER) membrane protein that binds to kinesin motor proteins, which are involved in intracellular organelle and transport of vesicles[101, 102].

1.2.1.2. Cdc42 subfamily

Cdc42 is another classical Rho GTPase that belongs to the Cdc42 subfamily together with RhoJ and RhoQ. Cdc42 and RhoQ are widely expressed[103], RhoJ expression is restricted to endothelial and tumor cells[104, 105]. Alan Hall and his colleagues showed that overexpression of Cdc42 stimulates filopodia in Swiss 3T3 fibroblast cells, leading to sequential activation of Rac1 and RhoA, respectively[106]. Filopodia are described as finger-like membrane extensions that are located at the leading edge of migrating cells[67]. The activation of nucleation promoting factors (NPFs) such as Wiscott-Aldrich Syndrome protein (WASP), neuronal (n-WASP) as well as WASP-family verprolin-homologous protein (WAVE)/suppressor of cAMP receptor (SCAR) are essential since the Arp2/3 complex itself is not sufficient for actin polymerization[39]. Cdc42 activates WASP and N-WASP complexes[107] (**Fig. 8**). Inactive N-WASP or WASP complexes are found in an autoinhibited state through the interaction of the C domain of the verprolin homology, central and acidic (VCA) module and the GTPase binding domain (GBD). This autoinhibition is relieved by the direct binding of GTP-loaded Cdc42 and PIP_2[108]. It has been shown that Cdc42 binds directly to the GBD domain and PIP_2 binds to a polybasic region, also known as the B motif[109]. Upon Cdc42 and PIP2 binding, active N-WASP or WASP can promote Arp2/3 driven actin polymerization. Similarly, RhoQ and RhoJ have been demonstrated to bind to N-WASP and promote Arp2/3-mediated actin polymerization[103], leading to filopodia formation[110]. IRSp53 is an effector for both Cdc42

and Rac1. IRSp53 binds to active Cdc42 through its Cdc42 and Rac interactive binding (CRIB) domain. Upon Cdc42 binding to IRSp53, the I-BAR domain of IRSp53 induces outward membrane curvature and promotes WASP-mediated Arp2/3-driven actin polymerization and subsequent filopodia formation[79].

In addition to its role in filopodia formation, Cdc42 is also involved in invadopodium formation[111]. It has been reported that VAV1, a GEF for Cdc42, Rac1 and RhoA, activates Cdc42 to stimulate invadopodia in DanG pancreatic cancer cells and Src-induced phosphorylation and activation Vav1 are required for invadopodia formation[112].

Cdc42 co-operates with Rac1 in the activation of several effectors such as PAK, PI5K, formins and IQGAP[95]. In mammals, formins such as mDia2, mDia3, Daam1, FMNL1, FMNL2 and INF2 have been reported to interact with Cdc42 and are involved in filopodia formation[113]. Overexpression of IQGAP increased the levels of GTP-loaded Cdc42, leading to the formation of filopodia in MCF-7 breast cancer cells[114]. Both IQGAP1 and IQGAP2 bind to Cdc42 via their GTPase-activating protein (GAP)-related domain (GRD)[115]. The crystal structure of Cdc42-GTP bound to the GRD domain of IQGAP2 showed that Cdc42 promotes IQGAP dimerization[115].

The signaling networks of RhoQ and RhoJ are less characterized compared to that of Cdc42. Endogenous RhoJ was localized to focal adhesions in endothelial HUVEC cells[116]. Vascular endothelial growth factor (VEGF) activates RhoJ, promoting endothelial cell migration and tube formation via actomyosin-mediated contractility and focal adhesions[74, 116]. Moreover, RhoJ and Cdc42 are both expressed in human corneal epithelial (HCET) cells and are involved in cell migration *in vitro*[74, 117].

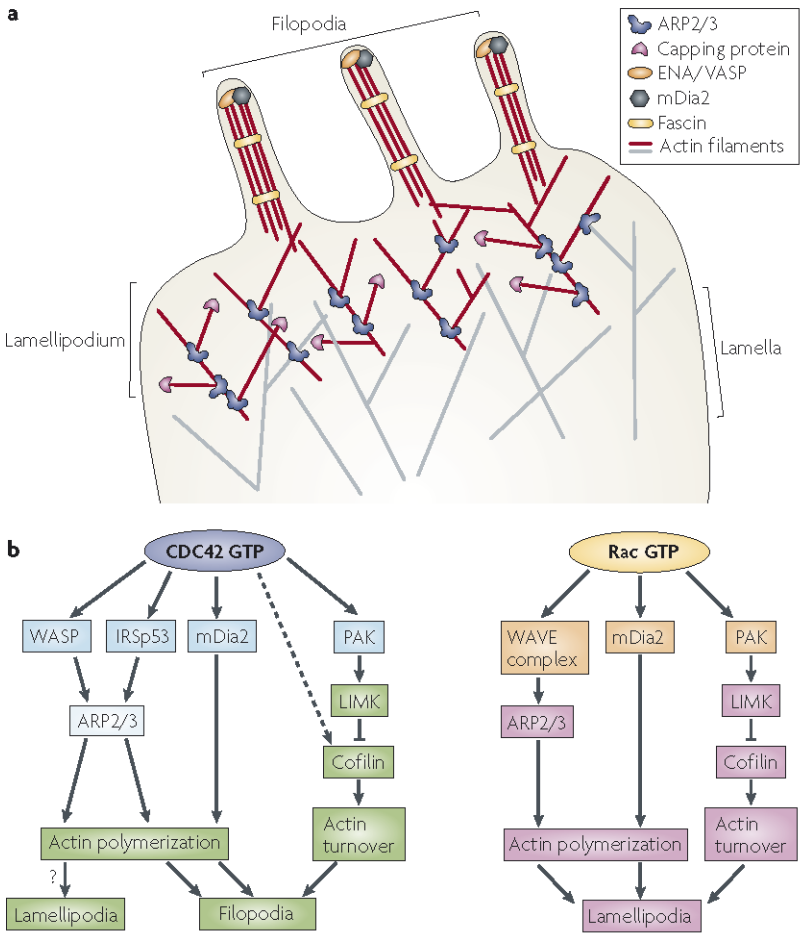

Fig. 8 | Lamellipodia and filopodia stimulation.

Reprinted by permission from [Springer]: [Nature]: [Nature Reviews Molecular Cell Biology]: [Mammalian Rho GTPases: new insights into their functions from in vivo studies, Sarah J. Heasman, Anne J. Ridley]: [Springer Nature: All rights reserved]: (2008)

1.2.1.3. RhoA subfamily

RhoA is one of the most studied Rho GTPases and belongs to the RhoA subfamily, which also includes RhoB and RhoC. The biochemical function of RhoA was first discovered by Alan Hall and his colleagues in 1990, when they microinjected $RhoA^{G14V}$, a constitutively active form of RhoA, in Swiss 3T3 fibroblast cells[118]. They reported that active RhoA induces morphological changes in the organization of actin filaments, without idea of what these induced cellular structures are and what they do[118]. In 1994, they identified that these cellular structures are stress fibers that are induced after lysophosphatidic acid (LPA) treatment and reported that active RhoA regulates focal adhesion assembly and stress fiber formation downstream of LPA cascade[74, 119, 120]. Thus, RhoA became the first Rho GTPase whose function was revealed[119].

RhoA, RhoB and RhoC activate downstream effectors such as mDia and Rock. Catalytically inactive Rock is kept in an autoinhibited conformation by a direct interaction of its N-terminal kinase domain with its C-terminal region including the coiled-coil domain, the PH domain and the cysteine-rich domain[121]. Rock is released from its autoinhibited conformation upon active RhoA binding to the RhoA-GTP binding (RB) domain of Rock[121]. Once activated by RhoA, catalytically active Rock can either directly phosphorylates MRLC or phosphorylates and inactivates the MYPT1, which, in turn, inhibits the myosin phosphatase activity so the MRLC is phosphorylated. MRLC phosphorylation promotes myosin II interaction with actin filaments and the assembly of stress fibers[39, 48, 74]. mDia, which is a member of the Diaphanous (Dia) formin subfamily, includes an N-terminal GBD domain and C-terminal Diaphanous autoinhibitory domain

(DAD)[122]. mDia, like ELMO, can be found in an autoinhibited state. Upon Rho binding to the catalytic formin homology 2 domain (FH2) of mDia, GBD is relieved from DAD, which, in turn, induces a conformational change that activates mDia, leading to the nucleation and polymerization of actin filaments[122-124]. Independent of its actin nucleation function, mDia exhibits a microtubule stabilization activity[125]. Moreover, Upon RhoA-binding, mDia co-operates with Rock for the formation of actomyosin bundles, like stress fibers[39]. However, mDia is found at the leading edge and rear of the cells and functions differently dependent on the cell type and the local Rho GTPase activity.

It has been thought that Rac and Cdc42 are found in an active state at the leading of migrating cells and promote protrusion formation such as lamellipodia, membrane ruffing or filopodia, whereas RhoA has been initially suggested to be active only at the rear or in the cell body to promote stress fibers, creating the mechanical force needed for retraction of the cells, followed by a forward movement[74]. Later, studies demonstrated that RhoA is also found in an active state at leading, prior to Rac and Cdc42 activation[74, 126, 127]. Studies showed evidence that following cell-cell contact, RhoA is activated at the initial cell-cell contact site, whereas Rac1 and Cdc42 are found inactive at this site but activated at leading edge of migrating cells[67]. Which GEFs, GAPs or PTMs are involved in this crosstalk between Rho GTPase-stimulated cell migration is not well elucidated[74].

FMNL2, an effector for both Rac1 and Cdc42, has also been shown to bind active RhoC, but not RhoA or RhoB. RhoC-specific FMNL2 activation is important for tumor invasion *in vitro*[128]. In addition, RhoC has also been shown to be essential for metastasis *in vivo*[129]. It is thought that FMN2 specificity of RhoC is due to RhoC-specific isoleucine residue at position 43, which may also determine GEF binding selectivity[16].

1.2.1.4. RhoD and RhoF subfamily

RhoD and RhoF are classified as classical Rho GTPases. However, a study has suggested that RhoD and RhoF need to be considered as atypical Rho GTPases since they show a high intrinsic nucleotide exchange activity and are largely found as GTP-bound[130]. It has been reported that RhoD localizes to the early endocytic vesicles and to the plasma membrane[74, 131]. It has been demonstrated that RhoD controls early endosomal dynamics and distribution. Moreover, it has been shown to be implicated in the disassembly of focal adhesions and stress fibers by antagonizing RhoA, affecting cell migration and cytokinesis[74, 132]. Like Cdc42, active RhoD stimulates filopodia and loss of RhoD reduces cell migration[133]. RhoD promotes Arp2/3-driven actin polymerization via the recruitment of WASP homolog associated with actin Golgi membranes and microtubules (WHAMM), an actin nucleation protein[133]. In addition, it promotes Filamin A (FLNa)-stimulated actin dynamics by interacting with FLNa-interacting protein (FILIP)[74, 133].

Interestingly, RhoF has been shown to induce filopodia formation independent of Cdc42, via the binding and activation of mDia2[74, 134]. In addition, RhoF binds to mDia1 to stimulate filopodia formation and the RhoF/mDia1 module seems to be independent of the traditional Cdc42/WASP/Arp2/3 axis[74, 135]. Surprisingly, RhoF is involved in the formation of stress fibers in HeLa cells. It has been shown that both RhoA and RhoF target the same downstream effector, mDia1, for stress fiber formation and mDia1 recruitment is Rock-dependent[136]. Active RhoF transiently interacts with Rock without significantly activating it, but it has been shown to increase the local concentration of Rock

activity[136].

1.2.2. Atypical Rho GTPases

Atypical Rho GTPases include the Rnd subfamily, the RhoBTB subfamily, the RhoU and RhoV subfamily and RhoH.

The Rnd subfamily of proteins are unable to hydrolyze GTP. Thus, they are considered as GTPase-deficient and are constitutively found in the GTP-loaded state[137]. Rnd1 and Rnd3 have been shown to interact with p190RhoGAP to antagonize the activity of RhoA, which results in the disassembly of stress fibers and causes cell rounding[33, 39, 138]. Rnd2 is mostly found in the cytoplasm, while Rnd1 and Rnd3 are membrane-associated and are not affected by RhoGDI activity[39]. Rnd phosphorylation at Ser240 followed by the recognition of the Rnd Cys241-farnesyl moiety by 14-3-3 results in translocation of Rnd proteins from the plasma membrane to the cytosol[38]. This process inactivates Rnd proteins and Rnd-stimulated cell rounding[38]. Rnd2 provides a positive feedback for RhoA, by interacting with Pragmin, an effector protein, which stimulates RhoA activity in a Rock-dependent manner[139]. Rnd2 and Pragmin stimulated contraction in HeLa cells, while abrogation of Pragmin expression affected neurite outgrowth[139]. Interestingly, Rnd2 promotes the RhoA activity through Pragmin, while Rnd1 and Rnd3 are known to antagonize the activity of RhoA[74, 139].

The RhoBTB subfamily of Rho GTPases includes RhoBTB1 and RhoBTB2. RhoBTB3 is excluded from the small Rho GTPases family due to differences in amino acid sequence alignment and possessing an unrecognizable GTP domain. It is thought

that RhoBTB3 does not even bind to GTP *in vitro*, which supports the idea of RhoBTB3 may have different biological outputs compared to RhoBTB1 and RhoBTB2[140]. The GTPase domain of RhoBTB1 and RhoBTB2 have some differences compared to that of other Rho proteins. These differences include a longer insert region and a deletion affecting the phosphate/magnesium binding region. However, it has been shown that these differences in the GTPase domain of RhoBTB2 do not hinder GTP binding[140, 141]. It is thought that the GTPase domain of RhoBTB1 may function similarly to that of RhoBTB2. *RhoBTB2* was first named as deleted in breast cancer 2 (*DBC2*) since the gene codes for the RhoBTB2 protein is homozygous deleted at region 8p21 in 3.5% of breast tumors[142]. In addition, *RhoBTB1* has been shown to be deleted at region 10q21 in head and neck cancer tumors[143]. Moreover, the expression of *RhoBTB2* showed a decrease in about 42% of breast cancer patients and that of RhoBTB1 showed a similar decrease, about 37%, in head and neck cancer patients, suggesting that the RhoBTB subfamily of Rho GTPases are implicated in tumorigenesis, possibly acting as tumor suppressors[140, 144]. T-47D breast cancer cell lines lack *RhoBTB2* transcripts[140]. Overexpression of RhoBTB2 in T-47D cells inhibits cell growth and promotes apoptosis in vitro[145]. RhoBTB2 overexpression in HOS (human osteosarcoma) cells caused a significant G1 phase arrest and apoptosis[146]. How RhoBTB2 induces cell growth arrest on T-47D cells is elucidated by cells Cyclin D1 (CCND1) downregulation[147]. Other roles of RhoBTB proteins, such as in vascular function, have been described[148, 149]. *RhoBTB1* was defined as a target of the peroxisome proliferator-activated receptor γ (PPARγ), a nuclear hormone receptor that is involved in adipogenesis but also in vascular protection of the smooth muscle and vascular endothelium[148, 149]. RhoBTB1 proteins levels are

significantly reduced in the aorta of mice which expresses a dominant negative PPARγ. The decrease in RhoBTB1 proteins levels are also correlated with a decrease in cullin 3. It has been suggested that RhoBTB1 controls cullin 3 activity, which, in turn, governs RhoA activity in smooth muscle[140, 148, 149].

RhoU and RhoV constitute a distinct subfamily among the small Rho GTPase family of proteins. RhoU has been shown to have a very high intrinsic nucleotide exchange activity and GTP-bound levels compared to that of Cdc42[150, 151]. It is therefore considered as an atypical Rho GTPase. Although the biochemical features of RhoV, such as the exchange of GDP for GTP or GTP hydrolsis, have not been studied yet, it is possible that RhoV may show a similar intrinsic nucleotide exchange activity due to its sequence homology with RhoU[41]. PAKs are the best-defined effectors of RhoU and RhoV. RhoU directly binds to and activates PAK1[152]. $RhoV^{G40V}$, an active mutant of RhoV, showed increased interaction with both PAK2 and PAK6, whereas these interactions were inhibited in the presence of $RhoV^{S45N}$ expression, a dominant negative RhoV mutant[41, 153, 154]. *In vitro*, RhoU promotes focal adhesion turnover, is involved in disassembly of stress fibers, cell adhesion and stimulation of filopodia in different cell lines[41, 155-157]. *In vivo*, RhoU has been demonstrated to be involved during the development of the mouse foregut[158, 159]. Overexpression of RhoV stimulates filopodia, lamellipodia or the formation of focal adhesions depending on the cell type. RhoV has also been shown to be implicated in development, during the differentiation of neural crest[41, 160]. The canonical Wnt pathway triggers transient expression of RhoV and loss of RhoV blocks the expression of neural crest transcription factors such as Twist, Slug or Sox9[41, 160].

RhoH is considered as a subfamily on its own. Like Rac2, it is widely expressed in

haematopoietic cells and tissues. RhoH is GTPase-deficient and it is believed that it is constitutively found in a GTP-loaded form without cycling. RhoH has been reported to be a component of the T cell receptor (TCR) signaling and is indispensable for the signaling molecule Zap70 to the TCR via its immunoreceptor tyrosine-based activation motifs (ITAMs)[39, 161]. It has been suggested that phosphorylation of the ITAMs of RhoH regulates its function[161]. Importantly, RhoH has been described as an antagonizer of the activity of other Rho GTPases by inhibiting the activation of NFκB[162]. The abrogation of RhoH expression leads to increased Rac1 activity, cytosol to plasma membrane translocation of Rac1 and colocalization of Rac1 with cortical filamentous-actin (F-actin) in hematopoietic progenitor cells (HPCs)[39, 163].

1.3. Characterization of the Rho GTPase signaling networks

1.3.1. Traditional PPI methods

A variety of traditional methods have been employed to determine Protein-Protein Interactions (PPIs). Large scale approaches permit screening for unbiased new binding partners. These methods include yeast two-hybrid (Y2H), affinity purification-mass spectrometry (AP-MS), protein microarrays and peptide phage display. Small scale approaches can be used to further validate a PPI and expand on the interactions. These approaches include förster resonance energy transfer or fluorescence resonance energy transfer (FRET), bioluminescence resonance energy transfer (BRET), co-

immunoprecipitation (co-ip), x-ray protein crystallography, nuclear magnetic resonance (NMR) spectroscopy and protein-fragment complementation[164]. These methods often combine biochemistry with biophysics and computational analyses. Each of these methods has its own advantages and disadvantages.

Y2H is one of the most commonly used methods to study PPIs. It was first introduced by Field and Song in 1989[165]. It was originally developed to detect PPIs in yeast *in vivo*, but it was also made available to reveal PPIs in bacteria or mammalian cells[166]. Before the introduction of Y2H in 1989, PPIs are mostly studied by using biochemical techniques *in vitro*[167]. Field and Song exploited the Gal4 transcription factor to develop Y2H. The classical Y2H consists of a bait which includes a protein of interest, X, fused to the DNA binding domain (DBD) of Gal4 and a prey, which comprises a potential interacting protein, Y, fused to the activation domain (AD) of Gal4[167]. Interaction between X and Y pieces together a functional transcriptional factor that could induce reporter gene expression. Y2H was later applied to other DNA-binding proteins such as the DBD of *E. coli* Lex4 or the AD of Herpes simplex virus (HSV) VP16 and others[167]. Y2H enables the detection of a direct interaction between bait and prey. However, it comes up with inconveniences such as false positive interactions or non-specific interactions. It disfavors detection of weak and transient PPIs. Proteins that undergo PTMs are unlikely to interact with each other in a typical Y2H. In traditional Y2H assays, proteins need to be localized to the nucleus to activate reporter genes, so interacting proteins that are not localized to the nucleus are mostly excluded unless they have an artificial NLS. Furthermore, proteins that are not found in their natural physiological environment might not fold properly to interact with each other[164, 168].

In AP-MS, separation of proteins by SDS-PAGE are followed by in-gel tryptic digestion and protein identification by MS. Native proteins can be subjected to in-solution tryptic digestion after immunoprecipitation. Mass spectrometers determine the mass to charge (m/z) ratio of molecules and measure the relative abundance of each peptide[169] (**Fig. 9**). Peptides of interest are selected based on their abundance and are fragmented by tandem MS (MS/MS). The amino acid sequence of fragmented peptides can be identified by search engines, which compare the fragment ion values of experimental samples with calculated fragment ion values of all protein sequences in a reference sequence database[169]. AP-MS enables the identification of thousands of proteins in a single analysis. It also identified proteins with PTMs. However, it has some disadvantages. False positives for proteins which are identified by only one or two peptides or identification of contaminant proteins that are found in transient interaction with a protein complex. Although the latter problem can be partially resolved by using IgG controls for endogenous IPs or tag controls such as Flag, GST, HA, contaminant proteins may still render the analysis of true interacting proteins difficult[169]. Weak and transient interactions may be disrupted due to detergents used for solubilization of proteins in cell lysates.

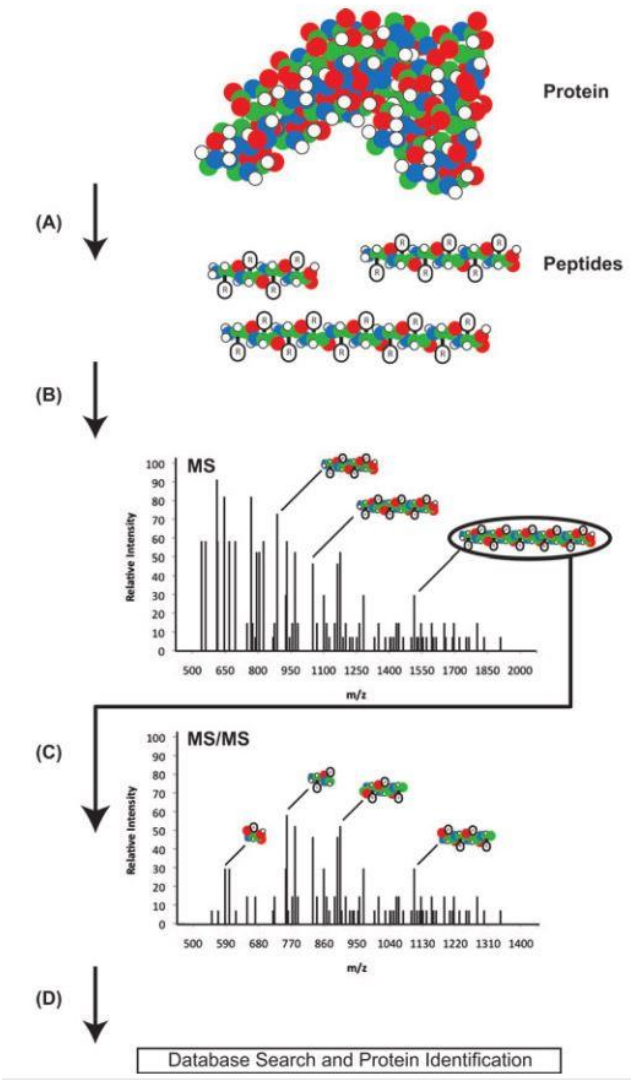

Fig. 9 | Overview of protein identification by AP-MS.

Reprinted by permission from [John Wiley and Sons]: [Proteomics]: [Affinity-purification coupled to mass spectrometry: Basic principles and strategies, Wade H. Dunham, Michael Mullin and Anne-Claude Gingras]: [John Wiley and Sons: All rights reserved]: (2012)

Protein microarrays, also known as protein chips, are commonly used to investigate PPIs (**Fig. 10**). Proteins of interest are immobilized on a solid surface and probed for interactions with a protein or peptide. Targeted proteins can be directly detected or via a

reporter antibody[170]. This method enables the study of PPIs in a high-throughput manner. Protein microarrays offer advantages such as the possibility of studying interactions relying on PTMs, such as phosphorylation. For example, protein microarrays of human phosphotyrosine binding (PTB) and Src homology 2 (SH2) domains have been used to discover phosphorylation-dependent interactions with 61 peptides representing tyrosine phosphorylation sites on the ErbB receptors[170, 171]. One of the drawback of this method is that it requires an intensive labor such as cloning, expressing and purifying proteins encoded in the human genome. Also, it is not possible to verify whether proteins are folded correctly and behave properly under a different set of conditions[170, 172].

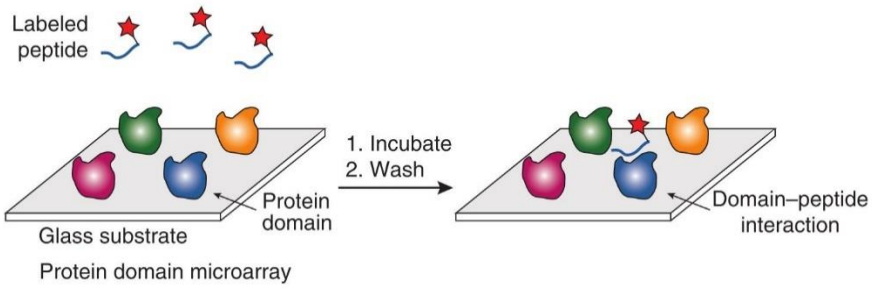

Fig. 10 | Protein microarray. Full-length proteins or protein domains can be immobilized on a solid surface and probed with fluorescently labeled peptides. After incubation and wash, targeted full-length proteins or protein domains can be detected by fluorescence.

Reprinted by permission from [Springer]: [Nature]: [Nature Protocols]: [Quantifying protein-protein interactions in high throughput using protein domain microarrays, Alexis Kaushansky, John E. Allen, Andrew Gordus, Michael A. Stiffler, Ethan S. Karp, Bryan H. Chang and Gavin MacBeath]: [Springer Nature: All rights reserved]: (2010)

Peptide phage display is one of the earliest methods to study PPIs (**Fig. 11**) Typically, polypeptides are fused to the gene-3 minor coat protein (P3) or the gene-8 major coat protein (P8) of the M13 filamentous phage, so they can be displayed on phage

particles containing the encoding DNA as well[173-175]. The phage library is then incubated with an immobilized solid surface that contains bait proteins to select for binding of displayed peptides with bait proteins. Unbound phages are then washed. Bound phages are eluted and amplified in *E. coli*. Amplified phage pools are then used for additional 3-5 rounds of selection. Bound polypeptides can be determined by DNA sequencing[173-175]. Compared to other methods, peptide phage display allows to identify the peptide binding domains and the generation of consensus motifs. It also enables the construction of diverse peptide libraries at a low cost[173-175]. However, it has some disadvantages. Luck and Travé showed that phage-display peptides can be very hydrophobic with high affinity, which is the case for tryptophan-containing peptides, while natural interaction motifs tend to be more hydrophilic with low affinity and high specificity[176]. They showed that interaction predictions for the two-thirds of the 54 human PDZ domains may be impaired due to a bias for hydrophobic amino acids[176]. Therefore, amino acid composition must be considered when utilizing peptide phage display to study PPIs.

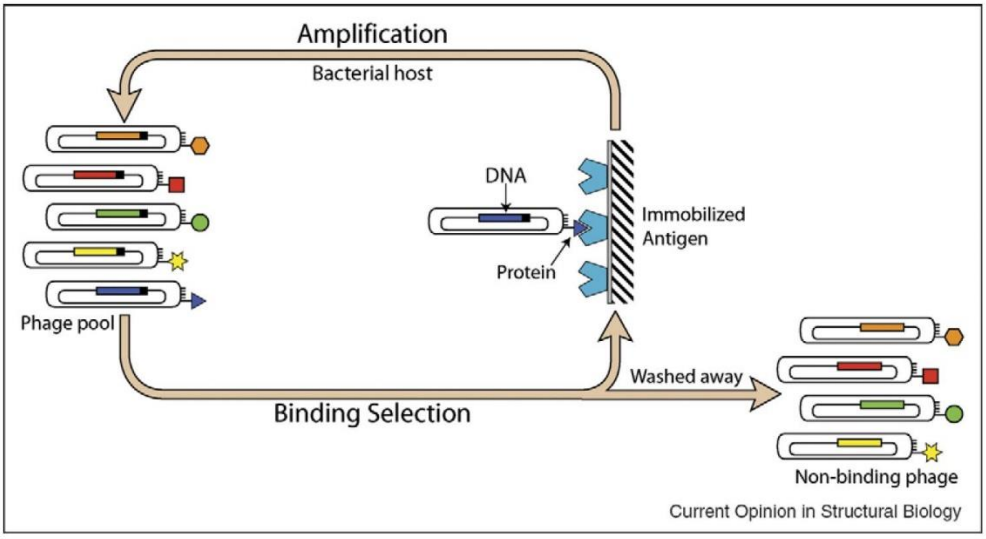

Fig. 11 | Overview of the peptide phage display method.

Reprinted by permission from [Elsevier]: [Current Opinion in Structural Biology]: [Phage display for engineering and analyzing protein interaction, Sachdev S. Sidhu and Shohei Koide]: [Elsevier: All rights reserved]: (2007)

FRET and BRET are two approaches relying on signal changes that occur via the use of fluorescence or bioluminescence following a PPI (**Fig. 12**). In FRET, an excited fluorescent molecule, the donor, transfers its energy to another fluorescent molecule, the acceptor, if they are found within a radius of ~50 Angstrom (Å) of each other[177]. FRET can be used a PPI method by fusing candidate proteins to the donor or acceptor fluorophore molecules. FRET efficiency depends on the spectral overlap of the donor emission and acceptor excitation as well as the relative orientation and distance between the donor and acceptor[178, 179]. A typical FRET assay is based on the use of aequorin as the donor, a photoprotein purified from the jellyfish *Aequorea*, and a GFP mutant as the

acceptor. When aequorin and mutant GFP are associated *in vivo*, aequorin transfers its energy to GFP so GFP can emit green light[177-179]. BRET was later developed and is based on bioluminescence[178]. In BRET, the donor can be a bioluminescent molecule, a luciferase, so it does not require fluorescence excitation. In the presence of a substrate, bioluminescence catalyzed by the luciferase excites the acceptor fluorophore, a GFP mutant by the same resonance energy transfer if they are found in the proximity of each other, within a radius of ~50 Angstrom (Å)[177]. Candidate proteins can be fused to the bioluminescent donor and fluorescent acceptor molecules to study PPIs in BRET both *in vivo* and *in vitro*[177-179]. FRET and BRET have many advantages. They can allow the investigation of the subcellular location of the interaction[180, 181]. In addition, since the energy transfer is a very rapid phenomenon, occurring in few nanoseconds, this renders determination of distances between proteins with nanometer precision[179]. FRET has disadvantages such as photobleaching, phototoxicity or autofluorescence[182]. Although BRET improved these problems found in FRET, it often comes with other problems such as weak signal or overlap of donor and acceptor emission peaks[183].

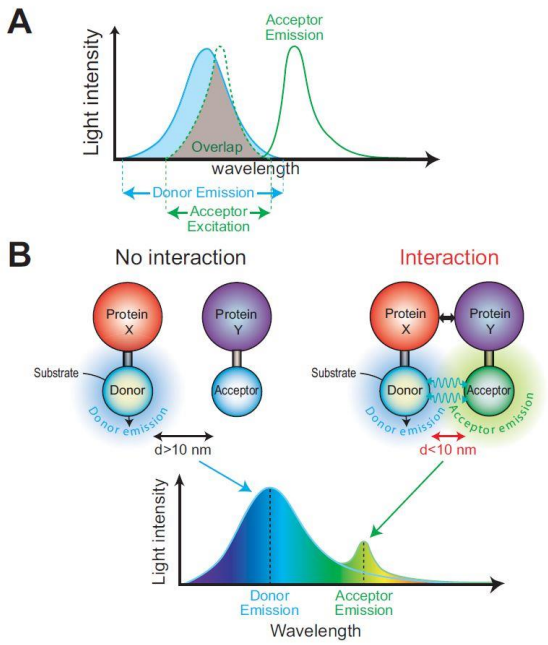

Fig. 12 | Overview of FRET and BRET assays. A) Overlap between the donor emission spectrum and acceptor excitation is necessary for energy transfer. B) The energy transfer occurs when the donor and acceptor are found in proximity upon interaction of the protein of interest with its binding partner.

Reprinted by permission from [John Wiley and Sons]: [Biotechnology Journal]: [The BRET technology and its application to screening assays, Johan Bacart, Caroline Corbel, Ralf Jockers, Stéphane Bach and Cyril Couturier]: [John Wiley and Sons: All rights reserved]: (2008)

The co-IP experiment is the mostly frequently used method to investigate PPIs. A protein complex that includes the target protein and its binding partners, can be precipitated using an immobilized antibody that recognizes a known epitope of one of the components of the protein complex[184]. Immunoprecipitated proteins are then subjected to sodium dodecyl sulfate-polyacrylamide gel electrophoresis (SDS-PAGE) and

immunoblot (also known as western blot) analysis. This method is commonly used to test whether proteins interact with each other *in vivo* or reveal novel interacting partners in a protein complex[184]. This method has many weaknesses such as the cross-reactivity of antibody, cell line- or tissue-specific expression of endogenous proteins, intensive labor for cloning and expressing fusion proteins, difficulty to assess weak and transient interactions, the possibility of impaired protein function due to large protein-tags, stringent biochemical conditions, has low throughput and time consuming[184]. Similar to co-IP, Glutathione-S-transferase (GST) pulldown consists of studying PPI between a GST-tagged bait and an unknown or known binding partner. GST-tagged bait, which is in complex with its binding partner, can be precipitated using GST agarose beads, subjected to SDS-PAGE and immunoblotting[185]. This method often reduces the precipitation of non-specific binding partners due to the cross-reactivity of an antibody that occurs during co-IP. However, certain proteins may non-specifically interact with GST. This technique has similar weaknesses as co-IP.

X-ray protein crystallography is used to determine the three dimensional structure of molecules such as proteins or nucleic acids[186]. It allows visualization of three-dimensional structure of proteins at the atomic level by showing how proteins interact with each other and their conformational states, providing insight at the level of residues and enabling understanding of protein function[164, 187]. However, proteins can undergo multiple conformational changes[187]. Once they are crystallized, it is only possible to visualize one conformation. Therefore, it is not possible to predict different conformational variations of proteins in their natural physiological environment *in vivo*[187]. Another limitation is that membrane proteins are not easy to crystallize since they can be precipitated out of

solution. Membrane proteins can be solubilized by using detergents, however detergents often affect their folding and stability in the crystal[188].

Some limitations of X-ray crystallography can be fixed by NMR spectroscopy, which is also used to determine protein structures at high-resolution[189]. NMR consists of the absorption of electromagnetic radiation at distinct frequencies by magnetically active nuclei in a strong magnetic field[190]. The chemical environment of each nucleus determines the distinct frequencies, which depend on atoms bound to the nucleus and the environment dynamics[190]. This technique offers many advantages. It is a powerful approach to determine PPIs in physiological or near-physiological environments. It also provides information for weak interactions (K_d > 100 µM) at the atomic level. However, it is not possible to study protein complexes with higher molecular weights, more than ~80-90 kDa[190].

Protein-fragment complementation consists of fusing each of the interacting proteins to complementary N- or C- terminal peptides of a reporter protein which is properly dissected[164, 191]. When two proteins interact with each other, complementary fragments of the reporter protein are brought into proximity. This allows them to fold together by reconstituting the reporter activity. Different reporters such as luciferase, GFP, cytosine deaminase or dihydrofolate reductase have been employed for protein-fragmentation complementation assays[191]. This technique enables the study of PPIs *in vivo* and *in vitro*. However, large tags may impair protein function or stability. PPIs investigated with fluorescent reporters may not be properly detected if the abundance of complexes is low to reconstitute a sufficient number of fluorescent proteins[191].

1.3.2. BioID: a proximity-based and powerful PPI method

1.3.2.1. Overview of the BioID method

BioID (proximity-dependent biotin identification) is a powerful proximity-based approach to identify PPIs. BioID consists of fusing a mutant form of *E. coli* biotin-ligase, $BirA^{R118G}$ (called BirA*), to a protein of interest (**Fig. 13**). It was developed based on the *E. coli* biotin-ligase (BirA). BirA is a 35 kDa protein, which functions as both an enzyme and a DNA-binding protein, that is responsible for the covalent attachment of biotin to proteins[192, 193]. This reaction occurs in two steps. In the first step, BirA catalyzes the formation of biotinoyl-5'-AMP (called bioAMP) in the presence of biotin and ATP. This intermediate product remains bound within the BirA active site. In the second step, biotinoyl-5'-AMP reacts with the nucleophilic ε-amino group of a specific lysine residue of a biotin-acceptor protein[192, 193]. Kwon and Beckett identified a couple of BirA mutants which have impaired enzymatic function[194]. Choi-Rhee et al. demonstrated that the $BirA^{R118G}$ mutant shows higher levels of self-biotinylation activity *in vivo* than other BirA proteins. They showed that activated biotin is released from the catalytic site of BirA* and it induces proximity-dependent non-specific biotinylation of neighboring proteins[195]. These results were later supported by another study[196]. Although Choi-Rhee et al. suggested that this system might be used to identify PPIs in living cells by fusing BirA* to a protein of interest, nobody employed this technique until 2012[195-197]. While some groups developed proximity-based techniques, none of these approaches have been largely adopted since they were less efficient than BioID[198]. Roux et al. revolutionized the PPIs

methods by employing BioID first time in living cells and identified proximal and interacting proteins of the human Lamin A (LaA), a component of the nuclear envelope[192]. They uncovered many candidates that are known interactors of LaA as well as unknown binding partners. For example, they identified an uncharacterized protein as a novel constituent of the nuclear envelope, which they have named SLAP75[192].

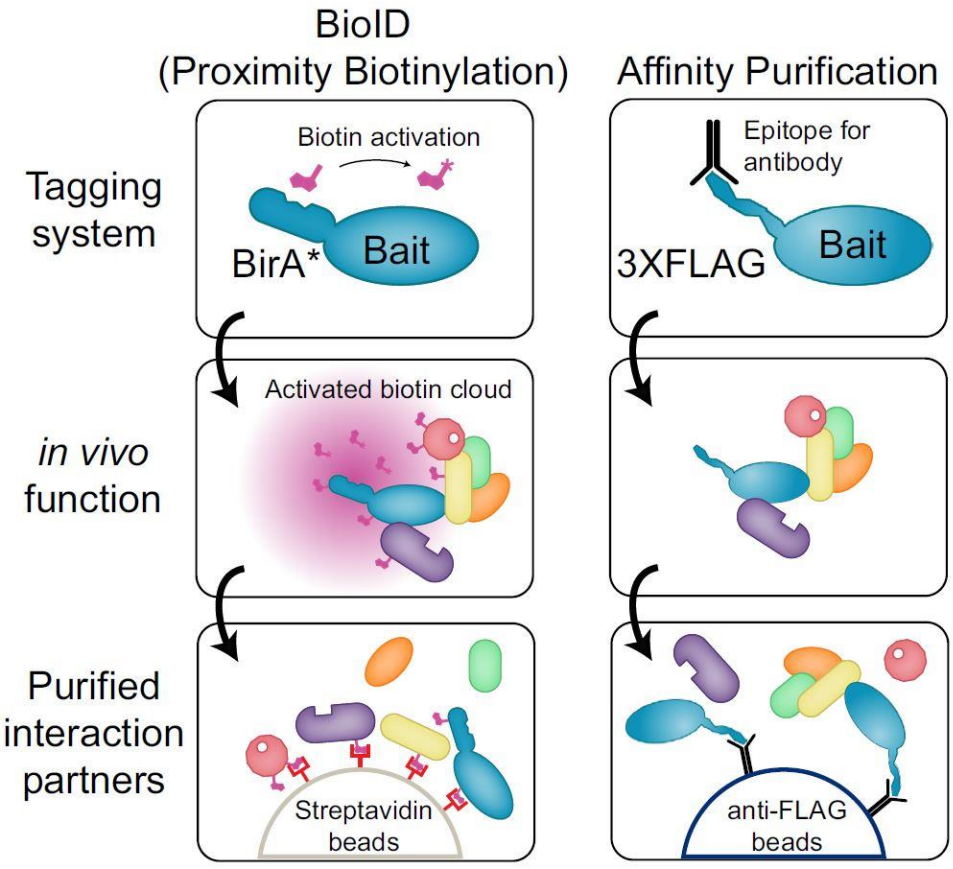

Fig. 13 | Comparison between the BioID and traditional AP-MS methods.

Reprinted by permission from [Elsevier]: [Journal of Proteomics]: [Proximity biotinylation and affinity purification are complementary approaches for the interactome mapping of chromatin-associated protein complexes, Jean-Philippe Lambert, Monika Tucholska, Christopher Go, James D.R. Knight and Anne-Claude Gingras]: [Elsevier: All rights reserved]: (2015)

BioID offers unprecedented advantages compared to traditional AP-MS methods. Unlike traditional Flag (or another tag-based) AP-MS methods, it takes its power from proximity-dependent biotinylation. Activated biotin is highly reactive and non-specifically biotinylates proximal proteins. The labeling radius of BioID is thought be about 10 nm around the BirA*-tagged protein of interest[199, 200]. Biotinylated-protein can be purified using Streptavidin-coated beads, trypsin-digested and identified by MS. BioID enables identification of more interacting partners than AP-MS. For example, Lambert et al. analyzed histone interaction partners and compared BioID with AP-MS[201]. BioID enabled identification of much more significant interacting partners compared AP-MS. A low number of binding partners were identified by both approaches[202]. BioID facilitates identification transient and weak interactions in living cells since biotinylation occurs prior to solubilization. Biotinylation is a covalent modification so there is no need to maintain PPIs. Therefore, proteins can be fully solubilized in most stringent conditions such as using RIPA buffers or lysis buffers containing 2% SDS or 500 mM NaCl[198]. This removes contaminant proteins that are detected in traditional AP-MS[198]. Although crosslinking of proteins also enables proximity-based labeling, crosslinking does only provide a snapshot of protein proximity while BioID provides a complete history of transient protein interactions that occurred over a given period of time in a natural cellular environment[198]. BioID enables identification of insoluble proteins such as integral membrane proteins or intermediate filament proteins, which is not easy to study by traditional AP-MS methods or Y2H[198].

Proximity labeling with Ascorbate Peroxidase (APEX) is another proximity-based approch that takes advantage of biotin, similarly to BioID. APEX generates biotin-phenolxyl radicals that reacts with amino acids such as Tyr, Trp, His or Cys[203]. The main disadvantage of APEX is that these radicals are dramatically short lived (<1 ms) compared to that of biotin-adenylate ester, which has a half-life of minutes, rendering BioID more advantageous than APEX in terms of labeling time period[204].

Like many approaches, BioID has its own limitations. BirA* tag is about 35 kDa and might compromise the function and localization of the protein of interest. Biotin labeling requires very long incubation times, from 6 hours to 24 hours, in order to accumulate a sufficient number of biotinylated proteins[204]. Covalent modification of lysine residues of primary amino groups by biotinylation might affect the function of labeled interacting proteins from further PTMs. In addition, some biotinylated proteins might be in the proximity of the protein of interest without physically interacting, causing false positive protein identifications. Many BioID studies demonstrated that the use of experimental controls such as BirA*, BirA*-GFP, BirA*-GFP with NLS or CAAX motifs significantly reduce the number of false positive protein identifications or non-specific biotin labeling[201, 205-209].

1.3.2.2. Exploitation of BioID for PPI

Traditional BioID has been successfully applied in mammalian cells and other systems. Roux et al. identified over 120 interacting partners in HEK293 cells for LaA, a key member of the nuclear lamina, including previously-reported LaA interactors such as

LAP1, LAP2, MAN1 and emerin[192, 205]. Roux and colleagues has also applied BioID to uncover novel members of the nuclear pore complex (NPC) in HEK293 cells[199]. They identified well-known NPC components as well as novel interacting partners. Expression and biotinylation of Flag-BirA*-CEP120 in HEK293 cells identified many centrosome proteins such as SPAP, SPICE1, CEP55, CEP59 and unknown interactions[210]. In addition, Pelletier and colleagues carried out BioID on 58 proteins and provided the most comprehensive interactome analysis of the human centrosome-cilium interface[208]. Another study identified proteins that are involved centriole duplication[211]. BioID has also been applied to cell junction proteins such as ZO-1, E-cadherin, Occludin, Claudin-4, MarvelD3 and α-catenin[205, 212-216]. Applications of BioID also include proteins that are involed in autophagy, signaling pathways such as Hippo pathway, nonsense-mediated mRNA decay, ubiquitin-mediated proteolysis, mitochondrial proteolysis, oncogenic transcription factors, mRNA-associated granules and bodies and others[205-207, 217-223].

Recently, an upgraded version of BioID have been developed. Roux and colleagues established BioID2, by using a smaller BirA promiscuous biotin ligase from *A. aeolicus*, about 27 kDa[224]. They showed that BioID2 improved localization of its fusion protein and is functionally comparable to BioID[224]. BioID2 allows more selective targeting of the bait and displays increased labeling of proximal proteins, as it has been successfully employed for Nup43, a constituent of the nuclear pore complex[224].

BioID has been successfully integrated with the protein-fragment complementation method to establish Split-BioID[225]. This technique consists of fusing two inactive fragments of BirA*, N-terminal and C-terminal fragments (NBirA* and CBirA*, respectively), with FK506-binding protein (FKBP) and FKBP-rapamycin-binding domain

(FRB). Similarly, to other protein-fragment complementation approaches, FKBP and FRB interact with each other in the presence of rapamycin, which bring N-terminal and C-terminal of BirA* into proximity. This allows BirA* folding and reconstitutes the reporter activity. During cell cycle, the G2/M transition-regulating protein phosphatase Cdc25C binds 14-3-3ε upon phosphorylation at Serine 216. Schopp et al. showed that transient NBirA*-14-3-3ε/CbirA*-Cdc25C^{WT} expression in the presence of rapamycin exhibited significantly higher biotinylation levels compared to that of NBirA*-14-3-3ε/CbirA*-Cdc25C^{S216A} or NBirA*-GFP/CbirA*-Cdc25C^{WT}, demonstrating the reliability of the Split-BioID approach[225]. By using Ago2/Dicer and Ago2/TNRC6C split-BioID samples, the same group identified known-components of miRNA-induced silencing complex (miRISC) such as TNRC6A, TNRC6B, CNOT1, CNOT4, PABPC1 and XRN1[225]. These data suggested that Split-BioID can be used as a powerful tool to reveal the proteomes of distinct protein complexes that are organized in a spatiotemporal manner[225].

Recently, another version of BioID has been developed and termed TurboID[226]. Two promiscuous mutants of the *E. coli* biotin ligase, TurboID (~35 kDa) and miniTurbo (~28kDa) have been generated. Both mutants are about 7-26 fold more active than BirA*, allowing biotin labeling of proximal proteins in about 10 minutes instead of ~6-24 hours. The study suggested that a one hour of TurboID assay produces more biotinylated proteins than that of 18 hours of BioID[226]. TurboID might be useful to monitor spatiotemporal proteome of ligand-treated cell surface receptors such as GPCRs or RTKs for drug screening.

1.4. Rationale and objectives

Historically, most studies on the Rho GTPase signaling pathways are relied on traditional PPIs methods such as biochemical assays, FRET- or BRET-based techniques, Y2H, AP-MS or other approaches. These studies paved the way for the identification and characterization of well-known Rho GTPase effectors and complexes such as the WAVE complex, the WASP complex, PAK, Rock and many others. Most of these studies focused on a single Rho GTPase-effector signaling networks, rather than globally covering the whole Rho GTPase network and interactome. The regulation of Rho GTPases and recruitment of their effectors often require weak or transient interactions that occur in a spatiotemporal manner in living cells, making their identification and characterization of signaling networks by traditional AP-MS based or other approaches challenging. There are most likely many effectors to be uncovered. Furthermore, GEF-Rho and GAP-Rho interactions have not been mapped in detail and how GEFs or GAPs achieve specific targeting of Rho GTPase-effector signaling couples have not been well investigated. GEFs and GAPs can regulate many Rho GTPases and this highly complex problematic is not yet understood.

In the recent years, BioID has emerged as the powerful approach of choice to characterize PPIs in living cells, in mice or other models. This method offers unprecedented advantages compared to all other known traditional PPIs methods in terms of efficiency, complexity or cost. We reasoned that BioID can be apply to Rho GTPases family of proteins to reveal their signaling pathways, uncovering novel effectors or regulatory proteins. The objectives of my thesis are the following:

1) To reveal the Rho GTPase interactome at large scale by BioID, uncovering novel Rho effectors and showing selective GEF-Rho or GAP-Rho interactions and specificity.

2) To characterize BioID-identified Rho GTPase effectors, elucidating their molecular mechanisms or biological functions in Rho GTPase-mediated signaling pathways.

CHAPTER 2: MATERIALS AND METHODS

2.1. Antibodies

The antibodies used in immunoblotting are the following: GST (1:1000; B-14, sc-138, Santa Cruz), Flag-HRP (1:8000; A8592, Sigma-Aldrich), p-ERM (1:2000; 3726S, Cell Signaling), ERM (1:2000; 3142S, Cell Signaling), p-SLK (T183) (1:1000; gift from Dr. Andrey Cybulsky, McGill University[227]), SLK (1:1000; gift from Dr. Luc Sabourin, Ottawa Hospital Research Institute[228]), Myc (1:1000; 9E10, sc-40, Santa Cruz), GAPDH (1:5000; FL-335, sc-25778, Santa Cruz), Tubulin (1:10000; T5168, Sigma-Aldrich), Calnexin (1:2000; H-70, sc-11397, Santa Cruz), KIAA0355 (1:6000; custom made, anti-peptide sequence is IVPEKKNSGSGGGLC, GenScript), mouse anti-rabbit secondary IgG-HRP (1:10000; sc-2357, Santa Cruz), goat anti-mouse secondary (1:5000; A4416, Sigma-Aldrich).

The antibodies used in immunofluorescence are the following: Hoechst (33342, Invitrogen), SlowFade Gold Antifade Mountant with DAPI (S36938, Thermo Fisher), Alexa Fluor 633 Phalloidin (A22284, Thermo Fisher), Mouse anti-Flag (F3165, Sigma-Aldrich), chicken anti-mouse Alexa Fluor 488 (A-21200, Thermo Fisher), goat anti-rabbit Alexa Fluor 568 (A-11011, Thermo Fisher), SLK (1:1000; gift from Dr. Luc Sabourin, Ottawa Hospital Research Institute), p-SLK (T183) (1:1000; gift from Dr. Andrey Cybulsky, McGill University).

2.2. Plasmids

Human Rho GTPAses, mostly in their constitutively active forms, in pDONR221 entry vectors generated previously in our laboratory[229] were cloned into pcDNA5-pDEST-FRT-BirA*-Flag destination vectors by using the Gateway® cloning system. For RhoBTB1 or RhoBTB2, only the GTPase domain was cloned into pcDNA5-pDEST-FRT-BirA*-Flag. pDONR221-SLK and pDONR221-SLK^{K63R} constructs were kindly provided by Dr. Arnaud Echard (Institut Pasteur). pEZYFlag and pEZY3 were gifts from Yu-Zhu Zhang (Addgene plasmids #17800 and #18672). mOrange-C1 was a gift from Dr. Michael Davidson (Addgene plasmid #54680). mOrange-Rac1^{WT} and mOrange-Rac1^{G12V} expression vectors were generated via 2-fragment Gateway® MultiSite recombination. pCMV-CFP-PLEKHG3 plasmid was a gift from Dr. Won Do Heo (Korea Advanced Institute of Science and Technology). Flp-In T-REx HeLa cell line was a gift and generated by Dr. Stephen Taylor (University of Manchester)[230]. The expression vectors generated by Gateway® cloning system which were used for functional assays are shown in the table below (**Table. 2**)

Entry Vector(s)	Destination Vector	Expression Vector	Expression Type
pDONR221-RhoA^{G14V}	pDEST27	pDEST27-GST-RhoA^{G14V}	Mammalian
pDONR221-Rac1^{G12V}	pDEST27	pDEST27-GST-Rac1^{G12V}	Mammalian
pDONR221-Cdc42^{G12V}	pDEST27	pDEST27-GST-Cdc42^{G12V}	Mammalian
pDONR221-SLK	pcDNA5-pDEST-FRT-3xFlag	pcDNA5-pDEST-FRT-3xFlag-SLK	Mammalian
pDONR221-SLK^{K63R}	pcDNA5-pDEST-FRT-3xFlag	pcDNA5-pDEST-FRT-3xFlag-SLK^{K63R}	Mammalian
pDONR221-SLK$^{1-338}$	pcDNA5-pDEST-FRT-3xFlag	pcDNA5-pDEST-FRT-3xFlag-SLK$^{1-338}$	Mammalian
pDONR221-SLK$^{339-788}$	pcDNA5-pDEST-FRT-3xFlag	pcDNA5-pDEST-FRT-3xFlag-SLK$^{339-788}$	Mammalian
pDONR221-SLK$^{789-1205}$	pcDNA5-pDEST-FRT-3xFlag	pcDNA5-pDEST-FRT-3xFlag-SLK$^{789-1205}$	Mammalian
pDONR221-SLK$^{1-788}$	pcDNA5-pDEST-FRT-3xFlag	pcDNA5-pDEST-FRT-3xFlag-SLK$^{1-788}$	Mammalian
pDONR221-SLK$^{1-996}$	pcDNA5-pDEST-FRT-3xFlag	pcDNA5-pDEST-FRT-3xFlag-SLK$^{1-996}$	Mammalian
pDONR221-SLK$^{1-1100}$	pcDNA5-pDEST-FRT-3xFlag	pcDNA5-pDEST-FRT-3xFlag-SLK$^{1-1100}$	Mammalian
pDONR221-RhoA^{WT}	pcDNA5-pDEST-FRT-3xFlag	pcDNA5-pDEST-FRT-3xFlag-RhoA^{WT}	Mammalian
pDONR221-RhoA^{G14V}	pcDNA5-pDEST-FRT-3xFlag	pcDNA5-pDEST-FRT-3xFlag-RhoA^{G14V}	Mammalian
pDONR221-Rac1^{WT}	pcDNA5-pDEST-FRT-3xFlag	pcDNA5-pDEST-FRT-3xFlag-Rac1^{WT}	Mammalian
pDONR221-Rac1^{G12V}	pcDNA5-pDEST-FRT-3xFlag	pcDNA5-pDEST-FRT-3xFlag-Rac1^{G12V}	Mammalian
pDONR221-KIAA0355	pcDNA5-pDEST-FRT-3xFlag	pcDNA5-pDEST-FRT-3xFlag-KIAA0355	Mammalian
pDONR221-KIAA0355$^{\Delta 240-480}$	pcDNA5-pDEST-FRT-3xFlag	pcDNA5-pDEST-FRT-3xFlag-KIAA0355$^{\Delta 240-480}$	Mammalian

pDONR221-RhoA^{G14V}	pCS-pDEST-6xMyc	pCS-pDEST-6xMyc-RhoA^{G14V}	Mammalian
pDONR221-KIAA0355	pCS-pDEST-6xMyc	pCS-pDEST-6xMyc-KIAA0355	Mammalian
pDONR221-RhoA^{G14V}	pTH35-pDEST-GST	pTH35-pDEST-GST-RhoA^{G14V}	Bacterial
pDONR221-Rac1^{G12V}	pTH35-pDEST-GST	pTH35-pDEST-GST-Rac1^{G12V}	Bacterial
pDONR221-RhoG^{WT}	pTH35-pDEST-GST	pTH35-pDEST-GST-RhoG^{WT}	Bacterial
pDONR221-RhoG^{G12V}	pTH35-pDEST-GST	pTH35-pDEST-GST-RhoG^{G12V}	Bacterial
pDONR221-PLEKHG3	pEZYflag	pEZYflag-PLEKHG3	Mammalian
pDONR221-L1-mOrange-L5r pDONR221-L5-Rac1^{WT}-L2	pEZY3	pEZY3-mOrange-Rac1^{WT}	Mammalian
pDONR221-L1-mOrange-L5r pDONR221-L5-Rac1^{G12V}-L2	pEZY3	pEZY3-mOrange-Rac1^{G12V}	Mammalian

Table 2 | Expression vectors used for functional assays.

2.3. Generation of KIAA0355-null cell lines by CRISPR/Cas9

To generate Flp-In T-REx HeLa cells with a deletion in the KIAA0355 genomic locus, we used a CRISPR/Cas9 approach described by Ran et al[231]. with the following modifications. We designed 2 sets of 2 gRNAs to engineer precise deletion in the Exon 2

of KIAA0355 using the CRISPR design webtool (http://tools.genome-engineering.org). The primers were as follows: CRISPR KIAA0355 Forward-1: 5'-CACCGTCGGCGATAGGAGTAGTGT-3'; CRISPR KIAA0355 Reverse-1: 5'-AAACACACTACTCCTATCGCCGAC-3'; CRISPR KIAA0355 Forward-2: 5'-CACCGCTCAGGCATCGGGTATTGC-3'; CRISPR KIAA0355 Reverse-2: 5'-AAACGCAATACCCGATGCCTGAGC-3'; CRISPR KIAA0355 Forward-3: 5'-CACCGTATGGCCGAGGTCAGCCGAC-3'; CRISPR KIAA0355 Reverse-3: 5'-AAACGTCGGCTGACCTCGGCCATAC-3'; CRISPR KIAA0355 Forward-4: 5'-CACCGTGGCACGGCAGAAGACGTTC-3'; CRISPR KIAA0355 Reverse-4: 5'-AAACGAACGTCTTCTGCCGTGCCAC-3'. Each gRNA (ordered from IDT) was clone into pSpCas9(BB)-2A-GFP (Addgene plasmid #48138) and insertions were verified by DNA sequencing. HeLa cells (6-well plates; 80% confluency) were transfected with 2.5 µg of each pair of gRNAs using Lipofectamine 3000 for 48 hrs. GFP-positive cells were then cloned as single cells in 96-well plates by FACS (IRCM flowcytometry core facility). Following expansion of the clones, genomic DNA was extracted using the Direct Lysis PCR reagent (302-C, Viagen). Each clone was analyzed for deletion in the KIAA0355 genomic locus by PCR using the following genotyping primers: Genotyping KIAA0355 Forward-1: 5'-GCCCAGGACAGTAAAATGGA-3'; Genotyping KIAA0355 Reverse-1: 5'-AAGTACTGGCACGGCAGAAG-3'; Genotyping KIAA0355 Forward-2: 5'-TACTCCTATCGCCGACATCC-3'; Genotyping KIAA0355 Reverse-2: 5'-TGTCCTGGAGACTGAATTCCT-3'. Positive clones were further expanded and frozen until used for protein-protein interaction experiments.

2.4. Cell culture and generation of stable cell lines

Stable Flp-In T-REx HEK293 or Flp-In T-REx HeLa cell lines expressing BirA*-Flag tagged Rho GTPases or other constructs were generated as mentioned elsewhere[232]. Briefly, Parental Flp-In T-REx HEK293 or Flp-In T-REx HeLa cells were grown in regular medium (DMEM medium supplemented with 10% (vol/vol) heat-inactivated fetal bovine serum (FBS) and 1% penicillin/streptomycin (450-201-EL, Wisent)). Cells were plated into 6-well dishes and were at ~75-85% confluency prior to transfection. 2 µg of pOG44 and 500 ng of expression vector were transfected using Lipofectamine 2000 (11668019, Thermo Fisher) according to the manufacturer's instructions. Next day, cells were trypsinized and transferred into 10-cm dishes in regular medium. 24 hours later, regular medium was replaced with selection medium (DMEM medium supplemented with 10% (vol/vol) heat-inactivated FBS, 1% penicillin/streptomycin and 200 µg/ml Hygromycin B (400052-Calbiochem)). Selection medium was replaced every 3-4 days for Flp-In T-REx HEK293 cells and 2-3 days for Flp-In T-REx HeLa cells. Isolated clones of ~1-2 mm in diameter were observed after 12-15 days for Flp-In T-REx HEK293 cells and 9-11 days for Flp-In T-REx HeLa cells. Isolated clones were trypsinized and replated into 6-cm or 10-cm plates depending on their number and size.

2.5. BioID and MS data analysis

BioID experiments were performed as described elsewhere, with modifications[209, 218]. Briefly, Flp-In T-REx HeLa or HEK293 cells expressing BirA*-Flag tagged Rho GTPases or controls (Empty Vector, BirA*-Flag-EGFP or BirA*-Flag-EGFP-CAAX) in a tetracycline-inducible manner in two 15-cm plates were treated with with 1 µg/ml tetracycline (TET701.10, Bioshop) and 50 µM biotin (BB0078, Bio Basic) for 24 h. Similar BioID assay and MS data analysis were carried out as described previously[209, 218]. Following 24 h of tetracycline and biotin treatment, ~90-95% confluent cells were washed 3 times with PBS and kept at -80°C. Thawed cell pellets were lysed in 1.5 ml of RIPA buffer supplemented with PMSF (P7626-1G, Sigma-Aldrich), 1 M DTT (15508013, Thermo Fisher) and protease inhibitor (P8340, Sigma-Aldrich) and transferred into 2 ml eppendorfs (72.695.500, Sarstedt). 1 µl of benzonase was added into each lysate. They were then sonicated for 30 sec at 30% amplitude with 10 sec bursts with 2 sec breaks in between, repeated 3 times. Following centrifugation for 30 min at maximum speed at 4°C, ~20-40 µl of supernatant were stored to monitor protein expression and biotinylation by immunoblotting. 70 µl of pre-washed streptavidin beads (17-5113-01, 5 ml, GE Healtcare) was incubated with each of the remaining lysate for 3 h on a rotator in cold room. Samples were then centrifuged for 1 min at 2000 RPM at 4°C. The supernatant was removed and beads were washed in RIPA buffer. Beads were washed in RIPA buffer 2 times more. Beads were then resuspended in 50 mM Ammonium Bicarbonate (ABC) (AB0032, 500G, Biobasic) and centrifuged for 1 min at 2000 RPM at 4°C. The washing step with ABC was

repeated 2 times more. Beads were then resuspended in 100 µl of 50 mM ABC and 1 µg of trypsin (T6567-5×20µg, Sigma-Aldrich) resuspended in 20 mM Tris-HCl, pH 8.0 was added into each sample prior to ~15-16 h of trypsin digestion at 37°C on a rotator. The following day, samples were trypsin-digested again for additionnal 2h. Following the second trypsin digestion, samples were centrifuged for 1 min at 2000 RPM at RT. Supernatants were transferred into new 1.5 ml eppendorfs, beads were washed 2 times with 100 µl of water (8801-7-40, 4L, Caledon), pooled with the collected supernatant and formic acid (94318-250ml, Sigma-Aldrich) was added into each solution for a final concentration of 5%. Samples were then centrifuged for 10 min at maximum speed at RT, supernatants were transferred into new 1.5 ml eppendorfs and drired in a SpeedVac for 3h at 30°C. Samples were resuspended in 15 µl of 5% formic acid and kept at -80°C. Samples originated from Flp-In T-REx HEK293 and Flp-In T-REx HeLa cell lines were injected into Orbitrap Velos (Thermo Fisher) and Orbitrap Q Exactive (Thermo Fisher) Mass Spectrometers, respectively. ProHits was used to analyze BioID-MS data[233]. RAW files were converted in .mzXML format by Proteowizard[234]. Peptide search was carried out by using Comet[235] and Mascot (Matrix Science) search engines by using the Human RefSeq Version 57 and processed through iProphet[236].

2.6. Protein network and interactome analysis

Protein network and interactome analyses were carried out by using Cytoscape, as described elsewhere, with few modifications[237, 238]. The SAINT file generated in ProHits was imported into Cytoscape. The protein-protein interaction data from IntAct was imported and merged with the BioID data[239]. MCL cluster was used to generate protein clusters or complexes[240]. Significance Analysis of INTeractome (SAINT) files were processed in ProHits-viz to perform dot plot analyses[241]. Only interactions with a Bayesian False Discovery Rate (BFDR)≤0.01 were taken into consideration and defined as high confidence. Functional annotation was carried out by using Gene Ontology (GO) terms. Protein networks illustrating the cellular components or biological processes were generated using SAFE[242].

2.7. Coimmunoprecipitation or GST pulldown

Interaction between SLK and active RhoA is validated by GST pulldown. Flp-In T-REx HeLa cells expressing Flag-SLK or Flag-SLKK^{63R} in a tetracycline-inducible manner were transfected with either GST, GST-RhoA^{G14V}, GST-Rac1^{G12V}, GST-Cdc42^{G12V} or with GST, GST-RhoA^{WT}, GST-RhoA^{G14V}. After two days of transfection, cells were treated with 1 µg/ml of tetracycline for 24 h. Cells were then lysed in CHAPS buffer (30 mM Tris-HCl pH 7.5, 150 mM NaCl, 5 mM $MgCl_2$ and 1% CHAPS) and subjected to GST pulldown using GST beads (L00206-10ml, GenScript). After 3h of GST pulldown, beads were

washed three times in CHAPS buffer. Proteins were denatured and subjecteded to SDS-PAGE. The precipitated proteins or expression levels were analyzed by immunoblotting with anti-Flag M2-HRP and mouse anti-GST antibodies.

Interaction between KIAA0355 and active Rac1 is validated by co-immunoprecipitation or GST pulldown. For validation by co-immunoprecipitation, Flp-In T-REx HEK293 cells expressing Flag-Rac1^{WT} or Flag-Rac1^{G12V} in a tetracycline-inducible manner were transfected with Myc-KIAA0355. After two days of transfection, cells were treated with 1 µg/ml of tetracycline for 24 h. Cells were then lysed in CHAPS buffer and subjected to co-immunoprepitation using Flag-M2 agarose beads (A2220, Sigma-Aldrich) for 3 h. After co-immunoprecipitation, beads were washed three times in CHAPS buffer, proteins were denatured and subjected to SDS-PAGE. The precipitated proteins and expression levels were analyzed by immunoblotting with mouse anti-Myc and anti-Flag M2-HRP. To validate endogenous KIAA0355 interaction with active Rac1, Flp-In T-REx Parental HeLa cell lines were co-transfected with Empty Vector, Flag-Rac1^{WT}, Flag-Rac1^{G12V} or Flag-Rac1^{G12V} together with Scrambled (siCtrl) or ON-target SmartPool KIAA0355 siRNA (siKIAA0355) and Flp-In T-REx HeLa KIAA0355$^{-/-}$ cell lines generated via CRISPR/Cas9 (#6, #7 and #9) were transfected with Flag-Rac1^{G12V}. After three days of transfection, cells were lysed in CHAPS buffer and subjected to co-immunoprecipitation using Flag-M2 agarose beads for 3 h. Following co-immunoprecipitation, beads were washed three times in CHAPS buffer, proteins were denaturated and subjected to SDS-PAGE. The precipitated proteins and expression levels were analyzed by immunoblotting with rabbit anti-KIAA0355 (custom made, GenScript, see Antibodies section), anti-Flag-M2-HRP or mouse anti-Tubulin antibodies. For validation by GST pulldown, GST or GST-

Rac1^{G12V} proteins expressed in bacteria were purified on Glutathione Resine (L00206, GenScript) as described elsewhere[229] and incubated for 3h with lysates of Flp-In T-REx HeLa cells expressing Flag-KIAA0355 or Flag-KIAA0355$^{\Delta 240\text{-}480}$. The precipitated proteins and expression levels were analyzed by immunoblotting with mouse anti-Tubulin and anti-Flag-M2-HRP or Coomassie.

Interaction between PLEKHG3 and active RhoG is validated by GST pulldown. HeLa cells were transfected with Flag-PLEKHG3 for 2 days, lysed in CHAPS buffer. GST, GST-RhoG^{WT} or GST-RhoG^{G12V} proteins expressed in bacteria were purified on glutathione-Sepharose beads were incubated with cell lysates for 3 h. The precipitated proteins and expression levels were analyzed by immunoblotting with mouse anti-Flag-M2-HRP or Coomassie.

2.8. Immunofluorescence and microscopy analysis

For IF analysis of BirA*-Flag tagged Rho GTPases, Flp-In T-REx HeLa cells expressing controls (Empty Vector, BirA*-Flag-EGFP or BirA*-Flag-EGFP-CAAX) or Rho GTPases, mostly in their constitutively active forms, were induced with tetracycline for 24 h on glass coverslips. Cells were gently washed with phosphate-buffered saline (PBS), fixed with 4% paraformaldehyde (PFA) in PBS for 15 min, washed 2 times with PBS, 0.1% Triton X-100 (PBST) for 10 min each for permeabilization and incubated in blocking solution PBST, 1% bovine serum albumin (PBST/BSA) for 1h at RT. Cells were then incubated with an anti-Flag M2 primary antibody (except BirA*-Flag-EGFP or BirA*-Flag-EGFP-CAAX) in PBST/BSA overnight in a humidity chamber in cold room. The following

day, cells were washed 3 times in PBS and incubated with a chicken anti-mouse Alexa Fluor 488 secondary antibody for 90 min at RT. Cells were washed 3 times in PBS and incubated with an Alexa Fluor 633 Phalloidin for 90 min at RT, washed 3 times in PBS and incubated with Hoechst in PBS. Cells were washed 3 times in PBS and the coverslips were mounted with Mowiol and sealed using nail polish. Images were taken on a Zeiss LSM710 confocal microscopy (Carl Zeiss) and analyzed using the Zen 2009 (Carl Zeiss) or ImageJ software.

For KIAA0355 colocalization with active Rac1, Flp-In T-REx HeLa cells expressing Empty Vector or Flag-KIAA0355 in a tetracycline-inducible manner were co-transfected with mOrange, mOrange-Rac1^{WT} or mOrangeRac1^{G12V} for 2 days. Cells were then plated on glass coverslips for 24 h in the presence of tetracycline. Similar IF procedure was performed as mentioned above, with modifications. Cells were incubated with a mouse anti-Flag M2 antibody. Images were taken on a DM6 fluorescence microscopy (Leica) and analyzed using the ImageJ software.

For RAC1-KIAA0355 IF experiments, Flp-In T-REx HeLa cells expressing Flag-Rac1^{G12V} in a tetracycline-inducible manner were co-transfected with siCTRL or siKIAA0355 for 2 days in 6-cm plates. Co-transfected Flag-Rac1^{G12V} and Flp-In T-REx HeLa cells expressing controls (Empty Vector, Flag-Rac1^{WT}), non-transfected (NT) Flag-Rac1^{G12V}, Flag-KIAA0355 or Flag-KIAA0355$^{\Delta 240\text{-}480}$ cells were plated on glass coverslips overnight in the presence of tetracycline. Similar IF procedure was performed as mentioned above.

For SLK colocalization experiments, Flp-In T-REx HeLa cells expressing Empty Vector, Flag-RhoA^{WT} or Flag-RhoA^{G14V} in a tetracycline-inducible manner were plated on

glass coverslips overnight in the presence of tetracycline. Similar IF procedure was performed as mentioned above, with modifications. The primary antibodies used are the following: rabbit anti-SLK or rabbit anti-pERM and anti-Flag M2. The secondary antibodies used are following: chicken anti-mouse Alexa Fluor 488 and goat anti-rabbit Alexa Fluor 568. The coverslips were mounted with SlowFade Gold Antifade reagent with DAPI. Images were taken on a DM6 fluorescence microscopy (Leica) and analyzed using the ImageJ software.

For ERM phosphorylation experiments, Flp-In T-REx HeLa cells expressing Flag-RhoA^{G14V} in a tetracycline-inducible manner were transfected with siCTRL or siSLK for 2 days in 6-cm plates. 1 µg/ml of tetracycline was added into medium to induce Flag-RhoA^{G14V} expression for 24h. The following day, tetracycline-induced and siCTRL or siSLK transfected cells and untreated controls (uninduced, untransfected) were plated on glass coverslips overnight. Similar IF procedure was carried out as above, with modifications. The primary antibodies used are the following: rabbit anti-pERM, mouse anti-Flag M2. The secondary antibodies used are following: chicken anti-mouse Alexa Fluor 488 and goat anti-rabbit Alexa Fluor 568. The coverslips were mounted with SlowFade Gold Antifade reagent with DAPI. Images were taken on a DM6 fluorescence microscopy (Leica) and analyzed using the ImageJ software.

2.9. In vitro kinase assays

In vitro kinase assays were carried out as previously described[243], with

modifications. Briefly, Lysates of Flp-In T-REx HeLa cells expressing the indicated constructs were subjected to co-immunoprepitation using Flag-M2 agarose beads (#A2220-1ml, Sigma-Aldrich) for 3 h. After co-immunoprecipitation, beads were washed 3 times in CHAPS buffer, 2 times in 2×Kinase Reaction Buffer (KRB) (50 mM Tris-HCl, pH7.5, 100 mM NaCl, 6 mM $MgCl_2$ and 1 mM $MnCl_2$), and resuspended in 15 µl of KRB buffer supplemented with 2 mM DTT, 50 µM ATP, 1 mM Na_2VO_4, 5 mM NaF, 2.5 mM sodium pyrophosphate and 100µl 10×PhosSTOP (04906845001, Roche) containing purified and eluted GST or GST- GST-Ezrin$^{479-585}$ from bacteria. The beads were incubated for 1h at 30°C. Proteins were denatured and subjected to SDS-PAGE. The phosphorylation and expression levels were analyzed by immunoblotting with the indicated antibodies or by coomassie.

2.10. Cell migration assays

Boyden migration assays were performed as previously described[243], with modifications. Tetracycline-treated Flp-In T-REx HeLa cells expressing Empty Vector, Flag-KIAA0355, Flag-KIAA0355$^{\Delta 240-480}$ or Flp-In T-REx HeLa KIAA0355$^{-/-}$ cells (KIAA0355 KO6, KO7 or KO9) generated via CRISPR/Cas9 were detached and harvest with the following solution: 1× Hank's balanced salt solution (HBSS), 25 mM HEPES pH 7.4, 5 mM EDTA and 0.01% Trypsin. Cell pellets were washed 2 times in Dulbecco's modified Eagle medium (DMEM) supplemented with 1% penicillin-streptomycin and 0.5% BSA by centrifugation for 5 min at 1000 RPM between each wash. Cell pellets were resuspended in 600 µl of DMEM supplemented with 1% PS. 75000 or 100000 cells were

plated in the upper chamber in triplicate for each condition in the presence of serum-starved DMEM. Cells were allowed to migrate through the Boyden Chamber (3422, Corning) containing DMEM with or without 10% fetal bovin serum (FBS) for 6h or 16 h. The lower side of Boyden Chambers is precoated or not, with fibronectin. Cells were fixed in 4% PFA for 15 min. Leftover cells in the upper chambers were cleaned using cotton swabs. Migrating cells were washed 3 times with PBS. The membrane was cut using a blade, placed on a microscopy slide and mounted using SlowFade Gold Antifade reagent with DAPI. Images were taken on a DM6 fluorescence microscopy (Leica).

Cell migration tracking experiments were carried out as previously described[244]. Briefly, the indicated cells were plated in 6 or 12-well plates and induced or not with Tetracycline 24 h prior imaging. Nuclei were stained using NucRed reagent (R37106, Thermo Fisher). Pictures were taken every 5 minutes for a course of 6h using a DM IRE2 microscope (Leica) with an automated stage (PECON) and images were acquired using an Orca-ER Model C-4742 digital camera (Hamamatsu). Migration speed was quantified using Volocity software (PerkinElmer Life and Analytical Sciences).

2.11. High-content imaging and microscopy analysis for siRNA screening of active RhoG

Flp-In T-REx HeLa cells expressing controls (Empty Vector, Flag-RhoG^{WT} or untransfected Flag-RhoG^{G12V}) or Flag-RhoG^{G12V} in a tetracycline-inducible manner were transfected with a set of siRNAs against BioID candidates for 2 days. Cells were plated on Cellbind surface 96-well plates (3340, Corning) overnight in the presence of

tetracycline. Similar IF procedure was performed as mentioned above, with modifications. The primary antibody used is an anti-Flag M2 antibody. The secondary antibody used is a chicken anti-mouse Alexa Fluor 488. Images were taken on a high-content microscopy (ImageXpress, Molecular Devices) and analyzed using MetaXpress (Molecular Devices) or ImageJ software. Membrane ruffles were quantified as described elsewhere[245], with modifications. ADAPT plug-in[246] for ImageJ was used for quantification. Briefly, membranes ruffles were identified by Phalloidin staining that colocalized with Flag-RhoG^{G12V} signal at the cell periphery. Flag or Phalloidin images in grayscale were opened in ADAPT. ImageJ's multi-point selector tool was used to select the cells in the Phalloidin image. The Phalloidin image was selected for the cytoplasmic channel and the Flag image was selected for the signal to be correlated. Auto Threshold and Generate Signal Distribution functions were both selected. The Huang method was used for thresholding. For the smoothing filter radius, a value between 1.0 and 2.0 was selected.

2.12. Statistics

Statistical analyses and quantification of all experiments were performed through the GraphPad Prism Software (GraphPad Software) by using Student *t* test or one-way ANOVA, followed by Bonferroni's multiple comparison test. P values < 0.05 were considered as significant for all analyses ($^{*}p < 0.05$; $^{**}p < 0.001$; $^{***}p < 0.0001$).

CHAPTER 3: DECIPHERING RHO GTPASE EFFECTORS AND RHO GTPASE/GEF-GAP INTERACTIONS BY BIOID-PROTEOMICS

3.1. A systematic BioID analysis to uncover new effectors and map Rho GTPase-GEF/GAP interactions

To better understand the signaling networks of Rho GTPases, uncover new effectors and map Rho GTPase-GEFs/GAPs interactions, we performed a systematic BioID analysis on 20 human Rho GTPases. To do this, we exploited a previously generated library of Gateway-system compatible pENTRY vectors encoding 84 human GTPases, including the 20 human Rho GTPase family of proteins, mostly in their constitutively active forms[229]. We recombined them into pDEST vectors to generate final expression vectors, in which BirA*-Flag is systemically fused to the N-terminal of 20 human Rho GTPases. To ensure the stable, efficient and rapid expression of BirA*-Flag tagged Rho GTPases, we generated human embryonic kidney (HEK) 293 or HeLa Flp-In T-REx cells. We then performed BioID on both cell lines to identify common or cell-specific interaction profiles.

We first verified by immunoblotting that BirA*-Flag-Rho GTPases are properly expressed in Flp-In T-REx HEK293 or Flp-In T-REx HeLa cells (**Figs. 14a and 14b**). Immunofluorescence staining of Flp-In T-REx HeLa cells stably expressing BirA*-Flag-Rho GTPases in a tetracycline-inducible manner displayed expected cytoskeletal effects (**Fig. 14c**). As expected, active forms of BirA*-Flag tagged Rac1, Rac2, Rac3 or RhoG induced membrane ruffling, BirA*-Flag-RhoA^{G14V} stimulated the formation of stress fibers, whereas BirA*-Flag-Cdc42^{G12V} led to the formation of filopodia. Moreover, expression of

other BirA*-Flag tagged Rho GTPases showed distinct morphological changes such as dorsal ruffles (BirA*-Flag-RhoBTB1), large clusters of filopodia (BirA*-Flag-RhoJ^{G40V}), round cells (BirA*-Flag-Rnd1^{WT}) (**Fig. 14c**). These results showed that BirA*-Flag tagged Rho GTPases are properly expressed and stimulate their associated characteristic morphological changes.

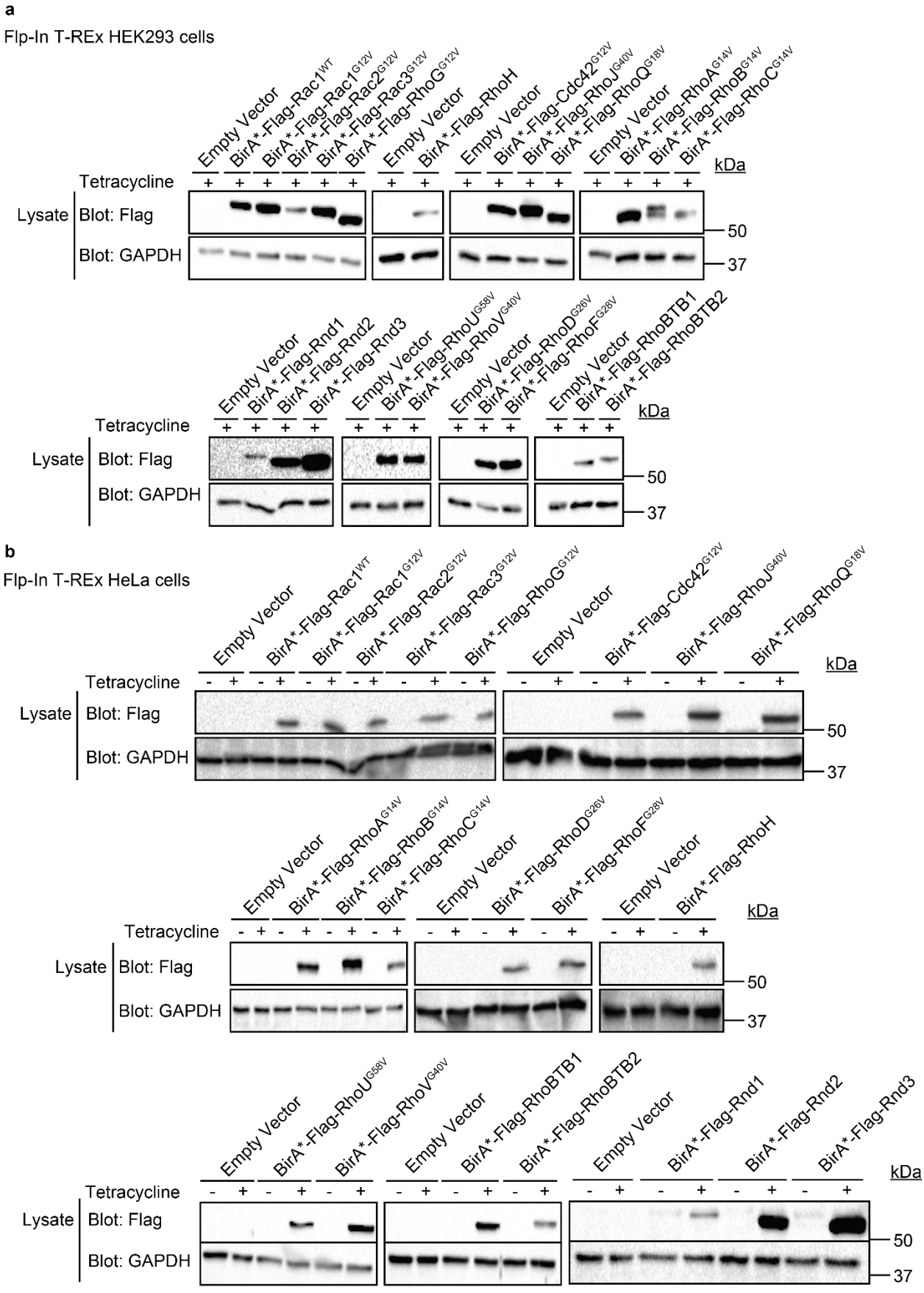
a
Flp-In T-REx HEK293 cells
Empty Vector
BirA*-Flag-Rac1WT
BirA*-Flag-Rac1G12V
BirA*-Flag-Rac2G12V
BirA*-Flag-Rac3G12V
BirA*-Flag-RhoGG12V
BirA*-Flag-RhoH
BirA*-Flag-Cdc42G12V
BirA*-Flag-RhoJG40V
BirA*-Flag-RhoQG18V
BirA*-Flag-RhoAG14V
BirA*-Flag-RhoBG14V
BirA*-Flag-RhoCG14V
kDa
Tetracycline
Lysate
Blot: Flag
Blot: GAPDH
50
37
Empty Vector
BirA*-Flag-Rnd1
BirA*-Flag-Rnd2
BirA*-Flag-Rnd3
BirA*-Flag-RhoUG58V
BirA*-Flag-RhoVG40V
BirA*-Flag-RhoDG26V
BirA*-Flag-RhoFG28V
BirA*-Flag-RhoBTB1
BirA*-Flag-RhoBTB2
kDa
Tetracycline
Lysate
Blot: Flag
Blot: GAPDH
50
37
b
Flp-In T-REx HeLa cells
Empty Vector
BirA*-Flag-Rac1WT
BirA*-Flag-Rac1G12V
BirA*-Flag-Rac2G12V
BirA*-Flag-Rac3G12V
BirA*-Flag-RhoGG12V
Empty Vector
BirA*-Flag-Cdc42G12V
BirA*-Flag-RhoJG40V
BirA*-Flag-RhoQG18V
kDa
Tetracycline
Lysate
Blot: Flag
Blot: GAPDH
50
37
Empty Vector
BirA*-Flag-RhoAG14V
BirA*-Flag-RhoBG14V
BirA*-Flag-RhoCG14V
Empty Vector
BirA*-Flag-RhoDG26V
BirA*-Flag-RhoFG28V
Empty Vector
BirA*-Flag-RhoH
kDa
Tetracycline
Lysate
Blot: Flag
Blot: GAPDH
50
37
Empty Vector
BirA*-Flag-RhoUG58V
BirA*-Flag-RhoVG40V
Empty Vector
BirA*-Flag-RhoBTB1
BirA*-Flag-RhoBTB2
Empty Vector
BirA*-Flag-Rnd1
BirA*-Flag-Rnd2
BirA*-Flag-Rnd3
kDa
Tetracycline
Lysate
Blot: Flag
Blot: GAPDH
50
37

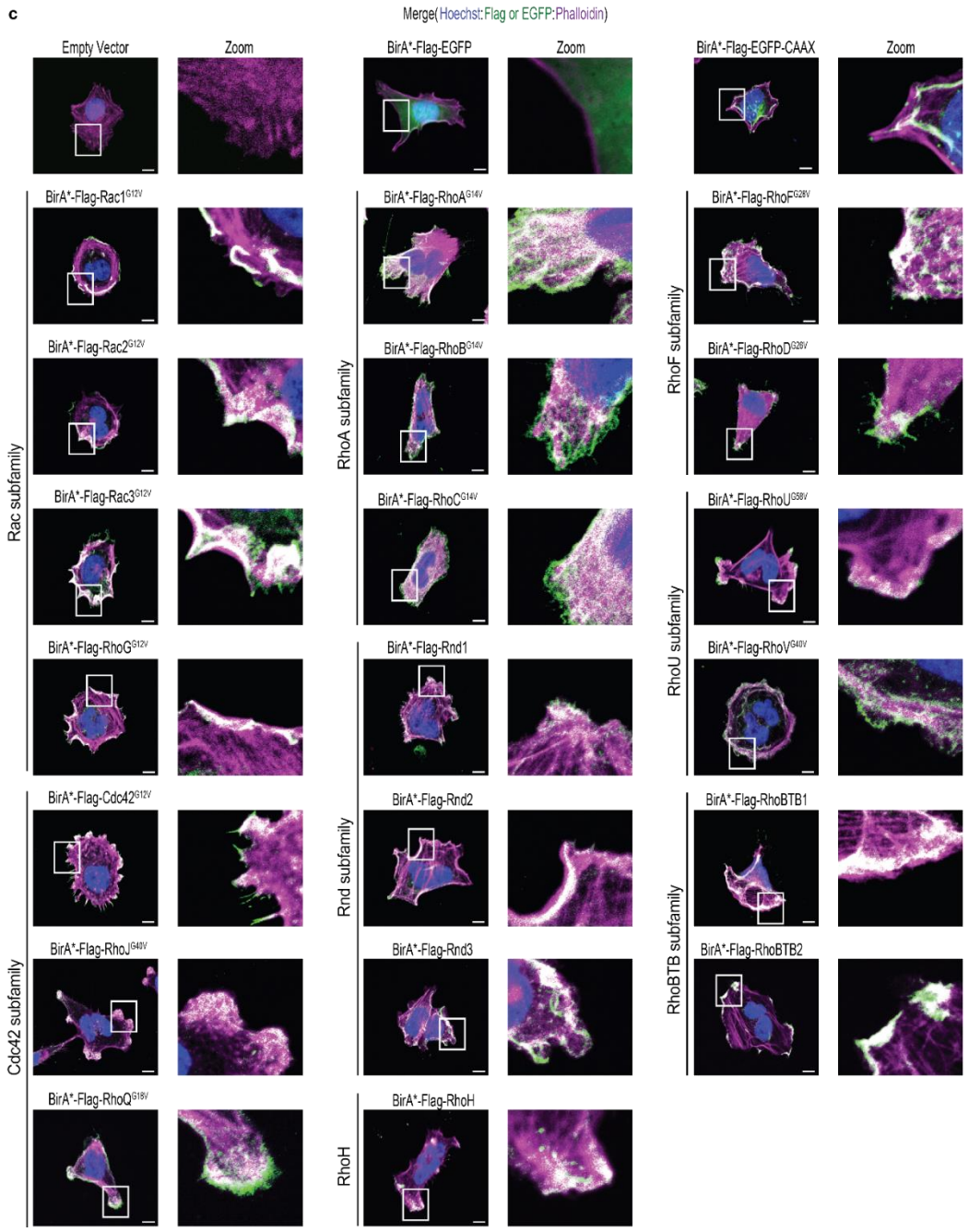

Fig. 14 | a, Immunoblotting of lysates from Flp-In T-REx HEK293 cells expressing the indicated constructs. **b**, Immunoblotting of lysates from Flp-In T-REx HeLa cells expressing the indicated constructs. **c**. Representative IF images of BirA*-Flag-tagged Rho GTPases**.** Empty Vector or BirA*-Flag-tagged constructs from Flp-In T-REx HeLa cells are expressed upon tetracycline induction, fixed and stained for Hoechst (blue), Flag or EGFP (green), Phalloidin (magenta) and analyzed with confocal microscopy (LSM710, Zeiss) (scale bar: 10 µm).

Following 24 hours of tetracycline induction and biotin treatment, we performed BioID in biological duplicates on Flp-In T-REx HEK293 or Flp-In T-REx HeLa cells (**Fig. 15**). We also performed BioID on experimental controls that express Empty Vector (EV), BirA*-Flag-EGFP or BirA*-Flag-EGFP fused to a CAAX motif to filter contaminants. In addition to these experimental controls, we used BirA*-Flag-Rac1^{WT}, BirA*-Flag-Cdc42^{WT}, BirA*-Flag-RhoA^{WT} or BirA*-Flag-RhoG^{WT} that express wild-type forms of the three most-studied Rho GTPases and that of RhoG to filter unspecific interactors, other than effectors or regulatory proteins. The nucleotide-free forms of BirA*-Flag tagged Rac1, Cdc42, RhoA or RhoG were also used to further identify GEF interactions.

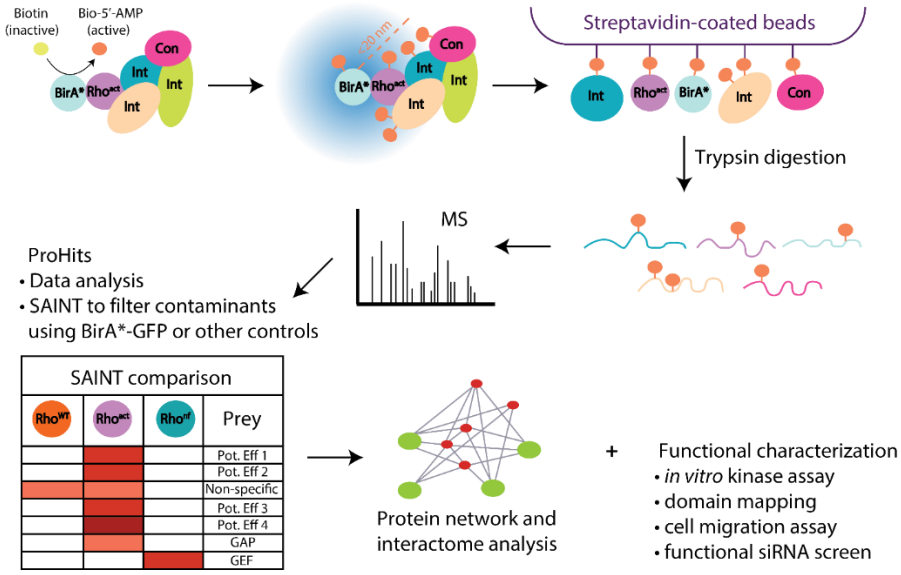

Fig. 15 | Schematic illustration of the experimental pipeline and expected outcome of Rho GTPase BioID screens. We performed BioID on 20 human Rho GTPases (mostly in constitutively active form) to gain insight into their protein networks, uncover new effectors and map Rho GTPase-GEF/GAP interactions. We conducted SAINT analyses to filter contaminants by using experimental controls. Our BioID screens mostly identified potential effector (Pot. Eff) or GAP interactions with constitutively active Rho GTPases (Rho^{act}) or GEF interactions with nucleotide-free Rho GTPases (Rho^{nf}). Protein network and interactome analysis carried out for each bait. Those analyses were supported by different functional assays.

3.2. BioID recovers known Rho GTPase effector complexes and biologically-relevant GO term profiles

We identified 10244 interactions with high confidence in our BioID screens that we carried out in Flp-In T-REx HEK293 cells and 14281 interactions in Flp-In T-REx HeLa cells. 4900 overlapping interactions were detected in both cell lines (**Fig. 16**). We first aimed to ask if our BioID proximity screen captured well-known Rho GTPase effectors reported in the literature. The members of the WAVE and GIT/PIX/PAK complexes were among those were identified in $Rac1^{G12V}$ BioID with high confidence score, recovering major protein complexes that are involved in the formation of lamellipodia and focal adhesion. Also, we identified the members of the WASP complex in $Cdc42^{G12V}$ that are essential for filopodia stimulation. Moreover, we recovered Diaph1, Diaph2, Diaph3, Rock1, Rock2 interactions that are known to be involved in RhoA-mediated stress fiber dynamics.

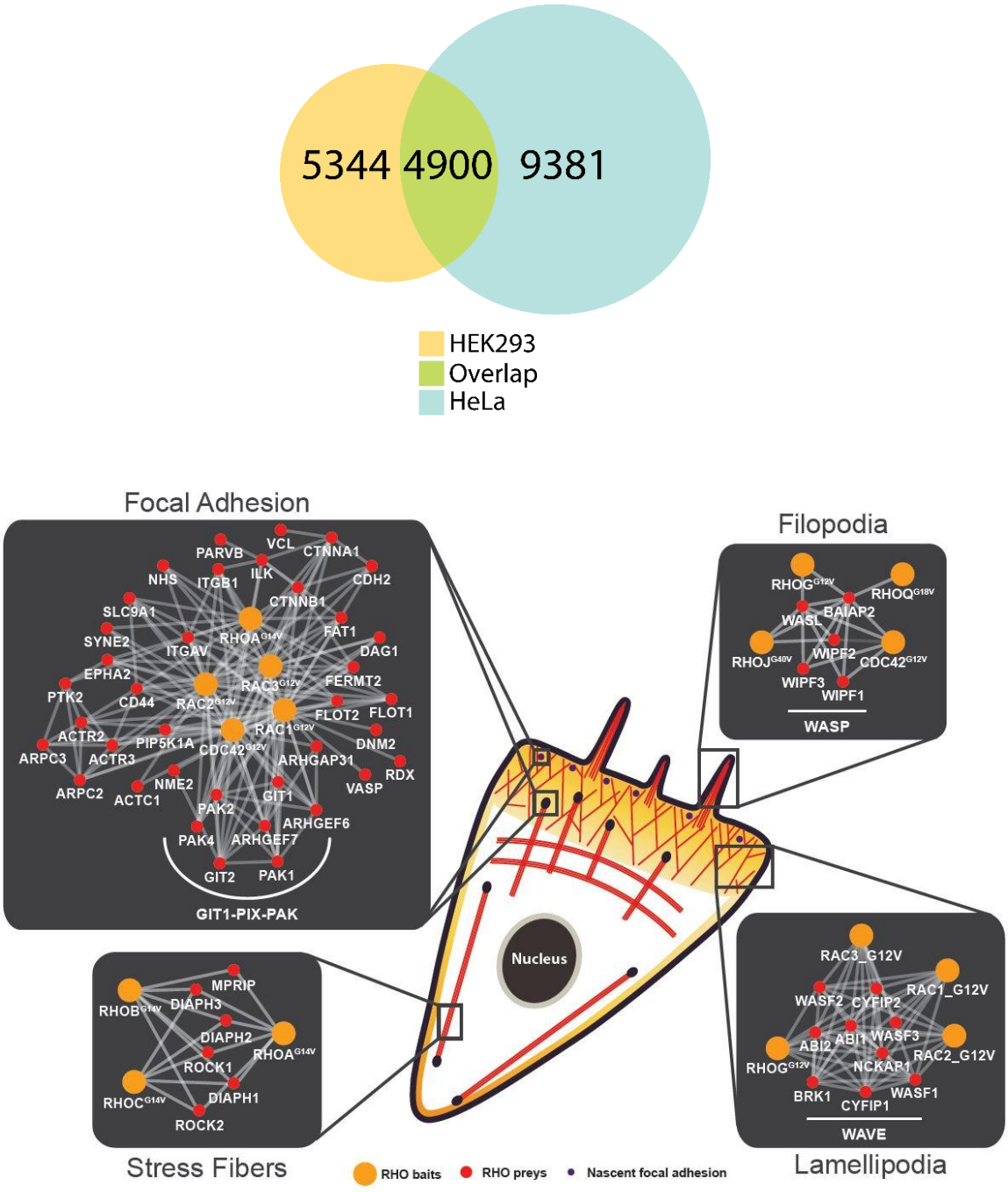

Fig. 16 | BioID recovers major Rho GTPase effector complexes that regulate lamellipodia, focal adhesion, filopodia and stress fiber formation downstream of active Rac1, Cdc42 and RhoA subfamilies.

To gain insight into localization and biological events of Rho GTPase networks, we investigated the significantly enriched cellular components and biological processes of GO terms identified in BioID screens of classical Rho GTPases (**Fig. 17**). The Rac subfamily BioID enriched cellular components which mostly localized to the lamellipodium & WAVE/SCAR complex, actin filament and focal adhesion as expected. It also enriched subcellular structures such as the mitochondrial inner chain complex and endosomal membrane. Moreover, the Rac subfamily BioID enriched proteins that are involved in a variety of known biological processes such the regulation of GTPase signal transduction, growth factor receptor signaling pathway, muscle contraction & muscle filament sliding, PI3K signaling pathway and others. These data are consistent with previous reports on Rac proteins. Rac1 is known to stimulate PI3K activation[86]. Rac2 has been shown to be essential for the maintenance of mitochondrial integrity[247]. We also recovered preys with biological processes, such as mRNA decay, that are not associated with Rac proteins. The role of Rac proteins in mRNA decay has not been well characterized.

The RhoA subfamily BioID recapitulated cellular components that are found in the heterotrimeric G-protein complex, endosome, the mitochondrial inner chain complex and others, whereas the Cdc42 subfamily BioID recovered cellular components that localized to the lamellipodium & focal adhesion & actin cytoskeleton, cell-cell junction & catenin complex and others (**Fig. 17**). The RhoD/RhoF subfamily BioID enriched proteins that localized to cellular components such as Actin & Arp2/3 complex, lamellipodium, cell-cell junction & Zonula Adherens and others. The RhoA subfamily BioID recovered proteins that are involved in the regulation of GTPase signal transduction, but also in the nucleus export disassembly & cellular regulation, vesicle fusion & regulation of protein to

membrane and others. Similarly, the Cdc42 subfamily BioID identified proteins that are involved in the regulation of GTPase signal transduction as well as membrane organization, phosphatidylinositol receptor signaling pathway and others. The RhoD/RhoG subfamily BioID enriched proteins that are implicated in the regulation of GTPase signal transduction, PI3K receptor signaling pathway, membrane organization and others. While we identified known biological processes such as the regulation of GTPase signal transduction and membrane organization, we also enriched unknown biological processes for these Rho GTPases. For example, it is unknown whether RhoD or RhoF play a role in mitochondrial electron transport from NADH to ubiquinone. Our findings might pave the way for revealing unknown roles of Rho GTPases in mitochondrial electron transport or other mechanisms.

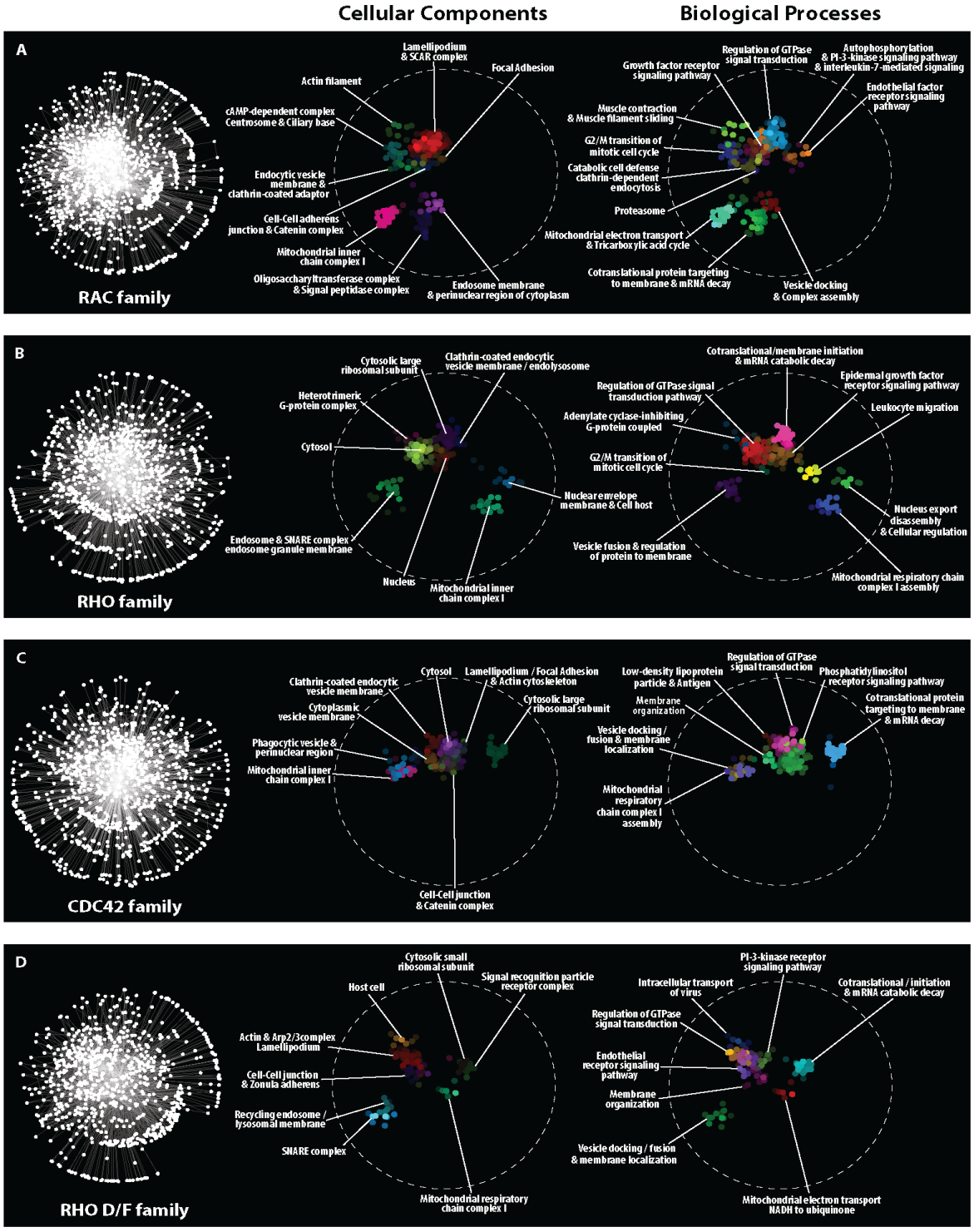

Fig. 17 | Significantly enriched cellular components and biological processes of GO terms identified in BioID screens of classical Rho GTPases.

Next, we analyzed GO cellular components and biological processes enrichment profiles of atypical Rho GTPases identified in our BioID screens (**Fig. 18**). We revealed that the RhoBTB subfamily BioID recovered cellular components that localized to the COP9 Signalosome. We identified protein complexes in the RhoBTB subfamily BioID that are involved in the nucleotide-excision repair damage or nuclear-transcribed mRNA catabolic nonsense-mediated decay. These data are consistent with a previous report of Manjarrez et al. which showed that RhoBTB2 forms a complex with Cullin3 and COP9 signalosome subunit 2 (COPS2)[141]. Moreover, we recovered preys with unknown biological processes for RhoBTB proteins. It is not known whether RhoBTB1 or RhoBTB2 are involved in nuclear-excision repair damage, which is one of the DNA repair systems.

The RhoH subfamily BioID cellular components were mostly enriched in the oligosaccharyltransferase complex & particle receptor recognition as well as phagocytic vesicle & SNARE complex. The RhoH subfamily recovered preys that are implicated in the regulation of Notch signaling pathway, vesicle fusion or phosphatidylinositol receptor signaling pathway. It has been shown that RhoH is essential for proper T-cell receptor (TCR) activation[248]. TCR complex/CD28 signaling modules can activate Notch signaling for T cell proliferation and activation[249]. It is possible that RhoH contributes to activation of Notch signaling via the TCR complex.

The Rnd subfamily BioID recapitulated protein interactions that are mostly found in the cytosolic particle receptor complex. We recovered Rnd preys that are involved in mRNA catabolic decay, the Notch signaling pathway or phosphatidlyinositol signaling

pathway. This is consistent with a previous study which showed that Rnd3-controlled lung cancer cell proliferation is regulated via Notch signaling[250]. The RhoU/V subfamily BioID enriched proteins that localized to the cytosolic small ribosomal subunit and cell-cell junction. We recovered RhoU/V preys with biological processes such as the regulation of small GTPase mediated signal, PI3K receptor signaling pathway and others. The role of Rnd proteins and RhoU/V subfamily on mRNA decay has not been elucidated.

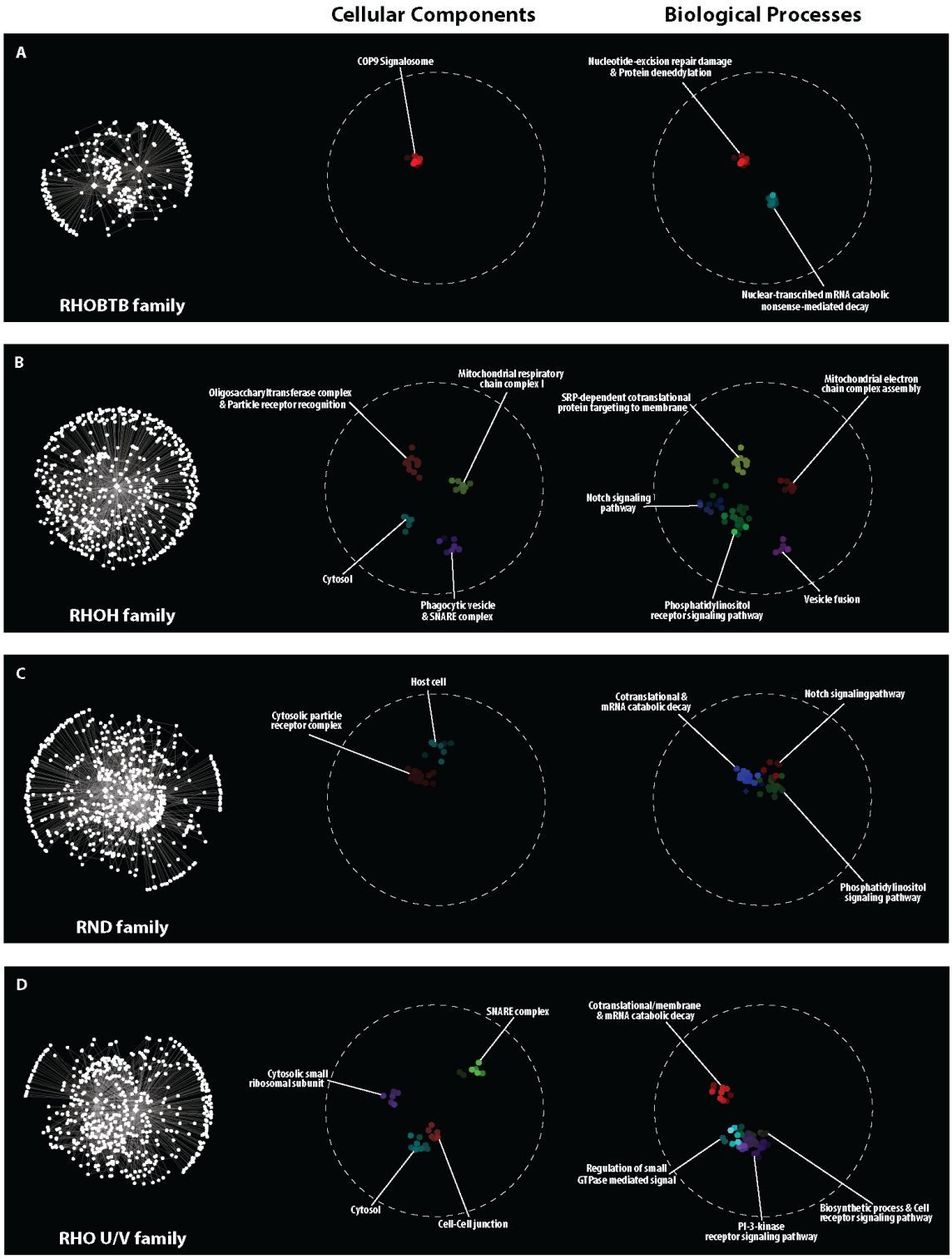

Fig. 18 | Significantly enriched cellular components and biological processes of GO terms identified in BioID screens of atypical Rho GTPases.

3.3. BioID reveals Rho GTPase-GEF/GAP interactions and specificity

We next aimed to define GEF and GAP specificity toward Rho GTPases by BioID. We performed BioID on nucleotide-free Rho GTPases to map GEF interactions. In addition, Rho GTPases in their constitutively active forms have been used to reveal GAP interactions.

Dock GEFs show specificity toward Rac1 and Cdc42, but not for RhoA[27]. Dock1, Dock2, Dock5, Dock3 and Dock4 activate Rac1 while Dock9, Dock10 and Dock11 achieve activation of Cdc42. Dock6, Dock7 and Dock8 can activate both Rac1 and Cdc42[27]. However, some of these reports are conflicting. Watabe-Ushida et al. showed that Dock7 binds to nucleotide-free Rac1, Rac3 but not Cdc42 and RhoA[251]. In contrast, Zhou et al. showed that Dock7 activates both Rac1 and Cdc42[252].

Consistent with the literature evidence, we found that the nucleotide-free Rac1, $Rac1^{G15A}$, significantly enriched Dock1, Dock4, Dock5, Dock6, Dock7 interactions in HEK293 or HeLa cells (**Fig. 19a and 19b**) compared to the wild-type Rac1 ($Rac1^{WT}$). Dock4 interaction was significantly enriched when we used the constitutively active form of Rac1 ($Rac1^{G12V}$) as a bait. It is known that GEFs catalyze the release of the nucleotide from small GTPases by affecting the nucleotide-binding site[253]. Thus, GEFs compete with the nucleotide for GTPase binding, favoring nucleotide exchanges[253]. However, the GEF

catalytic activity is completely reversible. It has been suggested that once GTPases are fully activated by GEFs and reach a theoretical maximum proportion, GEFs can be inhibitory by an increase in the intermediate GEF-GTPase protein complexes[254]. Therefore, GEFs can bind to GTP-loaded GTPases to catalyze the reverse nucleotide exchange, from GTP to GDP[254]. Consistent with this reversible GEF catalytic activity model, we identified GEF interactions with $Rac1^{G12V}$ such Dock4, ArhGEF7, Plekhg1, Plekhg2, Plekhg3, Plekhg4, Plekhg7, ArhGEF40 or Fgd6 in HEK293 or HeLa cells (**Figs. 19a and 19b**). Some of these GEFs, such as Dock4, ArhGEF7/β-Pix/Cool1, Plekhg1, Plekhg2/Slg, Plekhg3, Plekhg4, ArhGEF40/Solo, are already known to act as Rac1 GEFs[255-261]. Whether Plekhg7 or Fgd6, a known Cdc42 GEF, function as Rac1 GEFs has not been shown.

Next, we examined $Cdc42^{G15A}$-GEF interactions. We identified known DockGEFs for Cdc42 such as Dock6, Dock7, Dock9, Dock11 in both HEK293 and HeLa cells. Dock8 interaction was recovered in HEK293 cells, while Dock10 interaction was identified in HeLa cells. It is possible that these two Dock GEFs have different expression levels in those cell lines. We also recovered known Dbl GEFs for Cdc42, which includes DNMBP/Tuba, ArhGEF7, Vav2, Plekhg2, Plekhg3, Plekhg4, Mcf2l/ArhGEF14/Dbs/Ost, ArgGEF16, Fgd6[259-267]. ArhGEF26 displays a very weak GEF activity toward Cdc42[268]. Plekhg1 has been shown to target Cdc42 in a cyclic stretch assay, but whether it exhibits GEF activity toward Cdc42 has not been shown[257]. Moreover, whether ArhGEF40 or ArhGEF12 display GEF activity toward Cdc42 has not been shown.

As expected, we did not recover Dock GEF interactions when we performed BioID on $RhoA^{G17A}$. We identified many known Dbl GEFs for RhoA. Those include Obscn, Trio,

Ngef/Ephexin, ArhGEF5/Tim, ArhGEF12/Larg, ArhGEF11/Pdz-RhoGEF, ArhGEF1/p115-RhoGEF/Lsc, ArhGEF2/Gef-h1, ArhGEF12/Larg, ArhGEF17/p164-RhoGEF, ArhGEF18/p114-RhoGEF, Vav2, Akap13/akap-lbc, Ect2/ArhGEF31[264, 269-281]. It has not been tested if Plekhg3, a GEF for Rac1 and Cdc42, exhibits GEF activity toward RhoA or not.

Taken together, our BioID data on Rho GTPase-GEF interactions successfully recovered known GEFs with their target GTPases. In addition, we identified unknown Rho GTPase-GEF interactions, that might play a major role in the activation of distinct Rho GTPase-effector complexes.

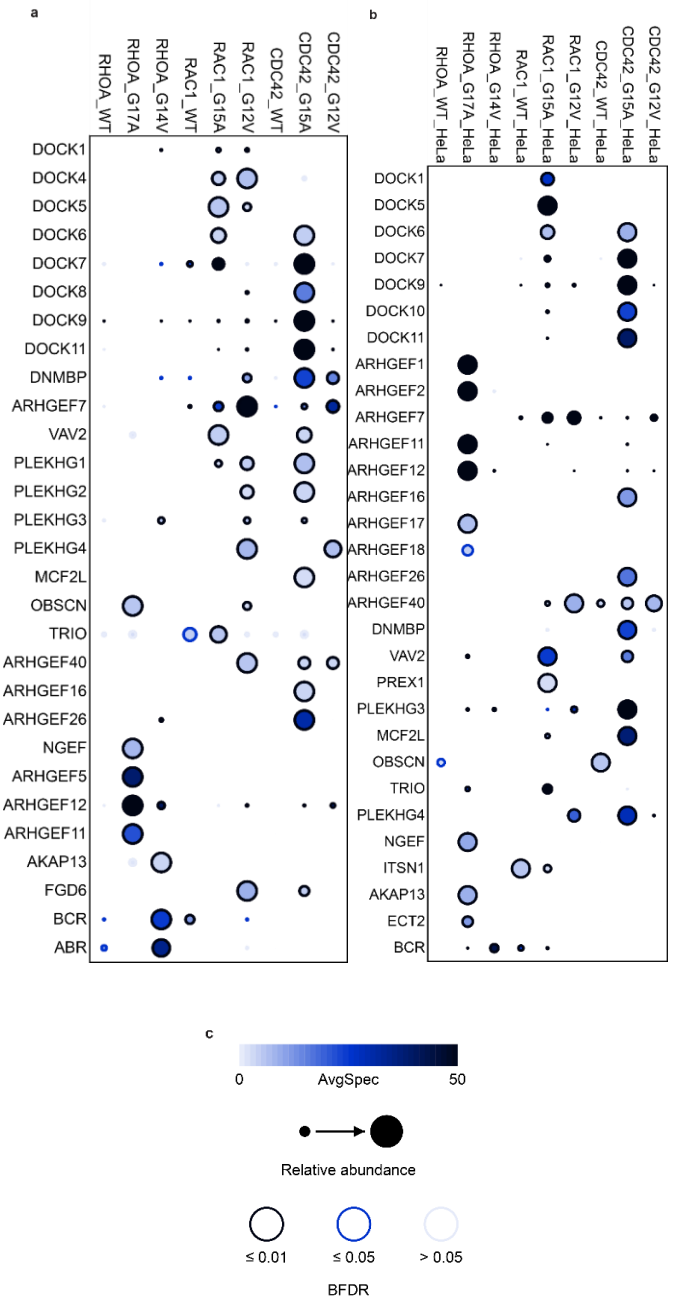

Fig. 19 | a, RhoA/Rac1/Cdc42-GEF interactions in Flp-In T-REx HEK293 cells. **b**, RhoA/Rac1/Cdc42-GEF interactions in Flp-In T-REx HeLa cells. **c**, The average spectral counts are shown in node color. The confidence score of the interaction (BFDR) is shown as edge color (BFDR ≤ 1% as high, 1% < BFDR ≤ 5% as medium or 5% < BFDR as low confidence). Circle size represents the relative abundance of prey over baits.

We next investigated the Rho GTPase-GAP interactions (**Fig. 20**). Both ArhGAP32/Grit has been known to act as a GAP for Rac1, Cdc42 and RhoA[282]. Consistent with the literature, we identified ArhGAP32 interaction in active forms of Rac1, Cdc42 and RhoA in HEK293 cells. We recovered ArhGAP39/CrGAP/Vilse in $Cdc42^{G12V}$ but also in $Rac1^{G12V}$. ArhGAP39 functions as a GAP for Cdc42, but whether it shows GAP activity toward Rac1 has not been shown[283]. We identified a highly enriched interaction between the RhoA GAP ArhGAP1/p50-RhoGAP and $RhoA^{G14V}$ in both HEK293 and HeLa cells. A previous report has identified Ophn1 as a GAP for Rac1, Cdc42 and RhoA[284]. Here, we recovered Ophn1 interaction only in $Cdc42^{G12V}$ and not in $Rac1^{G12V}$ or $RhoA^{G14V}$ in both HEK293 and HeLa cells. It is possible that Ophn1 might favor Cdc42 inactivation in those cells rather than Rac1 or RhoA. ArhGAP17/Rich-1 is known to be a RhoGAP for both Cdc42 and Rac1, but not for RhoA[285]. We successfully identified the ArhGAP17 interaction in $Cdc42^{G12V}$ in both HEK293 and HeLa cells and less slightly in $Rac1^{G12V}$ in HEK293 cells. However, we did not recover ArhGAP17 in $RhoA^{G14V}$ in both HEK293 and HeLa, which is consistent with the literature. ArhGAP42/Graf3 has been shown to inhibit RhoA activity in vascular smooth muscle cells to maintain proper blood pressure homoestasis[286]. Interestingly, we did not identify an interaction between ArhGAP42 and RhoA in HEK293 or HeLa cells, while we recovered ArhGAP42 in $Rac1^{G12V}$ in both cell lines. ArhGAP42 is specifically expressed in smooth muscle cells in humans and mice[286]. It is not tested whether ArhGAP42 exhibits GAP activity toward Rac1. It is therefore possible that ArhGAP42 activity is regulated differently in both HEK293 or HeLa cells by

engaging specific inactivation of Rac1.

Collectively, our results recovered many known Rho GTPase-GEF/GAP interactions as well as novel interactions in HEK293 or HeLa cells. Most GEFs such as Prex-1, Prex-2, ArhGEF2/Gef-h1, Dock1 act as tumor promoters while many GAPs such as ArhGAP7/Dlc1 function, like as tumor suppressor[61, 287-292]. However, some GAPs such as CdGAP can function to downregulate cancer metastasis[293]. Here, we identified novel Rho GTPase-GEF/GAP interactions that can be further validated and their roles on various biological processes can be investigated.

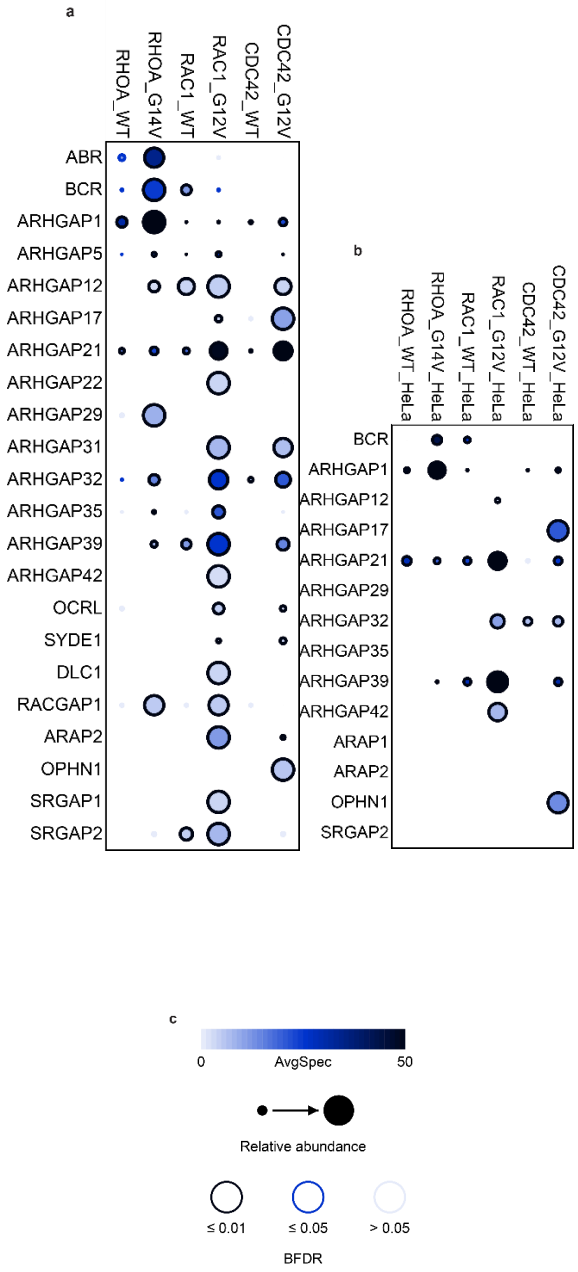

Fig. 20 | a, RhoA/Rac1/Cdc42-GAP interactions in Flp-In T-REx HEK293 cells. **b**, RhoA/Rac1/Cdc42-GAP interactions in Flp-In T-REx HeLa cells. **c**, The average spectral counts are shown in node color. The confidence score of the interaction (BFDR) is shown as edge color (BFDR ≤ 1% as high, 1% < BFDR ≤ 5% as medium or 5% < BFDR as low confidence). Circle size represents the relative abundance of prey over baits.

3.4. Identification of SLK as a novel RhoA effector

We first mined the BioID datasets to uncover novel candidate effector(s) of the classical RhoA GTPase which revealed the serine/theronine kinase SLK. SLK is a member of the SLK subfamily which also includes Serine/threonine kinase 10 (STK10, also known as LOK). The SLK subfamily belongs to the STE20 family of kinases which is part of the STE (homologs of yeast Sterile 7, Sterile 11, Sterile 20 kinases) group of serine/threonine protein kinases[294, 295]. It has been shown that SLK regulates a variety of processes such as apoptosis, cell cycle progression, cell adhesion and migration[294]. Studies have shown that SLK phosphorylate Ezrin/Radixin/Moesin (ERM) proteins, which are membrane-actin cytoskeleton linkers, to regulate spindle orientation, microvilli formation or epithelial integrity during tissue growth and other processes[296-299]. It is unknown whether SLK functions downstream of RhoA as an effector.

We first performed a dotplot analysis to visualize the SLK interaction in our BioID screen. Dotplot gives quantitative information about different parameters such as spectral counts, abundance of preys over baits or confidence scores[300]. The dotplot analysis showed that SLK significantly interacts, with high spectral counts, with only active forms of RhoA, RhoB and RhoC, but fails to interact with the wild-type form of RhoA ($RhoA^{WT}$) or other members of the Rho GTPase family (**Fig. 21a**). We also identified SLK-RhoA/RhoB/RhoC interaction in HeLa cells (data not shown), suggesting that SLK interaction with members of the RhoA subfamily is not specific to a single cell type. To

validate SLK-RhoA^{G14V} interaction, we performed GST-pulldown assays. In cells coexpressing Flag-SLK or the kinase-dead mutant of SLK (Flag-SLK^{K63R}) with either GST-RhoA^{G14V}, GST-Rac1^{G12V} or GST-Cdc42^{G12V}, both Flag-SLK or Flag-SLK^{K63R} interacted with only GST-RhoA^{G14V} (**Fig. 21b**), confirming the specificity of SLK for RhoA. In addition, we found that Flag-SLK binds to GST-RhoA^{G14V} and not to GST-RhoA^{WT}, validating our BioID screen (**Fig. 21c**). Taken together, these data suggest that SLK is a candidate novel RhoA effector.

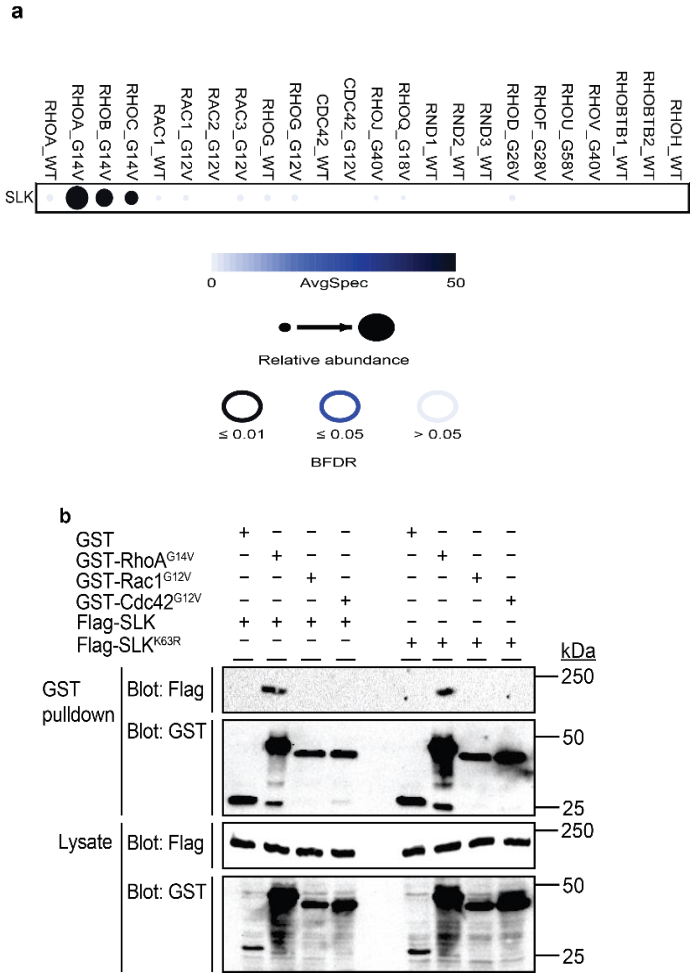

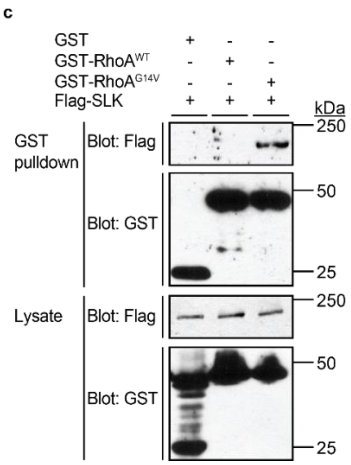

Fig. 21 | a, Dotplot showing BioID interactions between SLK and Rho GTPases in Flp-In T-REx HEK293 cells. The average spectral counts are shown in node color. The confidence score of the interaction (BFDR) is shown as edge color (BFDR ≤ 1% as high, 1% < BFDR ≤ 5% as medium or 5% < BFDR as low confidence). Circle size represents the relative abundance of prey over baits. **b**, Validation of SLK-RhoA^{G14V} interaction by GST pulldown. Flp-In T-REx HeLa cells expressing Flag-SLK or Flag-SLK^{K63R} in a tetracycline-inducible manner were transfected with either GST, GST-RhoA^{G14V}, GST-Rac1^{G12V} or GST-Cdc42^{G12V}. Lysates were incubated with glutathione sepharose beads. The precipitated proteins and expression levels were detected by immunoblotting with anti-Flag and anti-GST antibodies. **c**, SLK interacts with active RhoA but not with wild-type (WT) RhoA. Flp-In T-REx HeLa cells expressing Flag-SLK in a tetracycline-inducible manner were transfected with either GST, GST-RhoA^{WT}, GST-RhoA^{G14V}. Lysates were incubated with glutathione sepharose beads. The precipitated proteins and expression levels were detected by immunoblotting with anti-Flag and anti-GST antibodies.

3.5. SLK regulates ERM phosphorylation downstream of active RhoA

A previous 1999 study showed that active RhoA promotes ERM proteins phosphorylation through PI4P5K/ PIP_2 activation and other signaling pathways[301]. While

it is now established that ERM open conformation is stabilized via threonine phosphorylation (on residue T567), the identity of the kinase(s) promoting this phosphorylation downsteam of RhoA is a longstanding question[301, 302]. SLK family of kinases have been demonstrated to phosphorylate ERM for the regulation of cell shape and motility, microvilli formation, epithelial tissue integrity, cortical contractility and microtubule organization, spindle orientation or morphogenesis during mitosis[296-298, 303-305]. We here raised the question whether SLK is the missing kinase that regulates ERM phosphorylation downstream of active RhoA.

Consistent with previous reports, we found that active RhoA phosphorylates ERM[301, 306]. Our immunoblot data showed that expression of Flag-RhoA^{G14V}, but not Flag-RhoA^{WT}, induces endogenous ERMs phosphorylation in Flp-In T-REx HeLa cells (**Fig. 22a**). Immunofluorescence staining supported this observation (**Figs. 22b and 22c**). Furthermore, endogenous SLK showed higher colocalization with Flag-RhoA^{G14V} than Flag-RhoA^{WT} as shown by immunofluorescence staining (**Figs. 22d and 22e)**. Taken together, these results demonstrate that active RhoA promotes the phosphorylation of ERM proteins.

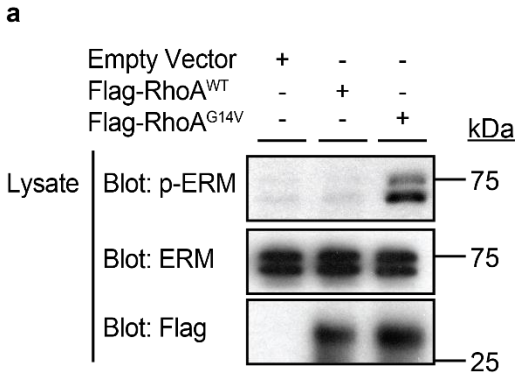

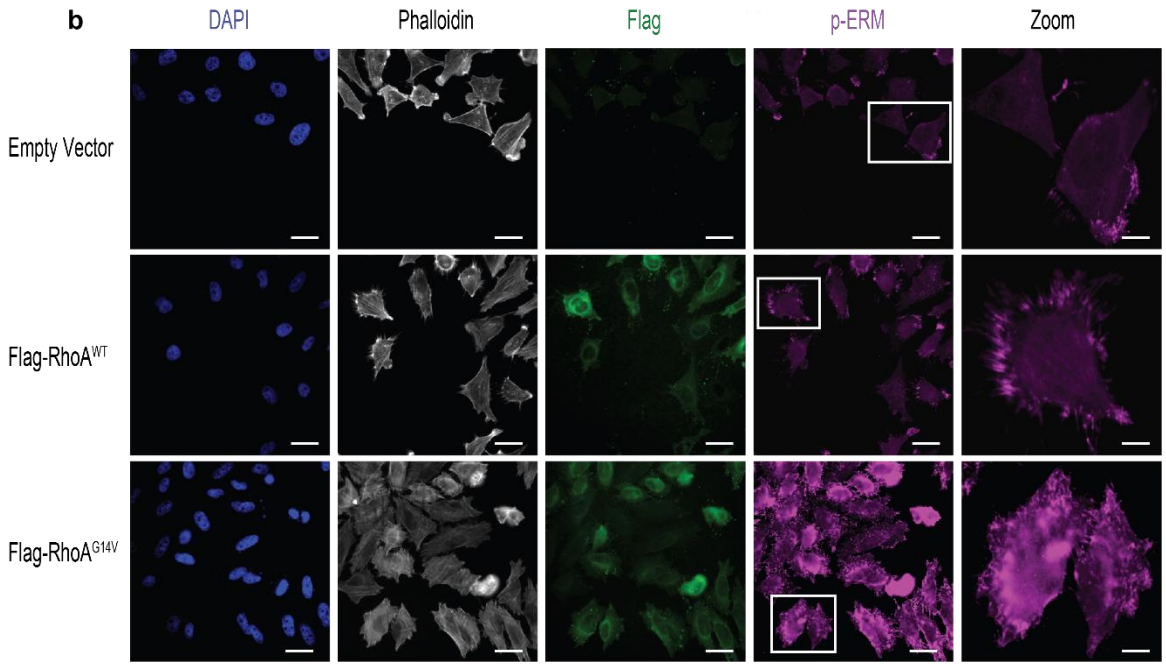
b
DAPI
Phalloidin
Flag
p-ERM
Zoom
Empty Vector
Flag-RhoA^WT
Flag-RhoA^G14V

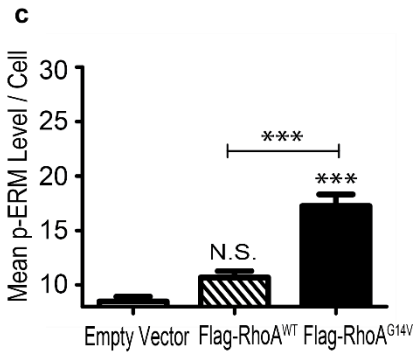
c
Mean p-ERM Level / Cell
30
25
20
15
10
***
***
N.S.
Empty Vector
Flag-RhoA^WT
Flag-RhoA^G14V

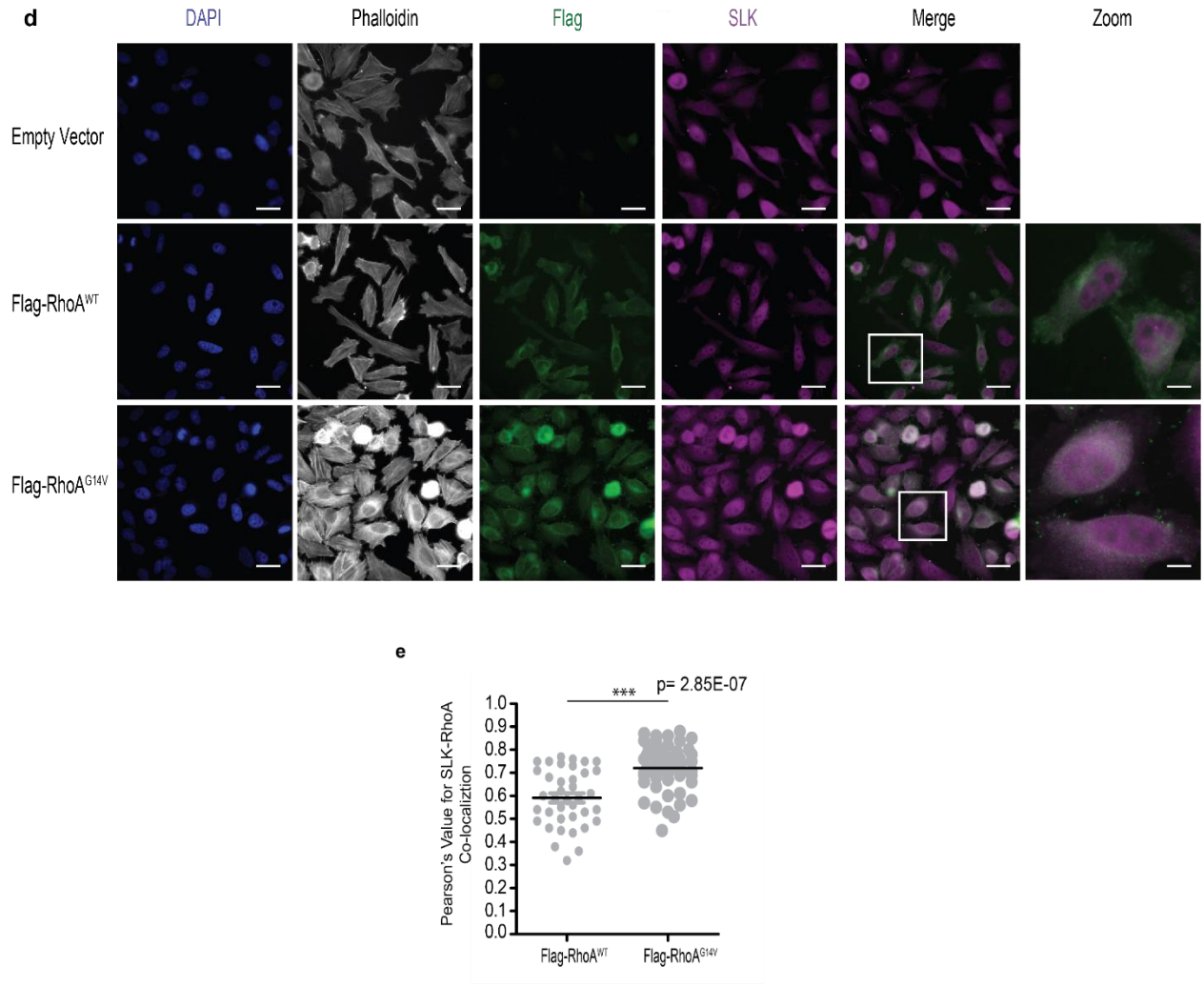

Fig. 22 | Active RhoA induces ERM proteins phosphorylation. **a**, Lysates from Flp-In T-REx HeLa cells expressing Empty Vector, Flag-RhoA^{WT} or Flag-RhoA^{G14V} were subjected to immunoblotting. The phosphorylation and expression levels were analyzed with anti-p-ERM, anti-ERM and anti-Flag antibodies. **b,** Empty Vector, Flag-RhoA^{WT} or Flag-RhoA^{G14V} constructs from Flp-In T-REx HeLa cells are expressed upon tetracycline induction, fixed, stained for DAPI (blue), Phalloidin (grayscale), Flag (green), p-ERM (magenta) and analyzed with fluorescence microscopy (DM6, Leica). Representative IF images were shown (scale bar: 4 µm). **c**, Quantification of ERM phosphorylation. Data were shown as mean ±S.E.M. The indicated *P*-values are calculated by one-way ANOVA, followed by a Bonferroni test; ***$P \leq 0.001$. **d**, Empty Vector, Flag-RhoA^{WT} or Flag-RhoA^{G14V} constructs from Flp-In T-REx HeLa cells are expressed upon tetracycline induction, fixed and stained for DAPI (blue), Phalloidin (grayscale), Flag (green), endogenous SLK (magenta) and analyzed with fluorescence microscopy (DM6, Leica) Zeiss). Representative IF images were shown (scale bar: 4 µm). **e**, Quantification of endogenous SLK colocalization with Flag-RhoA^{WT} or Flag-RhoA^{G14V}. Data were shown as mean ±S.E.M. The indicated *P*-values are calculated by one-way ANOVA, followed by a Bonferroni test; ***$P \leq 0.001$.

The missing kinase downstream of RhoA which is responsible for ERM phosphorylation remained undetermined. Here, we asked whether SLK is the missing kinase which phosphorylates ERM downstream of the RhoA signaling. First, we showed by immunoblotting that Flag-SLK, and not Flag-SLK^{K63R}, phosphorylates ERM (**Fig. 23a**). Lysates from cells expressing Flag-RhoA^{G14V} were treated with siCTRL or siSLK and the phosphorylation levels of ERM were evaluated. siRNA-mediated knockdown of SLK dramatically reduced ERM phosphorylation in Flag-RhoA^{G14V} expressed cells (**Fig. 23b**). Identical results were observed by immunofluorescence staining which showed a significant decrease in the phosphorylation levels of ERM in cells treated with siRNA to knockdown SLK expression (**Figs. 23c and 23d**). These results define SLK as an essential kinase in RhoA-induced ERM proteins phosphorylation.

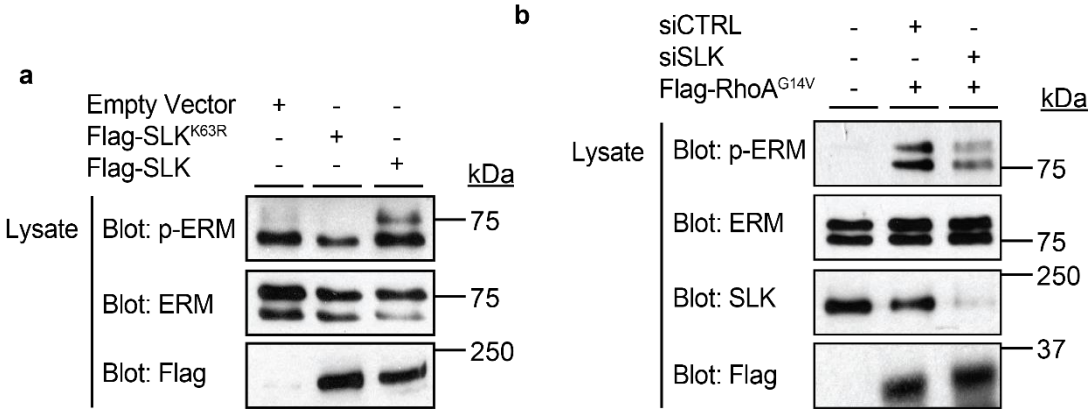

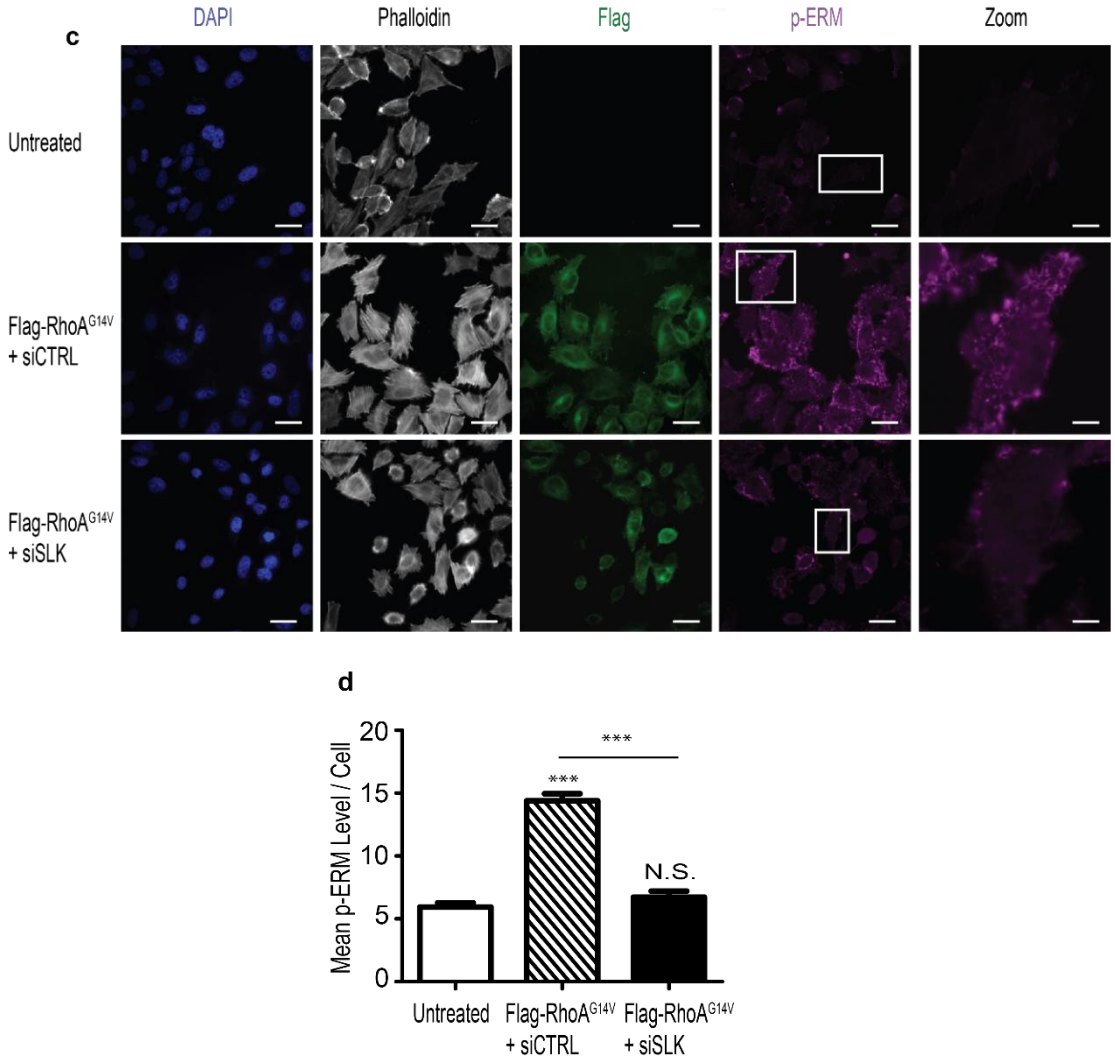

Fig. 23 | SLK is as essential kinase in RhoA-induced ERM proteins phosphorylation. **a**, SLK, but not SLK^{K63R}, phosphorylates ERM. Lysates from Flp-In T-REx HeLa cells expressing Empty Vector, Flag-SLK or Flag-SLK^{K63R} were subjected to immunoblotting. The phosphorylation and expression levels were analyzed with anti-p-ERM, anti-ERM and anti-Flag antibodies. **b**, Active RhoA induces the phosphorylation of ERMs via SLK. Lysates from Flp-In T-REx HeLa cells expressing Flag-RhoA^{G14V} in a tetracycline-inducible manner were transfected with Scrambled (siCTRL) or ON-target SmartPool SLK siRNA (siSLK) prior to tetracycline induction. The phosphorylation and expression levels were analyzed via immunoblotting with anti-p-ERM, anti-ERM, anti-SLK and anti-Flag antibodies. **c**, Flp-In T-REx HeLa expressing Flag-RhoA^{G14V} in a tetracycline-inducable manner are untreated or treated with tetracycline and co-transfected with either siCTRL or siSLK prior to tetracycline induction. Cells are fixed, stained for DAPI (blue), Phalloidin (grayscale), Flag (green) and p-ERM (magenta) and analyzed with fluorescence microscopy (DM6, Leica). Representative IF images were shown (scale bar: 4 μm). **d**, Quantification of p-ERM levels. Data were shown as mean ±S.E.M. The indicated *P*-values are calculated by one-way ANOVA, followed by a Bonferroni test; ***$P \leq 0.001$.

We next hypothesized that active RhoA may bind to SLK to promote its kinase activity. To test this possibility, we carried out an *in vitro* kinase assay. Lysates of HeLa cells coexpressing Flag-SLK with either Empty Vector, Myc-RhoA^{WT} or Myc-RhoA^{G14V} were immunoprecipitated and incubated with recombinant GST-Ezrin$^{479-585}$, which includes the C-terminal region of Ezrin with the T567 phosphorylation site that is targeted by SLK. We found that the active form of RhoA, but not the wild-type RhoA, significantly enhanced SLK-mediated Ezrin phosphorylation *in vitro* (**Fig. 24**). These data reveal active RhoA coupling to SLK stimulates SLK kinase activity.

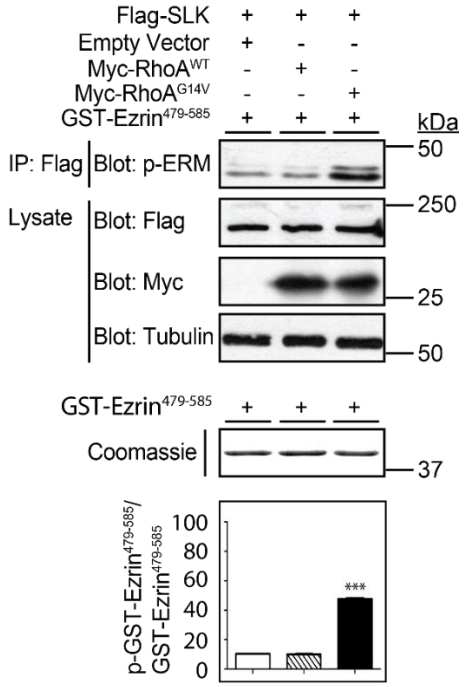

Fig. 24 | Active RhoA enhances SLK kinase activity. Lysates of HeLa cells were cotransfected with Flag-SLK with either Empty Vector, Myc-RhoA^{WT} or Myc-RhoA^{G14V} were subjected to immunoprecipitation using anti-Flag beads. The immunoprecipitated Flag-SLK proteins were then subjected to an *in vitro* kinase assay with GST-Ezrin$^{479-585}$. The phosphorylation and expression levels were analyzed by immunoblotting with anti-p-ERM, anti-Flag, anti-Myc and anti-Tubulin antibodies. p-GST-Ezrin$^{479-585}$ levels were quantified. Data were shown as mean ±S.E.M. The indicated *P*-values are calculated by one-way ANOVA, followed by a Bonferroni test; ***$P \leq 0.001$.

Studies established that autophosphorylation sites on SLK, such as T183, are essential for SLK kinase activity and activation[294]. A previous report showed that the SLK T183A mutant exhibited a 60% decrease in kinase activity compared to wild-type[307]. We therefore asked whether active RhoA is involved in SLK autophosphorylation and subsequent activation. In cells expressing Empty Vector, Flag-RhoA^{WT} or Flag-RhoA^{G14V}, expression of Flag-RhoA^{G14V} significantly increased SLK autophosphorylation levels on T183 compared to cells which express Flag-RhoA^{WT} (**Figs. 25a and 25b**). Taken together, these findings suggest that SLK binds to active RhoA, increasing SLK autophosphorylation on T183 and activation, which is crucial for subsequent ERM phosphorylation.

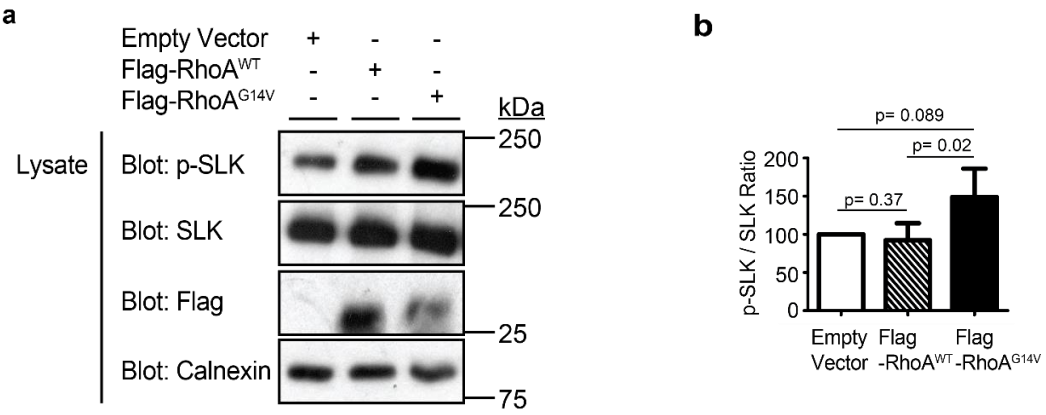

Fig. 25 | Active RhoA increases SLK autophosphorylation on T183. **a**, Lysates of Flp-In T-REx HeLa cells from the same representative experiment used for Fig. 1c were assessed for phosphorylation and expression levels using anti-p-SLK, anti-SLK, anti-Flag or anti-Calnexin antibodies. **b**, Quantification of pSLK levels. Data were shown as mean ±S.E.M. The indicated *P*-values are calculated by one-way ANOVA, followed by a Bonferroni test; ***$P \leq 0.001$.

To understand the molecular basis of RhoA-mediated SLK activation, we next aimed to map the SLK domain which binds active RhoA. We performed GST-pulldown assays where we expressed the N-terminal kinase (Flag-SLK$^{1-338}$), coiled-coil (Flag-SLK$^{339-788}$) or the C-terminal ATH domain (Flag-SLK$^{789-1205}$) in Flp-In T-REx HeLa cells and incubated with GST or GST-RhoA^{G14V}. The full-length SLK (Flag-SLK) or Flag-SLK$^{789-1205}$ interacted with GST-RhoA^{G14V}, whereas Flag-SLK$^{1-338}$ or Flag-SLK$^{339-788}$ failed to bind GST-RhoA^{G14V} (**Fig. 26**). This result shows that the ATH domain of SLK is responsible for binding to active RhoA.

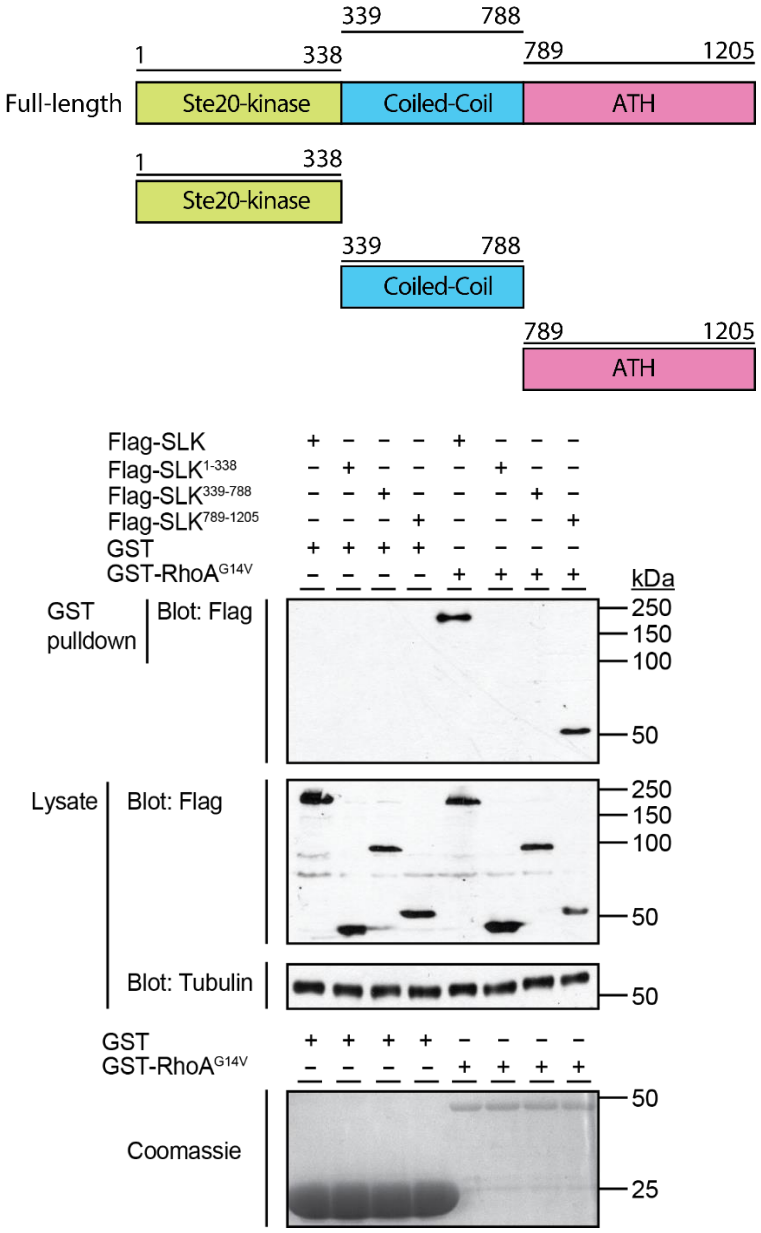

Fig. 26 | The ATH domain, but not the kinase or coiled-coil domains, of SLK mediates active RhoA binding *in vitro*. Lysates from Flp-In T-REx HeLa cells expressing the kinase (Flag-SLK$^{1-338}$), coiled-coil (Flag-SLK$^{339-788}$) or ATH domain (Flag-SLK$^{789-1205}$) in a tetracycline-inducible manner were incubated with GST or GST-RhoA^{G14V} bound to glutathione sepharose beads. The precipitated proteins and expression levels were detected by immonublotting with anti-Flag and anti-Tubulin antibodies.

To establish SLK as a bona fide effector of active RhoA, we aimed to construct a SLK mutant unable to bind RhoA. We used truncated forms of full length SLK with deletion in the ATH domain to further identify the minimal region responsible for binding to active RhoA. We conducted GST-pulldown assays where we expressed the SLK ATH domain (Flag-SLK$^{789-1205}$), the full-length SLK lacking the last 105 C-terminal amino acids (Flag-SLK$^{1-1100}$), the full-length SLK lacking the last 209 C-terminal amino acids (Flag-SLK$^{1-996}$) or the full-length SLK lacking the ATH domain (Flag-SLK$^{1-788}$). In these experiments, only Flag-SLK$^{789-1205}$ bound GST-RhoA^{G14V} suggesting that the last 105 amino acids at the C-terminal of SLK are required for binding to active RhoA (**Fig. 27a**). We next tested whether this region is essential for RhoA-induced increased in SLK activity. Lysates of HeLa cells coexpressing Flag-SLK or Flag-SLK$^{1-1100}$ with either Empty Vector or Myc-RhoA^{G14V} were immunoprecipitated and incubated with recombinant GST-Ezrin$^{479-585}$. Active RhoA significantly enhanced the kinase activity of full-length SLK, whereas it failed to increase the activity of Flag-SLK$^{1-1100}$ (**Fig. 27b**). Collectively, these results showed that the last 105 amino acids of the ATH domain in SLK act as a module to integrate the signal from active RhoA to promote kinase activity of SLK.

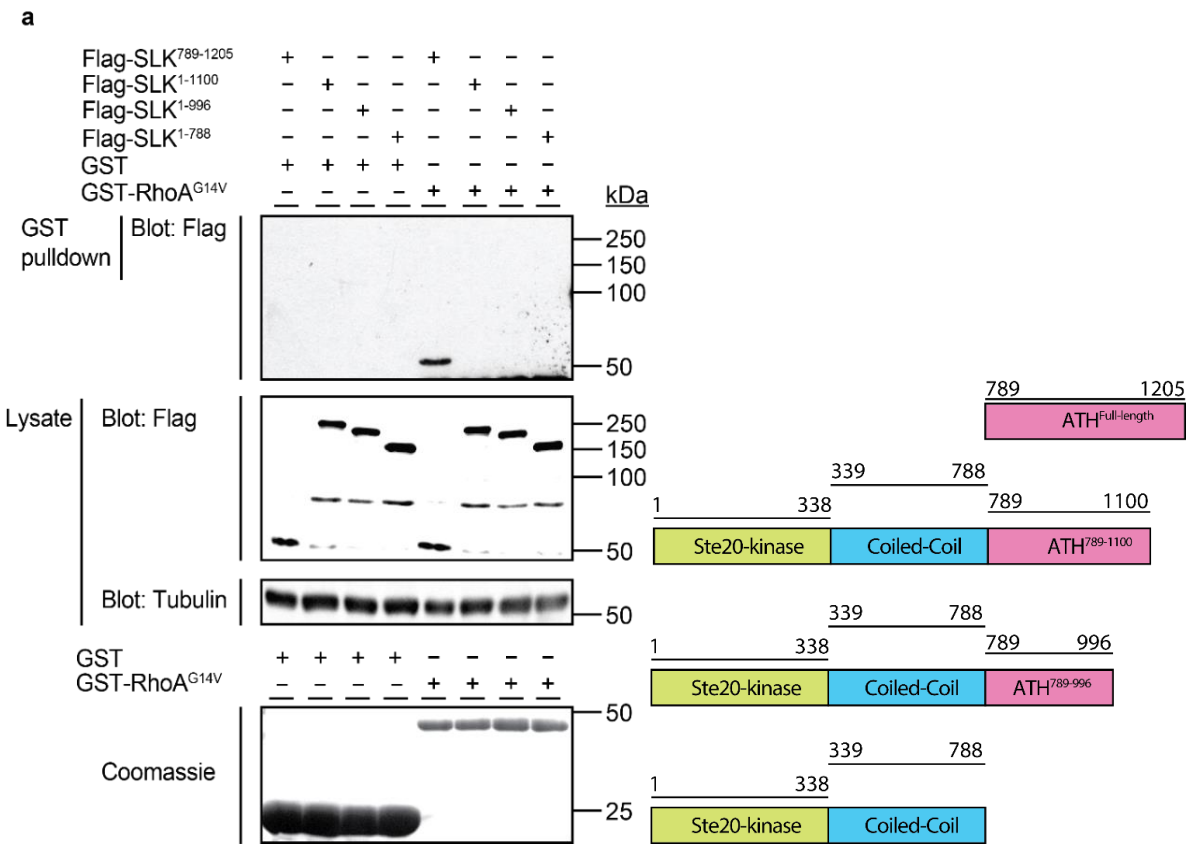
a
Flag-SLK789-1205
Flag-SLK1-1100
Flag-SLK1-996
Flag-SLK1-788
GST
GST-RhoAG14V
kDa
GST pulldown
Blot: Flag
250
150
100
50
Lysate
Blot: Flag
Blot: Tubulin
GST
GST-RhoAG14V
Coomassie
25
789
1205
ATHFull-length
339
788
1
338
1100
Ste20-kinase
Coiled-Coil
ATH789-1100
996
ATH789-996

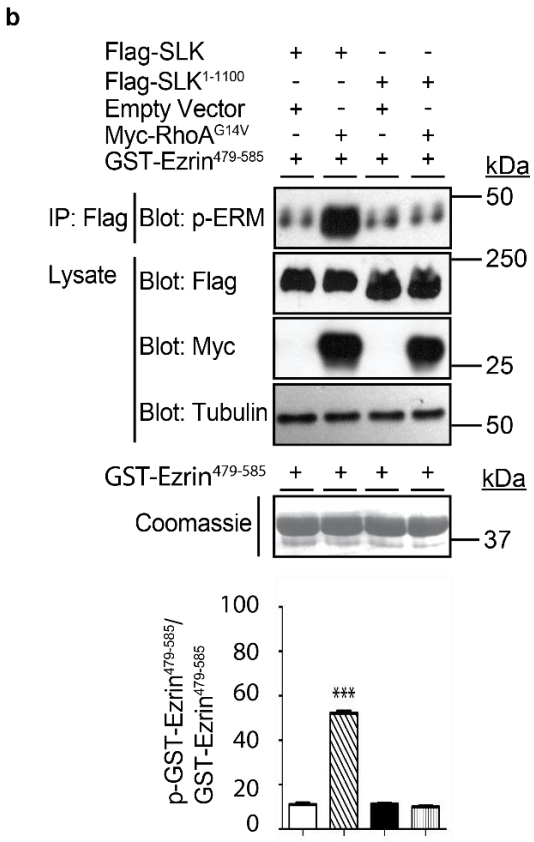

Fig. 27 | Amino acids at the C-terminal part of the SLK ATH domain integrates the signal from active RhoA to promote SLK kinase activity. **a**, The residues at the C-terminal end of SLK are required for active RhoA binding *in vitro*. Lysates from Flp-In T-REx HeLa cells expressing Flag-SLK$^{789-1205}$, Flag-SLK$^{1-1100}$, Flag-SLK$^{1-996}$ or Flag-SLK$^{1-788}$ in a tetracycline-inducable manner were incubated with GST or GST-RhoA^{G14V} bound to Glutathione Resin beads. The precipitated proteins and expression levels were detected by immonublotting with anti-Flag and anti-Tubulin antibodies. **b**, The residues at the C-terminal end of SLK are necessary to mediated SLK-dependent Ezrin phosphorylation downstream of active RhoA *in vitro*. Lysates of HeLa cells were cotransfected with Flag-SLK or Flag-SLK$^{1-1100}$ with either Empty Vector or Myc-RhoA^{G14V} were subjected to immunoprecipitation using anti-Flag beads. The immunoprecipitated Flag-SLK or Flag-SLK$^{1-1100}$ proteins were then subjected to an *in vitro* kinase assay with GST-Ezrin$^{479-585}$. The phosphorylation and expression levels were analyzed by immunoblotting with anti-p-ERM, anti-Flag, anti-Myc and anti-Tubulin antibodies. p-GST-Ezrin$^{479-585}$ levels were quantified. Data were shown as mean ±S.E.M. The indicated *P*-values are calculated by one-way ANOVA, followed by a Bonferroni test; ***$P \leq 0.001$.

3.6. KIAA0355, an uncharacterized Rac1 effector, is involved in cell migration

In search for novel Rac effectors, we looked at the prey interactions that were specifically recovered in active forms of the Rac subfamily members. We identified a specific interaction between the uncharacterized KIAA0355 protein and Rac subfamily of Rho GTPases in their active forms (**Fig. 28a**) in our BioID screens. We confirmed this data by showing that Myc-KIAA0355 can co-immunoprecipitate with Flag-Rac1^{G12V}, but not with Flag-Rac1^{WT} (**Fig. 28b**). Similarly, endogenous KIAA0355 immunoprecipitated with Flag-Rac1^{G12V}, but not with Flag-Rac1^{WT}, and this has been lost upon siRNA-mediated knockdown of KIAA0355 (siKIAA0355) or in KIAA-depleted cells generated by CRISPR/Cas9 (**Fig. 28c**). These results demonstrate that KIAA0355 is a novel binding partner of activated Rac1 therefore a potential effector molecule.

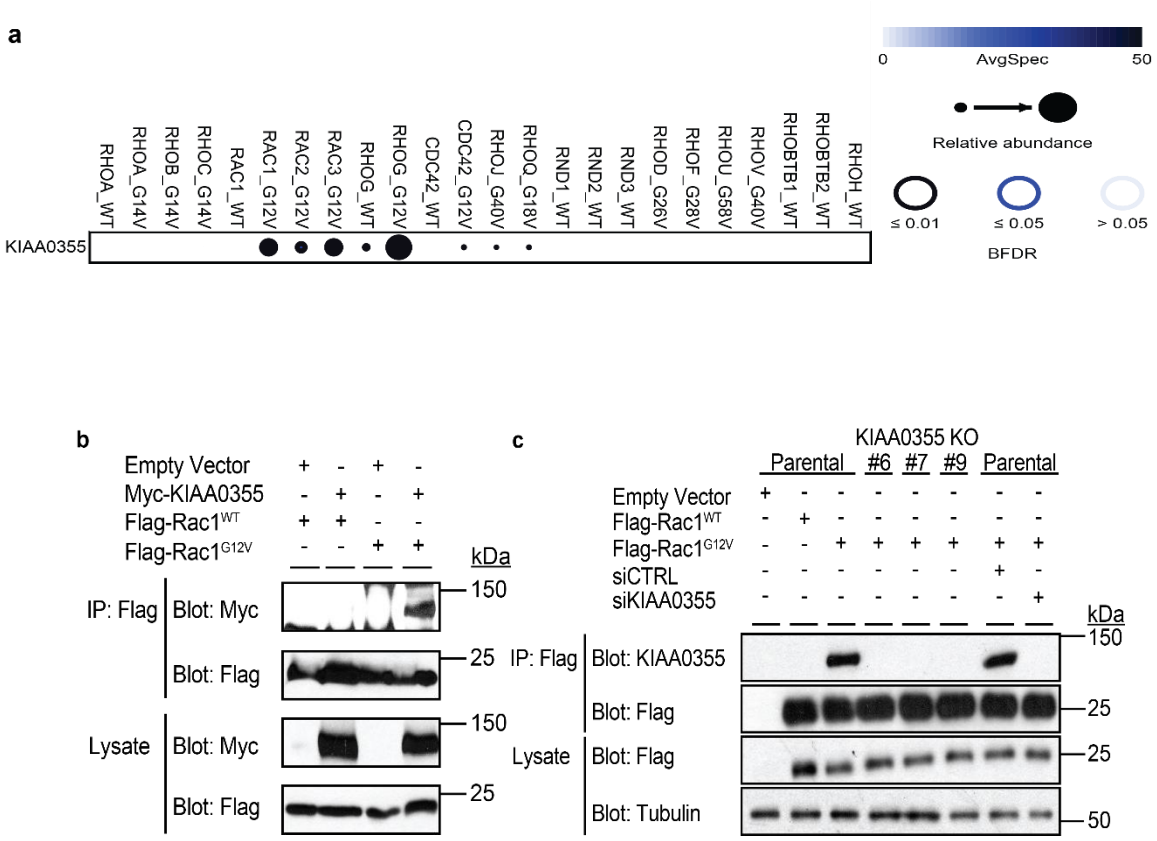

Fig. 28 | KIAA0355 is a novel binding partner of active Rac1. **a**, Dotplot showing BioID interactions between KIAA0355 and Rho GTPases in Flp-In T-REx HEK293 cells. The average spectral counts are shown in node color. The confidence score of the interaction (BFDR) is shown as edge color (BFDR ≤ 1% as high, 1% < BFDR ≤ 5% as medium or 5% < BFDR as low confidence). Circle size represents the relative abundance of prey over baits. **b**, Validation of KIAA0355-Rac1^{G12V} interaction by immunoprecitation analysis. Flp-In T-REx HEK293 cells expressing Flag-Rac1^{WT} or Flag-Rac1^{G12V} in a tetracycline-inducible manner were transfected with either Empty Vector or Myc-KIAA0355. Lysates were subjected to immunoprecipitation using anti-Flag beads. The precipitated proteins and expression levels were detected by immunoblotting with anti-Myc and anti-Flag antibodies. **c,** HeLa cells were cotransfected with Empty Vector, Flag-Rac1^{WT} or Flag-Rac1^{G12V} with either siCTRL or siKIAA0355 and KIAA0355$^{-/-}$ HeLa cells generated by CRISPR/Cas9 were transfected with Flag-Rac1^{G12V}. Lysates were subjected to immunoprecipitation using anti-Flag beads. The precipitated proteins and expression levels were detected by immunoblotting with anti-KIAA0355, anti-Flag or anti-Tubulin antibodies.

We next aimed to characterize the subcellular localization and dynamics of KIAA0355 as a potential Rac1 effector. Flag-KIAA0355 expression alone was associated with fine cytoplasmic speckles in Flp-In T-REx HeLa cells and this was not affected by the coexpression of mOrange-Rac1^{WT} (**Fig. 29a**). However, in cells that coexpress both mOrange-Rac1^{G12V} and Flag-KIAA0355, we found that Flag-KIAA0355 was no longer associated with cytoplasmic speckles and colocalized with mOrange-Rac1^{G12V}-induced membranes ruffles on the plasma membrane (**Figs. 29a and 29b**). To test whether KIAA0355 is essential for Rac1-induced membrane ruffling, we transfected Flp-In T-REx HeLa cells expressing Flag-Rac1^{G12V}, in a tetracycline-inducible manner, with siCTRL or siKIAA0355 and evaluated the membrane ruffling. Non-transfected (NT) Flag-Rac1^{G12V} or Flag-Rac1^{G12V}-expressing Flp-In T-REx HeLa cells transfected with siCTRL exhibited higher levels of membrane ruffles compared to cells that express Flag-Rac1^{WT} only (**Figs. 29c and 29d**). However, siRNA-mediated knockdown of endogenous KIAA0355 resulted in a dramatic loss of membrane ruffling in Flag-Rac1^{G12V}-expressing cells, diminishing it to near Flag-Rac1^{WT}-expressed cells. Taken together, these data suggest that KIAA0355 acts as an essential Rac1 effector and is spatiotemporally recruited to the plasma membrane by active Rac1 during membrane ruffling.

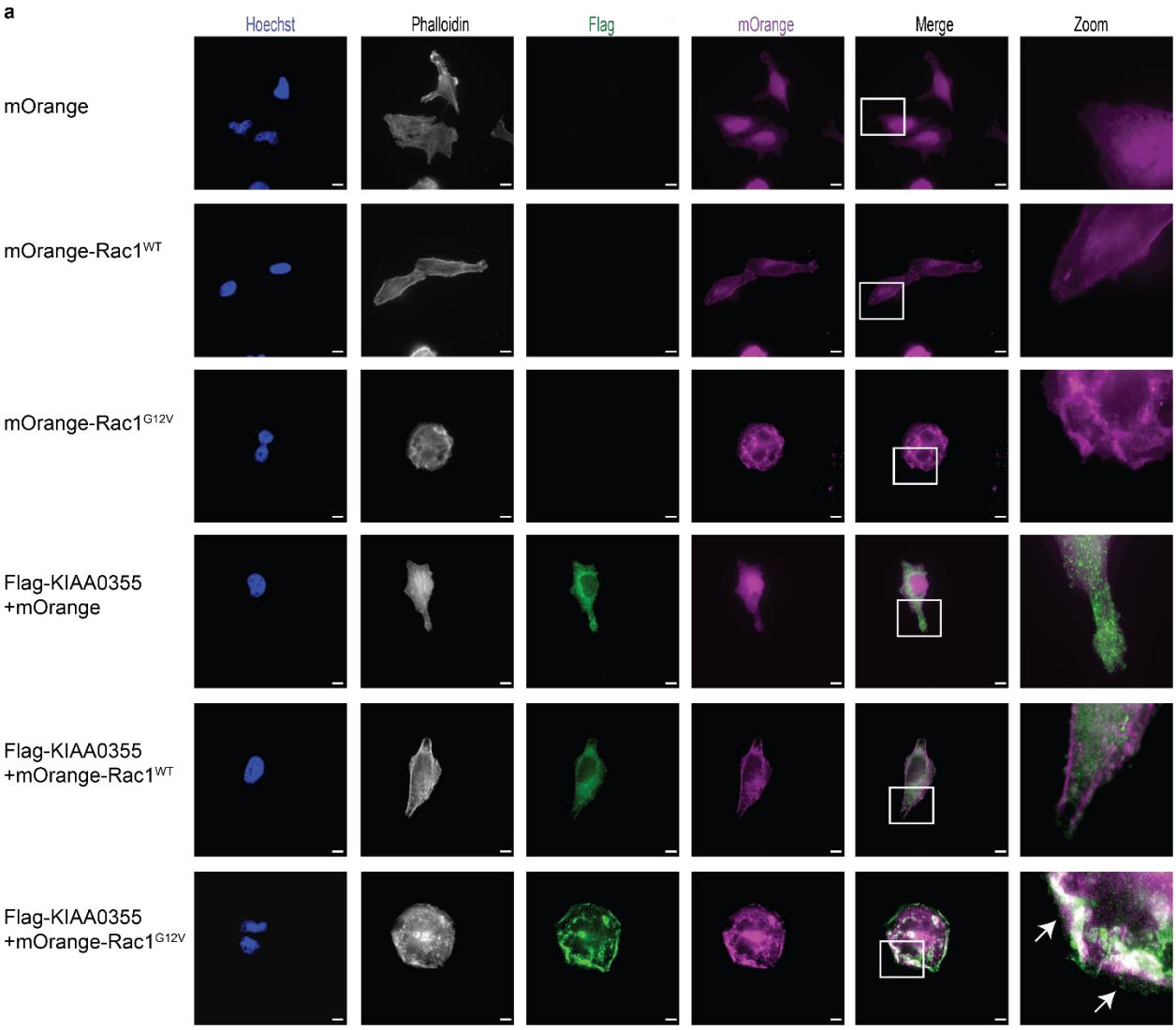
a
Hoechst
Phalloidin
Flag
mOrange
Merge
Zoom
mOrange
mOrange-Rac1WT
mOrange-Rac1G12V
Flag-KIAA0355
+mOrange
Flag-KIAA0355
+mOrange-Rac1WT
Flag-KIAA0355
+mOrange-Rac1G12V

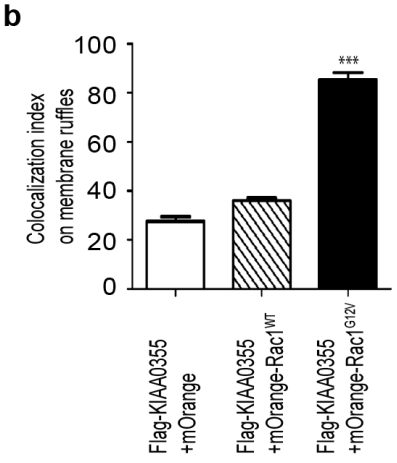
b
Colocalization index
on membrane ruffles
100
80
60
40
20
0
***
Flag-KIAA0355
+mOrange
Flag-KIAA0355
+mOrange-Rac1WT
Flag-KIAA0355
+mOrange-Rac1G12V

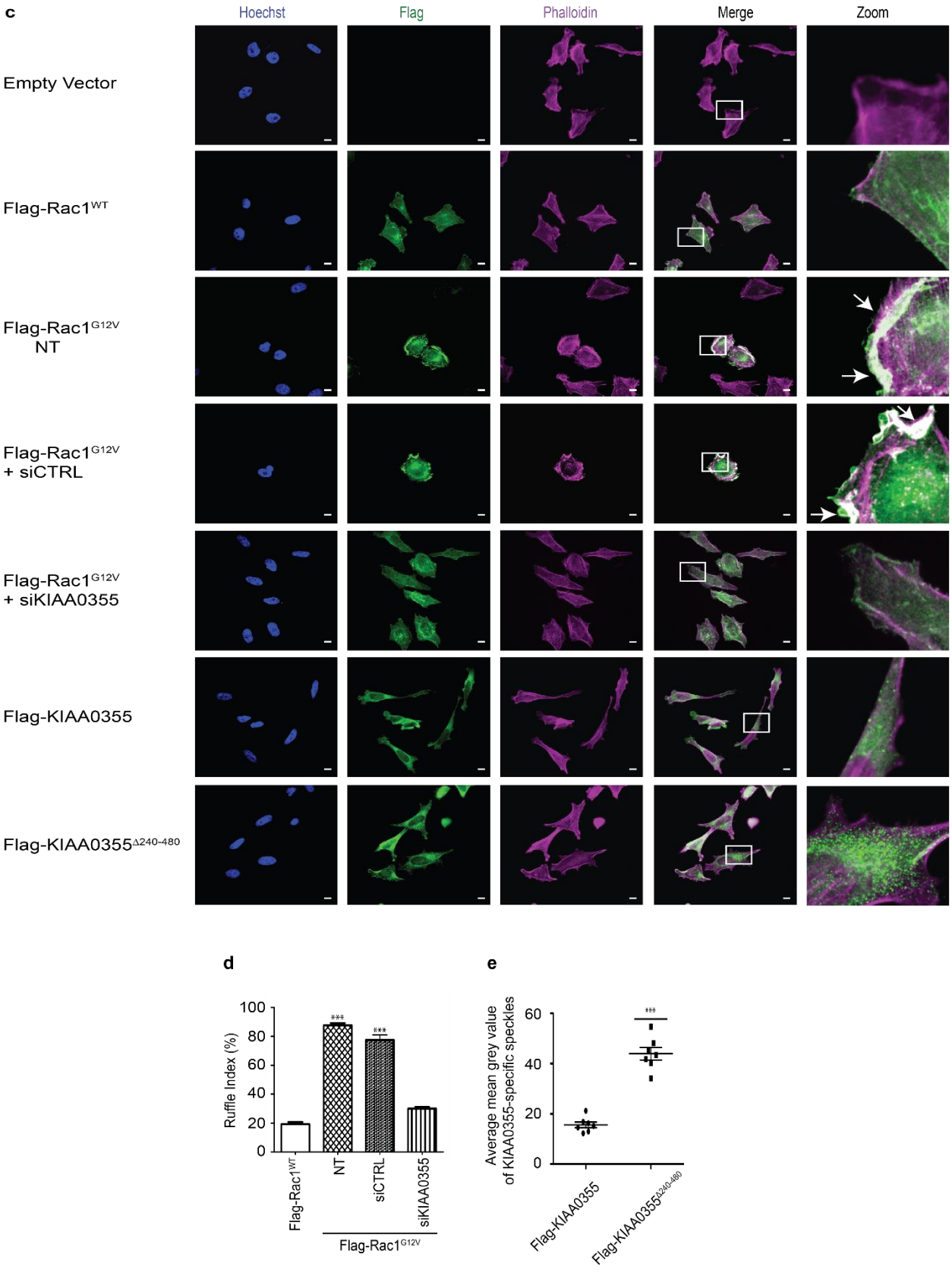
c
Hoechst
Flag
Phalloidin
Merge
Zoom
Empty Vector
Flag-Rac1WT
Flag-Rac1G12V NT
Flag-Rac1G12V + siCTRL
Flag-Rac1G12V + siKIAA0355
Flag-KIAA0355
Flag-KIAA0355Δ240-480
d
Ruffle Index (%)
100
80
60
40
20
0
***
***
Flag-Rac1WT
NT
siCTRL
siKIAA0355
Flag-Rac1G12V
e
Average mean grey value of KIAA0355-specific speckles
60
40
20
0
***
Flag-KIAA0355
Flag-KIAA0355Δ240-480

Fig. 29 | KIAA0355, an essential Rac1 effector, is involved in membrane ruffling. **a**, KIAA0355 is an essential effector of Rac1 for membrane ruffling. Flp-In T-REx HeLa cells expressing Flag-KIAA0355 in a tetracycline-inducable manner were transfected with mOrange, mOrange-Rac1^{WT} or mOrange-Rac1^{G12V}. Cells were fixed, stained for Hoechst (blue), Phalloidin (grayscale), Flag (green). Unstained mOrange-tagged constructs were shown in magenta. Representatives immunofluorescence (IF) images were shown (scale bar: 10 µm). **b**, Quantification of Flag-KIAA0355 colocalization with mOrange, mOrange-Rac1^{WT} or mOrange-Rac1^{G12V} on cell membrane. Data were shown as mean ±S.D. The indicated *P*-values are calculated by one-way ANOVA, followed by a Bonferroni test; ***$P \leq 0.001$. **c**, Flp-In T-REx HeLa cells expressing Flag-Rac1^{G12V} in a tetracycline-inducable manner were non-transfected (NT) or transfected with siCTRL or ON-target SmartPool KIAA0355 siRNA (siKIAA0355) prior to tetracycline induction. Empty Vector and Flag-Rac1^{WT} were used as controls. Flp-In T-REx HeLa cells expressing Flag-KIAA0355 or Flag-KIAA0355 that lacks the Rac1-binding domain (Flag-KIAA0355$^{\Delta 240\text{-}480}$) were subjected to immunofluorescence analysis. Cells were fixed, stained for Hoechst (blue), Flag (green) or Phalloidin (magenta). Representative IF images were shown (scale bar: 10 µm). **d**, Quantification of membrane ruffling. Data were shown mean ±S.D. The indicated *P*-values are calculated by one-way ANOVA, followed by a Bonferroni test; ***$P \leq 0.001$. **e**, Quantification of KIAA0355-specific speckles. Data were shown as mean ±S.E.M. The indicated *P*-values are calculated by using a two-tailed Student's *t*-test; ***$P \leq 0.001$.

We next aimed to define if KIAA0355 is involved in cell migration. Expression of Flag-KIAA0355 significantly increased cell migration compared to empty vector (EV) control as shown in Boyden migration assay (**Fig. 30a**). Identical results were obtained by cell tracking assay (**Fig. 30b**). Collectively, these results demonstrate that KIAA0355 promotes cell migration.

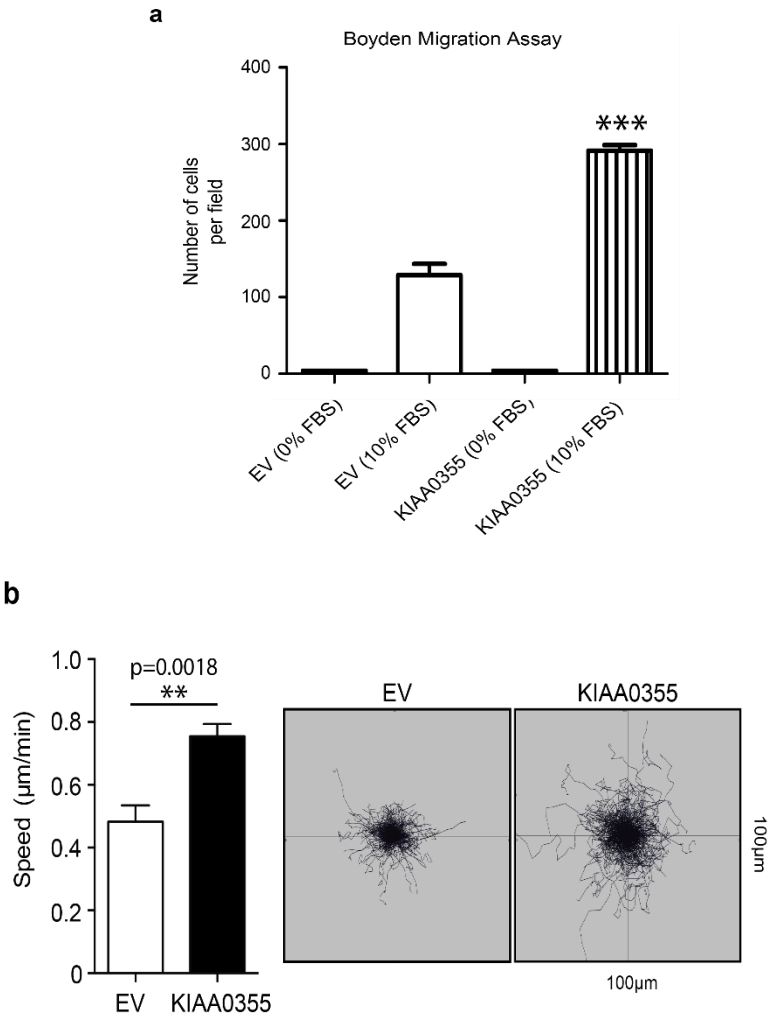

Fig. 30 | KIAA0355 expression enhances cell migration. **a**, Flp-In T-REx HeLa cells, incubated in the absence or presence of serum, expressing Empty Vector or Flag-KIAA0355 (KIAA0355) in a tetracycline-inducible manner, were incubated in the upper side of a Boyden chamber. Cells were allowed to migrate through the Boyden chamber for 6 h. The migration assay was carried out in triplicate. Data were shown as mean ±S.D. The indicated *P*-values are calculated by one-way ANOVA, followed by a Bonferroni test; ***$P \leq 0.001$. **b**, Cell tracking and quantification of migration speed. Flp-In T-REx HeLa cells expressing Empty Vector or Flag-KIAA0355 (KIAA0355) in a tetracycline-inducible manner were plated in 6-well plates. Nuclei were stained using NucRed reagent. Cells were then subjected to time-lapse microscopy analysis for tracking assay. Data were shown as mean ±S.E.M. The indicated *P*-values are calculated by using a two-tailed Student's *t*-test; ***$P \leq 0.001$.

To understand how KIAA0355 functions and integrates Rac1-GTP signal as an effector, we generated truncated forms of KIAA0355 and performed GST-pulldown assays (**data not shown**). We found that the deletion of amino acids from 240 to 480 of KIAA0355, Flag-KIAA0355$^{\Delta 240\text{-}480}$, led to complete abrogation of active Rac1 interaction (**Figs. 31a and 31b**). In Boyden migration assay, Flag-KIAA0355-expressed cells showed higher cell migration levels compared to those which expressed EV or Flag-KIAA0355$^{\Delta 240\text{-}480}$ (**Fig. 31c**). KIAA0355-depleted cells had similar migration levels to those of EV or KIAA0355$^{\Delta 240\text{-}480}$, suggesting that loss of endogenous KIAA0355 is not sufficient for loss-of-function in cell migration. Interestingly, *in vitro* cell tracking experiments showed that the expression of Flag-KIAA0355$^{\Delta 240\text{-}480}$ exhibited cell migration levels which were not significantly different than that of Flag-KIAA0355 (**Fig. 31d**), however it failed to reduce migration levels near that of EV-expressed cells. Collectively, our results suggest that KIAA0355 is a novel Rac1 effector and integrates the Rac1 signaling pathway for membrane ruffling and migration.

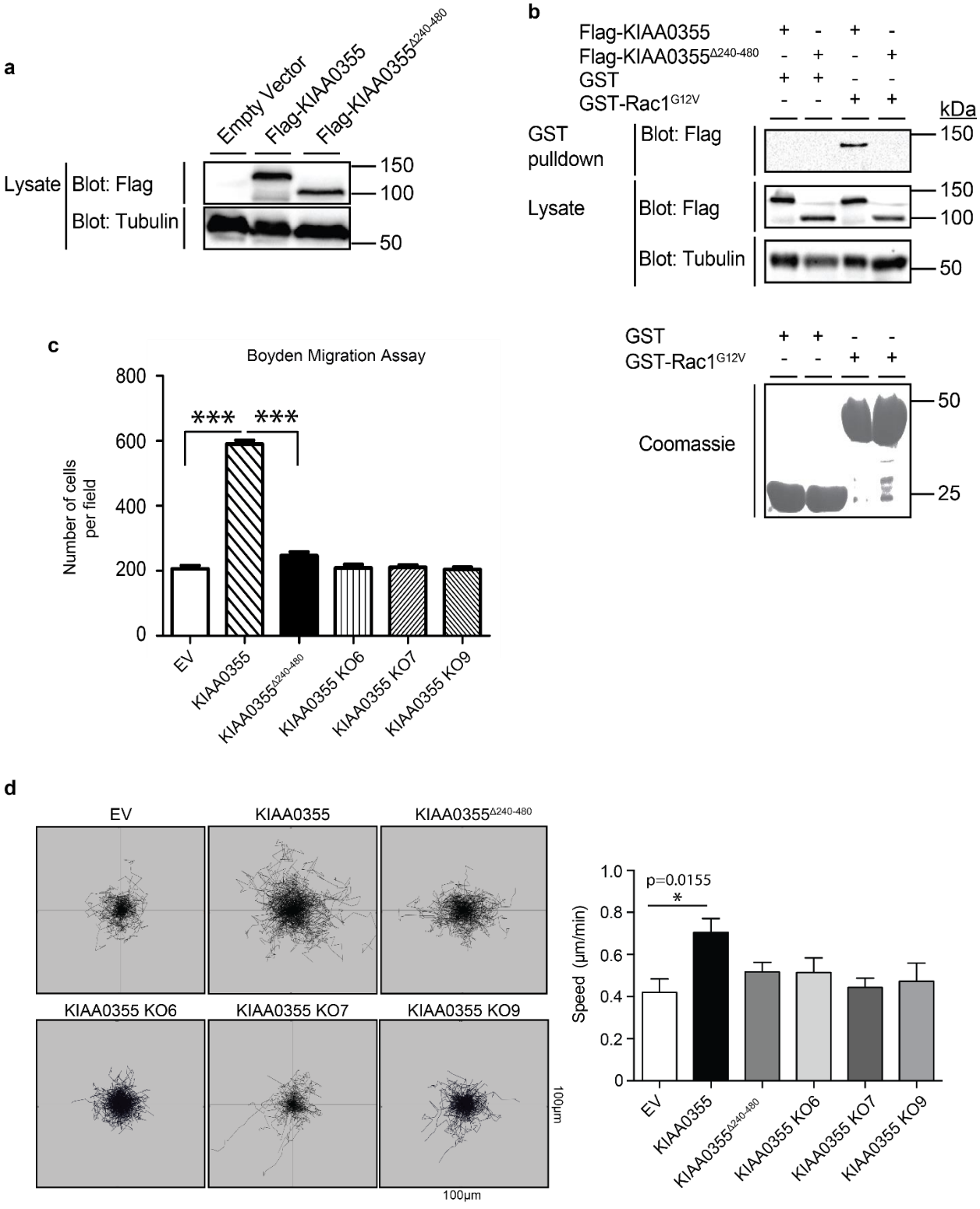
a
Empty Vector
Flag-KIAA0355
Flag-KIAA0355Δ240-480
Lysate
Blot: Flag
Blot: Tubulin
150
100
50
b
Flag-KIAA0355
Flag-KIAA0355Δ240-480
GST
GST-Rac1G12V
kDa
GST pulldown
Blot: Flag
Lysate
Blot: Flag
Blot: Tubulin
150
100
50
GST
GST-Rac1G12V
Coomassie
50
25
c
Boyden Migration Assay
Number of cells per field
800
600
400
200
0
***
***
EV
KIAA0355
KIAA0355Δ240-480
KIAA0355 KO6
KIAA0355 KO7
KIAA0355 KO9
d
EV
KIAA0355
KIAA0355Δ240-480
KIAA0355 KO6
KIAA0355 KO7
KIAA0355 KO9
100μm
100μm
Speed (μm/min)
1.0
0.8
0.6
0.4
0.2
0
p=0.0155
*
EV
KIAA0355
KIAA0355Δ240-480
KIAA0355 KO6
KIAA0355 KO7
KIAA0355 KO9

Fig. 31 | KIAA0355, a novel Rac1 effector, integrates the Rac1 signaling pathway for cell migration. **a**, Lysates of Flp-In T-REx HeLa cells showing expression of the indicated constructs. **b**, The amino acid residues between positions 240 and 480 of KIAA0355 are necessary for active Rac1 binding. Lysates from Flp-In T-REx HeLa cells expressing Flag-KIAA0355 or Flag-KIAA0355$^{\Delta 240\text{-}480}$ in a tetracycline-inducable manner were incubated GST or GST-Rac1^{G12V} bound to Glutathione Resin beads. The precipitated proteins and expression levels were detected by immonublotting with anti-Flag and anti-Tubulin antibodies. antibodies. **c**, KIAA0355 expression increases cell migration. The lower side of Boyden chambers is pre-coated with fibronectin. Serum-starved Flp-In T-REx HeLa cells expressing Empty Vector, Flag-KIAA0355 (KIAA0355), Flag-KIAA0355$^{\Delta 240\text{-}480}$ (KIAA0355$^{\Delta 240\text{-}480}$) in a tetracycline-inducible manner or serum-starved KIAA0355 Flp-In T-REx HeLa cell lines generated via CRISPR/Cas9 were incubated in the upper side of a Boyden chamber. Cells were allowed to migrate through the Boyden chamber for 16 h. The migration assay was carried out in triplicate. Data were shown as mean ±S.D. The indicated *P*-values are calculated by one-way ANOVA, followed by a Bonferroni test; ***$P \leq 0.001$. **d**, Cell tracking and quantification of migration speed. Flp-In T-REx HeLa cells expressing Empty Vector, Flag-KIAA0355 (KIAA0355), Flag-KIAA0355$^{\Delta 240\text{-}480}$ (KIAA0355$^{\Delta 240\text{-}480}$) in a tetracycline-inducible manner or KIAA0355 Flp-In T-REx HeLa cell lines generated by CRISPR/Cas9 were plated in 12-well plates. Nuclei were stained using NucRed reagent. Cells were then subjected to time-lapse microscopy analysis for tracking assay. Data were shown as mean ±S.E.M.

3.7. A functional siRNA screen of RhoG interacting proteins defines essential interactors for membrane ruffling

RhoG belongs to the Rac subfamily of Rho GTPases and its interactors and signaling pathways are not as well revealed as other Rac proteins. To uncover novel RhoG effectors or regulatory proteins that regulates membrane ruffling, we conducted a functional siRNA screening of RhoG interactors that we identified in our BioID screens (**Figs. 32a and 32b**). To do this, we carried out a high throughput screen in Flp-In T-REx HeLa cells, in which we expressed Flag-RhoG^{G12V} and treated with a set of siRNAs targeting 24 human genes encoding top RhoG interactors that we identified by BioID with

high spectral counts, abundance and confidence. We then proceeded for immunofluorescence staining in 96-well plates and automated microscope-based high content screening before quantifying the ruffle index in a semi-automated manner.

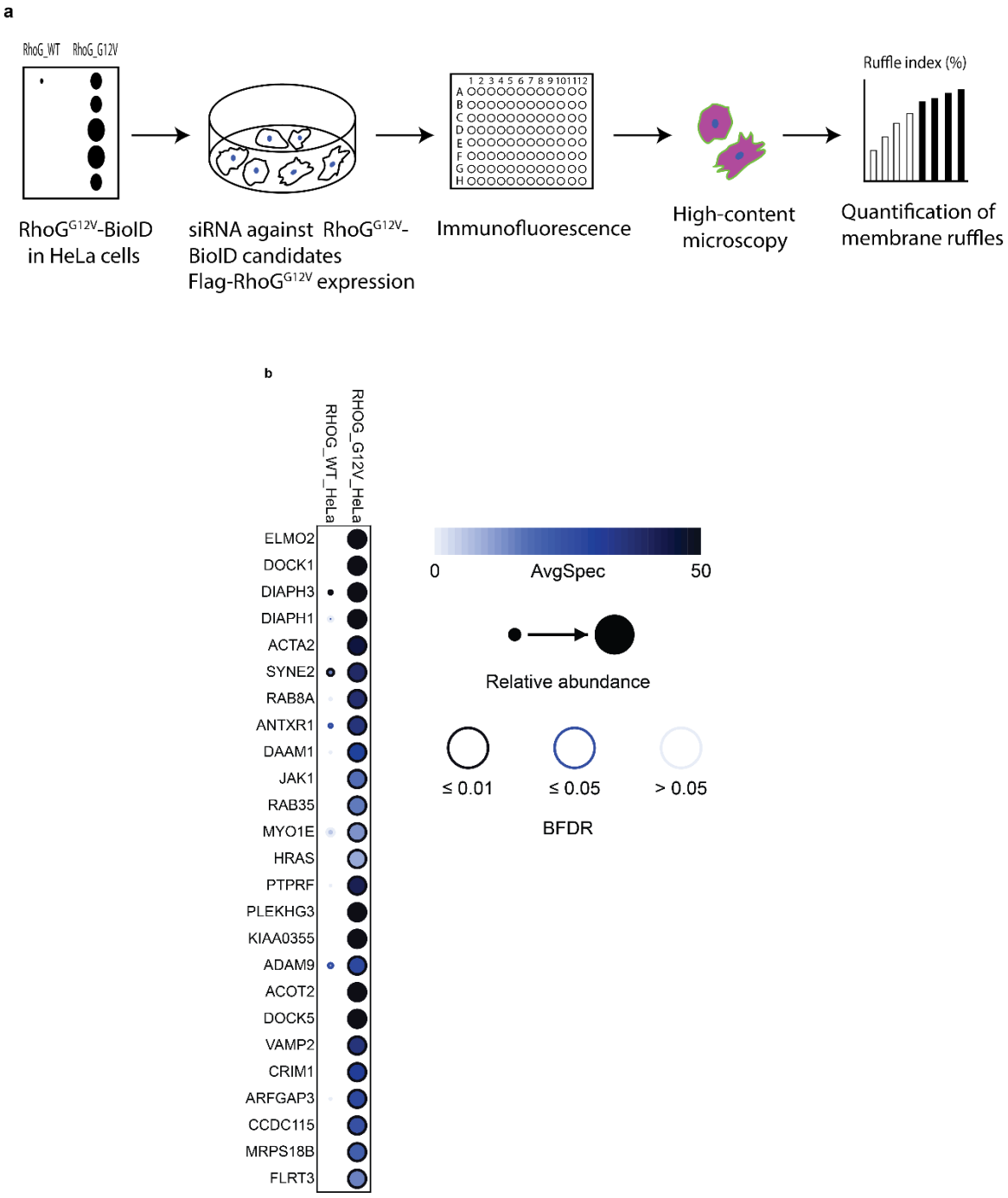

Fig. 32 | a, Schematic illustration of the functional siRNA screening for RhoG. **b**, Dotplot showing top BioID interactors identified in RhoG^{WT} and RhoG^{G12V} in Flp-In T-REx HeLa cells. The average spectral counts are shown in node color. The confidence score of the interaction (BFDR) is shown as edge color (BFDR ≤ 1% as high, 1% < BFDR ≤ 5% as medium or 5% < BFDR as low confidence). Circle size represents the relative abundance of prey over baits.

As expected, we identified the well-known ELMO2 and DOCK1 interactions in GTP-loaded BirA*-Flag-RhoG^{G12V} BioID screen, and not in that of BirA*-Flag-RhoG^{WT}, as previously reported in the literature[98]. By siRNA screening, we tested if some of these candidates are essential for RhoG-mediated membrane ruffling. Among 24 candidates, knockdown of 11 of them showed a significant decrease in Flag-RhoG^{G12V}-induced membrane ruffling, including *ELMO2*, *DOCK5* but also newly-identified BioID candidates such as *DIAPH1*, *DIAPH3*, *KIAA0355*, *PLEKHG3* and others (**Figs. 33a and 33d**). siRNA-mediated knockdown of KIAA0355 resulted in lower membrane ruffling in Flag-RhoG^{G12V} expressed cells than that of the controls (siCTRL or Untransfected), showing that KIAA0355 is recruited, not only by Rac1, but also by other members of the Rac1 subfamily, such as RhoG, during membrane ruffling. A previous report showed that PLEKHG3 enhances cell polarity and migration by activating Rac1 and Cdc42[260]. Here, we found that siRNA-mediated knockdown of PLEKHG3 significantly showed lower membrane ruffling levels (**Figs. 33a and 33b**). We also confirmed the PLEKHG3-RhoG^{G12V} interaction by GST-pulldown (**Fig. 33c**), suggesting that PLEKHG3 possibly acts as a RhoG-effector to activate Rac1 and is involved in RhoG-dependent membrane ruffling.

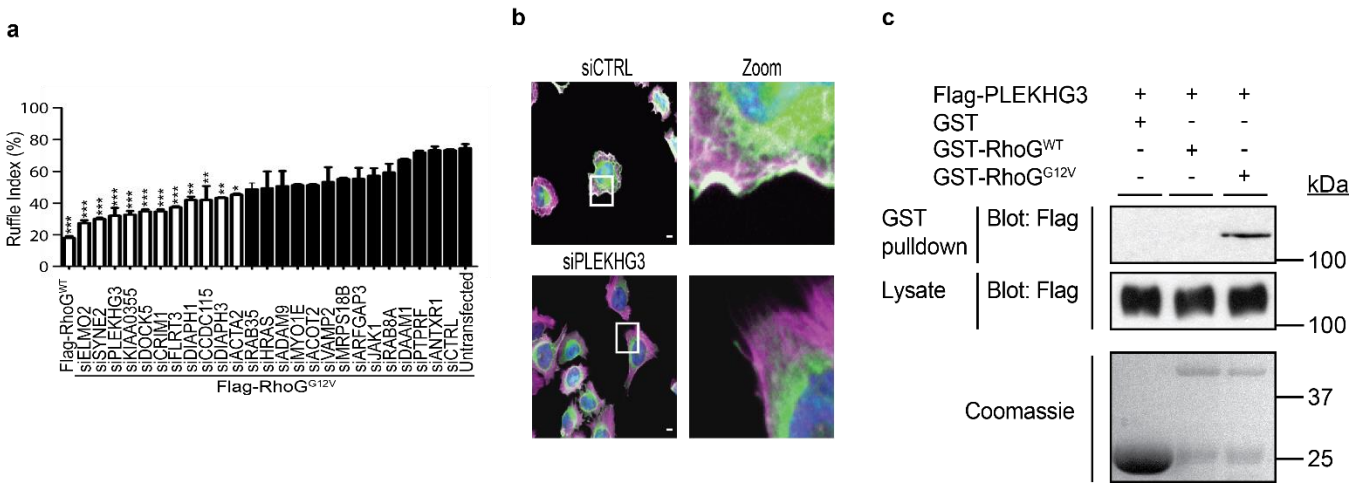
a
Ruffle Index (%)
100
80
60
40
20
0
Flag-RhoG^WT
siELMO2
siSYNE2
siPLEKHG3
siKIAA0355
siDOCK5
siCRIM1
siFLRT3
siDIAPH1
siCCDC115
siDIAPH3
siACTA2
siRAB35
siHRAS
siADAM9
siMYO1E
siACOT2
siVAMP2
siMRPS18B
siARFGAP3
siJAK1
siRAB8A
siDAAM1
siPTPRF
siANTXR1
siCTRL
Untransfected
Flag-RhoG^G12V
b
siCTRL
Zoom
siPLEKHG3
c
Flag-PLEKHG3 + + +
GST + - -
GST-RhoG^WT - + -
GST-RhoG^G12V - - +
kDa
GST pulldown
Blot: Flag
100
Lysate
Blot: Flag
100
Coomassie
37
25

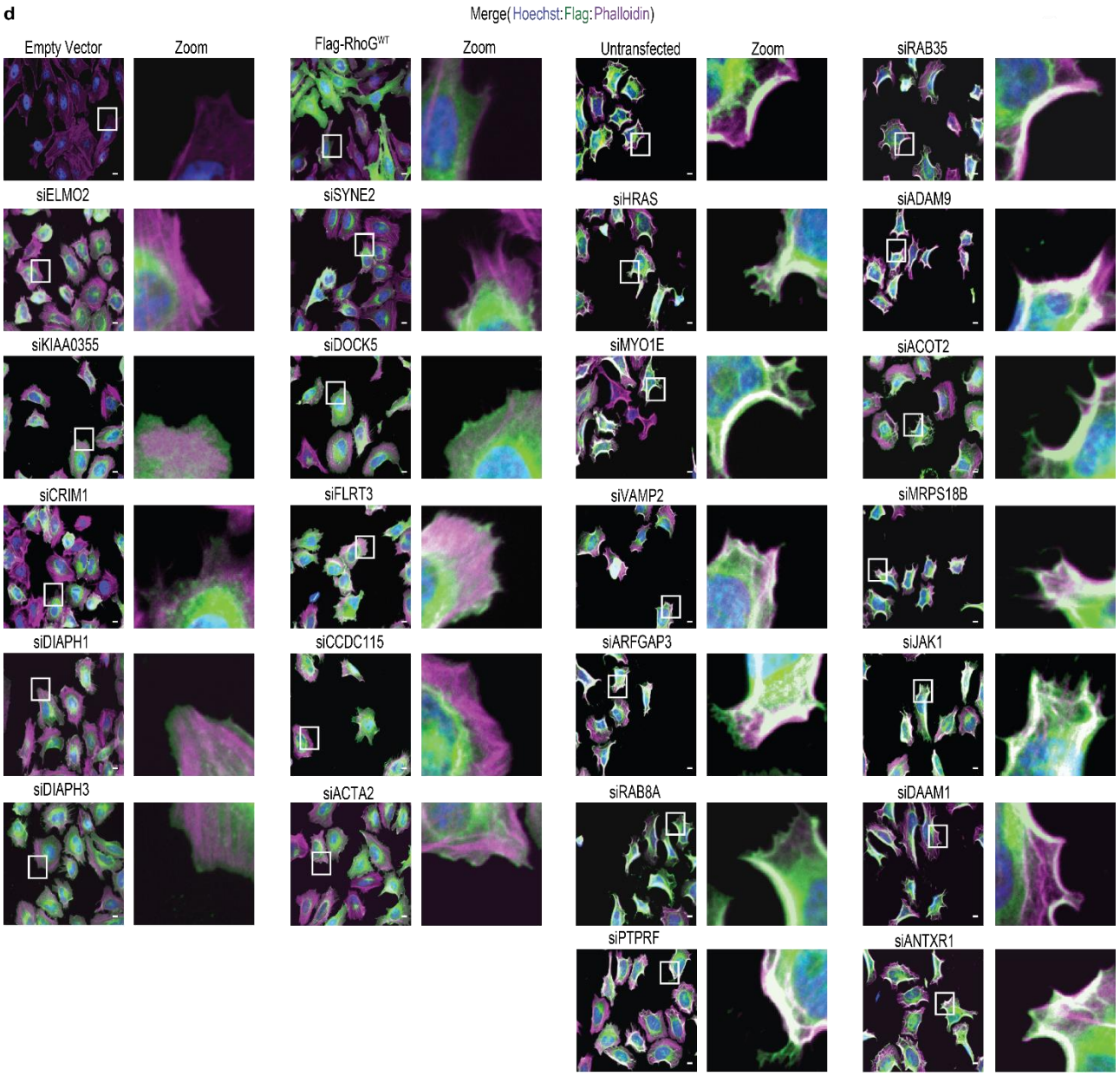
d
Merge(Hoechst:Flag:Phalloidin)
Empty Vector
Zoom
Flag-RhoG^WT
Zoom
Untransfected
Zoom
siRAB35
siELMO2
siSYNE2
siHRAS
siADAM9
siKIAA0355
siDOCK5
siMYO1E
siACOT2
siCRIM1
siFLRT3
siVAMP2
siMRPS18B
siDIAPH1
siCCDC115
siARFGAP3
siJAK1
siDIAPH3
siACTA2
siRAB8A
siDAAM1
siPTPRF
siANTXR1

Fig. 33 | A functional siRNA screening for RhoG reveals potential effectors that are essential for membrane ruffling. **a**, Quantification of membrane ruffling. Flp-In T-REx HeLa cells expressing Flag-RhoG^{G12V} in a tetracycline-inducible manner were transfected with a set of ON-target SmartPool siRNAs against the indicated genes prior to tetracycline induction and were subjected to immunofluorescence. Data were shown mean ±S.D. The indicated *P*-values are calculated by one-way ANOVA, followed by a Bonferroni test; **P* ≤ 0.05, ***P* ≤ 0.01 and ****P* ≤ 0.001. Flp-In T-REx HeLa cells expressing Empty Vector, Flag-RhoG^{WT}, untransfected Flag-RhoG^{G12V} or Flag-RhoG^{G12V} transfected with siCTRL were used as controls. **b**, Representative IF images showing Flp-In T-REx HeLa cells expressing Flag-RhoG^{G12V} transfected with either siCTRL or siPLEKHG3 (scale bar: 10 µm). **c**, Validation of PLEKHG3-RhoG^{G12V} interaction by GST pulldown. Flp-In T-REx HeLa cells expressing Flag-PLEKHG3 in a tetracycline-inducible manner were transfected with either GST, GST-RhoG^{WT}, GST-RhoG^{G12V}. Lysates were incubated with Glutathione Resin beads. The precipitated proteins and expression levels were detected by immunoblotting with an anti-Flag antibody. **d**, Representative IF images of Flp-In T-REx HeLa cells expressing Flag-RhoG^{G12V} in a tetracycline-inducible manner and transfected with with a set of ON-target SmartPool siRNAs against the indicated genes prior to tetracycline induction. Cells were fixed, stained for Hoechst (blue), Flag (green), Phalloidin (magenta) and analyzed with high-content fluorescence microscopy (scale bar: 10 µm).

CHAPTER 4: GENERAL DISCUSSION AND CONCLUSIONS

4.1. BioID-Proteomics reveals well-known, but also many novel Rho GTPase effectors

By employing the power of BioID as an approach to gain insight into the Rho GTPase signaling dynamics, our study was the first to uncover the global interactome of Rho GTPases revealing novel effectors and Rho GTPase-GEF/GAP interactions. By using a dataset of 56 baits in both HEK293 and HeLa cell lines, we generated a network of proteins with >5000 interactions in HEK293 and >9000 interactions in HeLa cell lines. About 92% of interactions identified in HEK293 were also recovered in HeLa cells. Those include the well-known effector complexes such as WAVE, GIT/PIX/PAK, WASP but also novel candidate effectors that we characterized in this study such as SLK and KIAA0355. GO term analysis of preys identified known biological processes such as regulation of GTPase signal transduction pathways, but also unknown processes such as mRNA decay.

Our BioID screens provided a detailed PPI interface for RhoA, Rac1 and Cdc42 as well as atypical Rho GTPases. Little is known about the signaling pathways of atypical Rho GTPases. Further decipherment of effector signaling networks of the atypical Rho GTPases by functional assays might provide a better understanding of their physiological impact.

Domains are functional units of proteins that mediate PPIs. Which effector domains are specifically involved downstream of each Rho GTPase signal remains to be investigated. Uncovering domain-domain interaction (DDI) profiles of Rho GTPase-effector couples will provide key evidence for their interaction mechanisms.

4.2. Rho/GEF-GAP interactions and specificity revealed by BioID

A longstanding question in the field is how GEFs and GAPs achieve specific engagement of Rho GTPase-effector signaling couples. Why a single GEF or GAP can regulate many Rho GTPases is not well understood. Moreover, GEF-Rho and GAP-Rho interactions have not been fully mapped.

4.2.1. Rho-GEF interactions

Here, we attempted to answer these major questions by BioID-proteomics. We used the nucleotide-free forms of three major Rho GTPases (RhoA, Rac1 and Cdc42) as well as that of RhoG to uncover GEF-Rho interactions. In humans, there are about 70 Dbl Rho GEFs and 11 Dock GEFs. We identified 9 Dock GEF-Rho interactions in HEK293 cells except Dock2, Dock3 and Dock10, which corresponds to 73% of the Dock GEF family. In Hela cells, we mapped 7 Dock GEF-Rho interactions except Dock2, Dock3, Dock4 and Dock8, which is about 64% of the Dock proteins. Dock GEFs are known to show

specificity toward Rac1 and Cdc42, but not RhoA. Consistent with the literature, we revealed the known Dock-A/B/C interactions for Rac1 and Dock-C/D for Cdc42. In addition, we recovered less enriched Dock-C (Dock9, Dock10 and Dock11) interactions with Rac. This might be due to the fact BioID is a very powerful method and detects very sensitive, low affinity interactions that cannot be shown by other methods such as GST pulldown assays. Furthermore, we mapped 29 Dbl GEF-Rho interactions in HEK293 and 30 Dbl GEF-Rho interactions in HeLa cells. Since some of these Dock or Dbl GEFs are cell-specific expression, it is possible that performing BioID in other cell lines can allow identification of Rho-GEF interactions that have not been recovered in HEK293 or HeLa cells.

We generated Internal Ribosome Entry Site (IRES)-containing bicistronic vectors enabling the simultaneous coexpression of BirA*-Flag-Rac1^{WT} and Myc-tagged Rac1 GEFs such as ArhGEF7, Dock1, Vav2, Sos1 and Prex1. We reasoned that Rac1 GEFs can activate BirA*-Flag-Rac^{WT} in its natural physical environment and achieve specific recruitment of Rac1-effector complexes that might be mapped by BioID. We performed BioID screens and identified specific Rac1-effector complexes that are recruited downstream of different Rac1 GEFs (data not shown). Further investigation of these studies might help for better understanding of the GEF specificity toward Rho GTPase-effector signaling pathways.

Our study successfully revealed known Rho-GEF interactions but also unknown interactions. We also showed by BioID-proteomics the specificity of Dock GEFs toward Rac1 and Cdc42. Our screens provide an unprecedented resource for the specificity of Dock and Dbl RhoGEF for their target Rho GTPases. Characterization of these

interactions can help to understand the molecular basis of recruitment of Rho GTPase-effector signaling pathways by GEFs.

4.2.2. Rho-GAP interactions

In humans, there are about 80 Rho GAPs. Here, we identified 20 Rho-GAP in HEK293 and 15 Rho-GAP in HeLa cells. Similar to GEFs, it is possible that we did not recover some Rho-GAP interactions due to cell-specific expression of Rho GAPs. We identified known Rho-GAP interactions such as ArhGAP1-RhoA, ArhGAP32-Rac1 and ArhGAP39-Cdc42 as well as many unknown interactions that have not been previously identified. Rho GAPs are much less studied and characterized compared to Rho GEFs. Validation of these Rho-GAP interactions and their characterization can allow to understand how Rho GAPs achieve inactivation of specific Rho GTPase-effector signaling pathways.

4.3. SLK, a novel RhoA effector, is involved in RhoA-mediated ERM phosphorylation

ERM proteins are membrane-actin linkers and are implicated in the reorganization of actin filaments, cell migration and adhesion, membrane dynamics[308]. ERM proteins phosphorylation and activation have been shown to be downstream of RhoA[301]. It has

been shown that the SLK kinase is involved in the phosphorylation of ERM proteins.

Here, we established SLK as a potential RhoA effector which is essential for RhoA-mediated ERM phosphorylation. Our BioID screens revealed the SLK specificity for RhoA, but not for Rac1 and Cdc42, which we also confirmed by GST pulldown. It has been suggested that SLK can be found in closed or open conformation[294]. Autophosphorylation sites on SLK, such as T183, have been shown to be important for kinase activity and activation. Moreover, opening of SLK is thought to be essential for substrate phosphorylation such as ERM proteins[294]. We found that active RhoA significantly increases SLK autophosphorylation on T183. Interestingly, another report showed that SLK phosphorylates RhoA on Ser188, promoting RhoA-mediated vasodilation induced by AT_2R activation in vascular smooth muscle cells[309]. These data suggest that RhoA recruits SLK and increases autophosphorylation levels of SLK, promoting its kinase activity, which might trigger SLK-induced phosphorylation of RhoA, generating a positive feed back between two proteins to increase subsequent ERM phosphorylation. It is possible that RhoA mediated SLK-dependent phosphorylation of substrates other than ERM proteins.

In parallel with BioID screens on Rho GTPases, we conducted BioID mapping on SLK and SLK^{K63R} and identified potential SLK interactors (data not shown). Whether some of these interactors act as substrates for SLK remains to be elucidated.

4.4. KIAA0355, a novel Rac1 effector, is involved in membrane ruffling and migration

Our BioID screens on Rho GTPases identified many interactions. We identified a couple of Rho-uncharacterized protein interactions. In search for novel Rac effectors, we recovered a highly-specific KIAA0355-Rac interaction. KIAA0355 showed specific interaction with all members of the Rac1 subfamily in both HEK293 and HeLa cells, suggesting the possibility of KIAA0355 involvement in Rac signaling. We discovered that KIAA0355 is necessary for Rac1-induced membrane ruffles and overexpression of KIAA0355 promotes cell migration. How KIAA0355 is recruited downstream of Rac1 and promotes Rac1-mediated formation of membrane ruffles remains to be uncovered. The molecular basis of the Rac1-KIAA0355 signaling axis needs further investigation.

Furthermore, by using a mutant that lacks N-terminal amino acids of KIAA0355 (Flag-KIAA0355$^{\Delta 240\text{-}480}$), we found that Flag-KIAA0355$^{\Delta 240\text{-}480}$ partially impairs cell migration of individual assays and might not be the only region of KIAA0355 which is involved in cell migration. Interestingly, expression of Flag-KIAA0355$^{\Delta 240\text{-}480}$ resulted in higher association with cytoplasmic speckles than that of Flag-KIAA0355 (**Figs. 29c and 29e**). In a previous study, we reported that KIAA0355 forms a complex with GW182 and AGO2, which are involved in siRNA or microRNA (miRNA)-mediated posttranscriptional gene expression regulation[206]. Whether KIAA0355 is involved in AGO2-GW182-mediated mRNA decay in a Rac1-dependent manner remains to be explored.

4.5. A functional siRNA screening of RhoG BioID candidates reveals potential interactors that are essential for membrane ruffling

Among the members of the Rac1 subfamily, the signaling networks and effectors of RhoG is poorly characterized. We combined BioID-proteomics with a functional siRNA screen to explore new potential RhoG effectors that might be involved in membrane ruffling. Unsurprisingly, we identified KIAA0355 among 11 candidates which showed a significant decrease in RhoG-mediated membrane ruffling, which highlighted the specificity of KIAA0355 for the Rac1 subfamily of proteins. We confirmed RhoG-PLEKHG3 interaction. Interestingly, it has been shown that PLEKHG3 functions as a GEF for both Rac1 and Cdc42. It is known that RhoG recruits ELMO to promote ELMO/DOCK1-mediated Rac1 activation[98]. Whether RhoG recruits the Rac1 GEF PLEKHG3 to promote Rac1 activation remains to be elucidated.

4.6. Conclusion

In this thesis, we employed a powerful proteomics method to uncover the Rho GTPase interactome, including effectors and regulatory proteins. While we revealed many known and novel Rho interactions, our screens provided insight into Rho-GEF/GAP interactions. We characterized the SLK serine/threonine kinase and elucidated its role

downstream of RhoA-regulated ERM proteins phosphorylation. In addition, we discovered an uncharacterized protein, KIAA0355, as a potential Rac1 effector and discovered a role of this protein in the formation of membrane ruffles and migration. Moreover, we conducted a functional siRNA screening of RhoG BioID candidates and identified potential effectors that are involved in membrane ruffling downstream of this less-characterized Rho GTPase.

Our work provides a unique, unprecedented resource for the Rho GTPase signaling networks and will be a cornerstone for deciphering the Rho GTPase dynamics, effector recruitment, GEF and GAP specificity.

CHAPTER 5: REFERENCES

1. Alberts, B. *Molecular biology of the cell*. (2015).
2. Reig, G., Pulgar, E. & Concha, M.L. Cell migration: from tissue culture to embryos. *Development* **141**, 1999-2013 (2014).
3. Eming, S.A., Martin, P. & Tomic-Canic, M. Wound repair and regeneration: mechanisms, signaling, and translation. *Sci Transl Med* **6**, 265sr266 (2014).
4. Madri, J.A. & Graesser, D. Cell migration in the immune system: the evolving inter-related roles of adhesion molecules and proteinases. *Dev. Immunol.* **7**, 103-116 (2000).
5. Yamaguchi, H., Wyckoff, J. & Condeelis, J. Cell migration in tumors. *Curr. Opin. Cell Biol.* **17**, 559-564 (2005).
6. Vedula, P. & Kashina, A. The makings of the 'actin code': regulation of actin's biological function at the amino acid and nucleotide level. *J. Cell Sci.* **131** (2018).
7. Perrin, B.J. & Ervasti, J.M. The actin gene family: function follows isoform. *Cytoskeleton (Hoboken)* **67**, 630-634 (2010).
8. Wagner, C.R., Mahowald, A.P. & Miller, K.G. One of the two cytoplasmic actin isoforms in Drosophila is essential. *Proc. Natl. Acad. Sci. U. S. A.* **99**, 8037-8042 (2002).
9. Nayal, A. *et al.* Paxillin phosphorylation at Ser273 localizes a GIT1–PIX–PAK complex and regulates adhesion and protrusion dynamics. *The Journal of Cell Biology* **173**, 587-589 (2006).
10. Vega, F.M. & Ridley, A.J. Rho GTPases in cancer cell biology. *FEBS Lett.* **582**, 2093-2101 (2008).
11. Jaffe, A.B. & Hall, A. Rho GTPases: biochemistry and biology. *Annu. Rev. Cell. Dev. Biol.* **21**, 247-269 (2005).
12. Heasman, S.J. & Ridley, A.J. Mammalian Rho GTPases: new insights into their functions from in vivo studies. *Nat. Rev. Mol. Cell Biol.* **9**, 690-701 (2008).
13. Milburn, M.V. *et al.* Molecular switch for signal transduction: structural differences between active and inactive forms of protooncogenic ras proteins. *Science* **247**, 939-945 (1990).
14. Pai, E.F. *et al.* Refined crystal structure of the triphosphate conformation of H-ras p21 at 1.35 A resolution: implications for the mechanism of GTP hydrolysis. *EMBO J.* **9**, 2351-2359 (1990).
15. Mott, H.R. & Owen, D. Structures of Ras superfamily effector complexes: What have we learnt in two decades? *Crit. Rev. Biochem. Mol. Biol.* **50**, 85-133 (2015).
16. Schaefer, A., Reinhard, N.R. & Hordijk, P.L. Toward understanding RhoGTPase specificity: structure, function and local activation. *Small GTPases* **5**, 6 (2014).
17. Ihara, K. *et al.* Crystal structure of human RhoA in a dominantly active form complexed with a GTP analogue. *J. Biol. Chem.* **273**, 9656-9666 (1998).
18. Hodge, R.G. & Ridley, A.J. Regulating Rho GTPases and their regulators. *Nat. Rev. Mol. Cell Biol.* **17**, 496-510 (2016).
19. Pawson, T. & Jorgensen, C. Chapter 11 - Signal Transduction by Growth Factor Receptors A2 - Mendelsohn, John, in *The Molecular Basis of Cancer (Third Edition)*. (eds. P.M. Howley, M.A. Israel, J.W. Gray & C.B. Thompson) 155-168 (W.B. Saunders, Philadelphia; 2008).
20. Cherfils, J. & Zeghouf, M. Regulation of small GTPases by GEFs, GAPs, and GDIs. *Physiol. Rev.* **93**, 269-309 (2013).
21. Gadea, G. & Blangy, A. Dock-family exchange factors in cell migration and disease. *Eur. J. Cell Biol.* **93**, 466-477 (2014).

22. Lawson, C.D. & Ridley, A.J. Rho GTPase signaling complexes in cell migration and invasion. *J. Cell Biol.* **217**, 447-457 (2018).
23. Cook, D.R., Rossman, K.L. & Der, C.J. Rho guanine nucleotide exchange factors: regulators of Rho GTPase activity in development and disease. *Oncogene* **33**, 4021-4035 (2014).
24. Rossman, K.L., Der, C.J. & Sondek, J. GEF means go: turning on RHO GTPases with guanine nucleotide-exchange factors. *Nat. Rev. Mol. Cell Biol.* **6**, 167-180 (2005).
25. Meller, N., Merlot, S. & Guda, C. CZH proteins: a new family of Rho-GEFs. *J. Cell Sci.* **118**, 4937-4946 (2005).
26. Cote, J.F., Motoyama, A.B., Bush, J.A. & Vuori, K. A novel and evolutionarily conserved PtdIns(3,4,5)P3-binding domain is necessary for DOCK180 signalling. *Nat. Cell Biol.* **7**, 797-807 (2005).
27. Laurin, M. & Cote, J.F. Insights into the biological functions of Dock family guanine nucleotide exchange factors. *Genes Dev.* **28**, 533-547 (2014).
28. Yang, J., Zhang, Z., Roe, S.M., Marshall, C.J. & Barford, D. Activation of Rho GTPases by DOCK exchange factors is mediated by a nucleotide sensor. *Science* **325**, 1398-1402 (2009).
29. Kulkarni, K., Yang, J., Zhang, Z. & Barford, D. Multiple factors confer specific Cdc42 and Rac protein activation by dedicator of cytokinesis (DOCK) nucleotide exchange factors. *J. Biol. Chem.* **286**, 25341-25351 (2011).
30. Huang, G.-H., Sun, Z.-L., Li, H.-J. & Feng, D.-F. Rho GTPase-activating proteins: Regulators of Rho GTPase activity in neuronal development and CNS diseases. *Mol. Cell. Neurosci.* **80**, 18-31 (2017).
31. Guerrier, S. *et al.* The F-BAR domain of srGAP2 induces membrane protrusions required for neuronal migration and morphogenesis. *Cell* **138**, 990-1004 (2009).
32. Soderling, S.H. *et al.* The WRP component of the WAVE-1 complex attenuates Rac-mediated signalling. *Nat. Cell Biol.* **4**, 970 (2002).
33. Wennerberg, K. *et al.* Rnd proteins function as RhoA antagonists by activating p190 RhoGAP. *Curr. Biol.* **13**, 1106-1115 (2003).
34. Arthur, W.T. & Burridge, K. RhoA inactivation by p190RhoGAP regulates cell spreading and migration by promoting membrane protrusion and polarity. *Mol. Biol. Cell* **12**, 2711-2720 (2001).
35. Garcia-Mata, R., Boulter, E. & Burridge, K. The 'invisible hand': regulation of RHO GTPases by RHOGDIs. *Nat. Rev. Mol. Cell Biol.* **12**, 493-504 (2011).
36. Xie, F. *et al.* Role of Rho-specific guanine nucleotide dissociation inhibitor α regulation in cell migration. *Acta Histochem.* **119**, 183-189 (2017).
37. Boulter, E. *et al.* Regulation of Rho GTPase crosstalk, degradation and activity by RhoGDI1. *Nat. Cell Biol.* **12**, 477-483 (2010).
38. Riou, P. *et al.* 14-3-3 Proteins Interact with a Hybrid Prenyl-Phosphorylation Motif to Inhibit G Proteins. *Cell* **153**, 640-653 (2013).
39. Haga, R.B. & Ridley, A.J. Rho GTPases: Regulation and roles in cancer cell biology. *Small GTPases* **7**, 207-221 (2016).
40. Chenette, E.J., Mitin, N.Y. & Der, C.J. Multiple sequence elements facilitate Chp Rho GTPase subcellular location, membrane association, and transforming activity. *Mol. Biol. Cell* **17**, 3108-3121 (2006).
41. Hodge, R.G. & Ridley, A.J. Regulation and functions of RhoU and RhoV. *Small*

GTPases, 1-8 (2017).
42. Navarro-Lerida, I. *et al.* A palmitoylation switch mechanism regulates Rac1 function and membrane organization. *EMBO J.* **31**, 534-551 (2012).
43. Law, A.L. *et al.* Lamellipodin and the Scar/WAVE complex cooperate to promote cell migration in vivo. *J. Cell Biol.* **203**, 673-689 (2013).
44. Rolli-Derkinderen, M. *et al.* Phosphorylation of serine 188 protects RhoA from ubiquitin/proteasome-mediated degradation in vascular smooth muscle cells. *Circ. Res.* **96**, 1152-1160 (2005).
45. Ellerbroek, S.M., Wennerberg, K. & Burridge, K. Serine phosphorylation negatively regulates RhoA in vivo. *J. Biol. Chem.* **278**, 19023-19031 (2003).
46. Nusser, N. *et al.* Serine phosphorylation differentially affects RhoA binding to effectors: implications to NGF-induced neurite outgrowth. *Cell. Signal.* **18**, 704-714 (2006).
47. Takemoto, K., Ishihara, S., Mizutani, T., Kawabata, K. & Haga, H. Compressive Stress Induces Dephosphorylation of the Myosin Regulatory Light Chain via RhoA Phosphorylation by the Adenylyl Cyclase/Protein Kinase A Signaling Pathway. *PLoS One* **10**, e0117937 (2015).
48. Kumper, S. *et al.* Rho-associated kinase (ROCK) function is essential for cell cycle progression, senescence and tumorigenesis. *eLife* **5**, e12994 (2016).
49. Chang, F., Lemmon, C., Lietha, D., Eck, M. & Romer, L. Tyrosine Phosphorylation of Rac1: A Role in Regulation of Cell Spreading. *PLoS One* **6**, e28587 (2011).
50. Kwon, T., Kwon, D.Y., Chun, J., Kim, J.H. & Kang, S.S. Akt protein kinase inhibits Rac1-GTP binding through phosphorylation at serine 71 of Rac1. *J. Biol. Chem.* **275**, 423-428 (2000).
51. Wang, H.R. *et al.* Regulation of cell polarity and protrusion formation by targeting RhoA for degradation. *Science* **302**, 1775-1779 (2003).
52. Wei, J. *et al.* A new mechanism of RhoA ubiquitination and degradation: Roles of SCF(FBXL19) E3 ligase and Erk2. *Biochim. Biophys. Acta* **1833**, 10.1016/j.bbamcr.2013.1007.1005 (2013).
53. Yu, L. *et al.* SND1 Acts Downstream of TGFbeta1 and Upstream of Smurf1 to Promote Breast Cancer Metastasis. *Cancer Res.* **75**, 1275-1286 (2015).
54. Nethe, M. & Hordijk, P.L. The role of ubiquitylation and degradation in RhoGTPase signalling. *J. Cell Sci.* **123**, 4011-4018 (2010).
55. Visvikis, O. *et al.* Activated Rac1, but not the tumorigenic variant Rac1b, is ubiquitinated on Lys 147 through a JNK-regulated process. *FEBS J.* **275**, 386-396 (2008).
56. Mettouchi, A. & Lemichez, E. Ubiquitylation of active Rac1 by the E3 ubiquitin-ligase HACE1. *Small GTPases* **3**, 102-106 (2012).
57. Zhao, J. *et al.* SCF E3 ligase F-box protein complex SCF(FBXL19) regulates cell migration by mediating Rac1 ubiquitination and degradation. *FASEB J.* **27**, 2611-2619 (2013).
58. Torrino, S. *et al.* The E3 ubiquitin-ligase HACE1 catalyzes the ubiquitylation of active Rac1. *Dev. Cell* **21**, 959-965 (2011).
59. Castillo-Lluva, S., Tan, C.T., Daugaard, M., Sorensen, P.H. & Malliri, A. The tumour suppressor HACE1 controls cell migration by regulating Rac1 degradation. *Oncogene* **32**, 1735-1742 (2013).
60. Goka, E.T. & Lippman, M.E. Loss of the E3 ubiquitin ligase HACE1 results in enhanced Rac1 signaling contributing to breast cancer progression. *Oncogene* **34**, 5395-5405

(2015).
61. Laurin, M. *et al.* Rac-specific guanine nucleotide exchange factor DOCK1 is a critical regulator of HER2-mediated breast cancer metastasis. *Proc. Natl. Acad. Sci. U. S. A.* **110**, 7434-7439 (2013).
62. Baczyk, D., Audette, M.C., Drewlo, S., Levytska, K. & Kingdom, J.C. SUMO-4: A novel functional candidate in the human placental protein SUMOylation machinery. *PLoS One* **12**, e0178056 (2017).
63. Flotho, A. & Melchior, F. Sumoylation: a regulatory protein modification in health and disease. *Annu. Rev. Biochem.* **82**, 357-385 (2013).
64. Castillo-Lluva, S. *et al.* SUMOylation of the GTPase Rac1 is required for optimal cell migration. *Nat. Cell Biol.* **12**, 1078-1085 (2010).
65. Yu, J. *et al.* RhoGDI SUMOylation at Lys-138 increases its binding activity to Rho GTPase and its inhibiting cancer cell motility. *J. Biol. Chem.* **287**, 13752-13760 (2012).
66. Ridley, A.J., Paterson, H.F., Johnston, C.L., Diekmann, D. & Hall, A. The small GTP-binding protein rac regulates growth factor-induced membrane ruffling. *Cell* **70**, 401-410 (1992).
67. Mayor, R. & Etienne-Manneville, S. The front and rear of collective cell migration. *Nat. Rev. Mol. Cell Biol.* **17**, 97-109 (2016).
68. Borm, B., Requardt, R.P., Herzog, V. & Kirfel, G. Membrane ruffles in cell migration: indicators of inefficient lamellipodia adhesion and compartments of actin filament reorganization. *Exp. Cell Res.* **302**, 83-95 (2005).
69. Bellanger, J.M. *et al.* The Rac1- and RhoG-specific GEF domain of Trio targets filamin to remodel cytoskeletal actin. *Nat. Cell Biol.* **2**, 888-892 (2000).
70. Matsui, T., Yonemura, S., Tsukita, S. & Tsukita, S. Activation of ERM proteins in vivo by Rho involves phosphatidyl-inositol 4-phosphate 5-kinase and not ROCK kinases. *Curr. Biol.* **9**, 1259-S1253 (1999).
71. Mahankali, M., Peng, H.-J., Cox, D. & Gomez-Cambronero, J. THE MECHANISM OF CELL MEMBRANE RUFFLING RELIES ON A PHOSPHOLIPASE D2 (PLD2), GRB2 AND RAC2 ASSOCIATION. *Cell. Signal.* **23**, 1291-1298 (2011).
72. Eden, S., Rohatgi, R., Podtelejnikov, A.V., Mann, M. & Kirschner, M.W. Mechanism of regulation of WAVE1-induced actin nucleation by Rac1 and Nck. *Nature* **418**, 790-793 (2002).
73. Chen, Z. *et al.* Structure and control of the actin regulatory WAVE complex. *Nature* **468**, 533-538 (2010).
74. Sadok, A. & Marshall, C.J. Rho GTPases: masters of cell migration. *Small GTPases* **5**, e29710 (2014).
75. Chen, B. *et al.* The WAVE regulatory complex links diverse receptors to the actin cytoskeleton. *Cell* **156**, 195-207 (2014).
76. Machesky, L.M. & Insall, R.H. Scar1 and the related Wiskott–Aldrich syndrome protein, WASP, regulate the actin cytoskeleton through the Arp2/3 complex. *Curr. Biol.* **8**, 1347-1356 (1998).
77. Miki, H., Yamaguchi, H., Suetsugu, S. & Takenawa, T. IRSp53 is an essential intermediate between Rac and WAVE in the regulation of membrane ruffling. *Nature* **408**, 732-735 (2000).
78. Lane, J., Martin, T., Weeks, H.P. & Jiang, W.G. Structure and role of WASP and WAVE in Rho GTPase signalling in cancer. *Cancer Genomics Proteomics* **11**, 155-165 (2014).

79. de Kreuk, B.J. & Hordijk, P.L. Control of Rho GTPase function by BAR-domains. *Small GTPases* **3**, 45-52 (2012).
80. de Kreuk, B.J. *et al.* The F-BAR domain protein PACSIN2 associates with Rac1 and regulates cell spreading and migration. *J. Cell Sci.* **124**, 2375-2388 (2011).
81. Frank, S.R. & Hansen, S.H. The PIX-GIT complex: a G protein signaling cassette in control of cell shape. *Semin. Cell Dev. Biol.* **19**, 234-244 (2008).
82. Brown, M.C. & Turner, C.E. Paxillin: adapting to change. *Physiol. Rev.* **84**, 1315-1339 (2004).
83. Zhang, Z.M., Simmerman, J.A., Guibao, C.D. & Zheng, J.J. GIT1 Paxillin-binding Domain Is a Four-helix Bundle, and It Binds to Both Paxillin LD2 and LD4 Motifs. *The Journal of Biological Chemistry* **283**, 18685-18693 (2008).
84. Zhou, W., Li, X. & Premont, R.T. Expanding functions of GIT Arf GTPase-activating proteins, PIX Rho guanine nucleotide exchange factors and GIT-PIX complexes. *J. Cell Sci.* **129**, 1963-1974 (2016).
85. Bamburg, J.R. & Bernstein, B.W. Roles of ADF/cofilin in actin polymerization and beyond. *F1000 Biology Reports* **2**, 62 (2010).
86. Campa, C.C., Ciraolo, E., Ghigo, A., Germena, G. & Hirsch, E. Crossroads of PI3K and Rac pathways. *Small GTPases* **6**, 71-80 (2015).
87. Pasini, S. *et al.* Activating Transcription Factor 4 (ATF4) modulates Rho GTPase levels and function via regulation of RhoGDIalpha. *Sci Rep* **6**, 36952 (2016).
88. Barber, M.A. *et al.* Membrane translocation of P-Rex1 is mediated by G protein betagamma subunits and phosphoinositide 3-kinase. *J. Biol. Chem.* **282**, 29967-29976 (2007).
89. Hodakoski, C. *et al.* Regulation of PTEN inhibition by the pleckstrin homology domain of P-REX2 during insulin signaling and glucose homeostasis. *Proceedings of the National Academy of Sciences* **111**, 155 (2014).
90. Zheng, Y., Bagrodia, S. & Cerione, R.A. Activation of phosphoinositide 3-kinase activity by Cdc42Hs binding to p85. *J. Biol. Chem.* **269**, 18727-18730 (1994).
91. Bokoch, G.M., Vlahos, C.J., Wang, Y., Knaus, U.G. & Traynor-Kaplan, A.E. Rac GTPase interacts specifically with phosphatidylinositol 3-kinase. *Biochem. J.* **315 (Pt 3)**, 775-779 (1996).
92. Marei, H. & Malliri, A. GEFs: Dual regulation of Rac1 signaling. *Small GTPases* **8**, 90-99 (2017).
93. Marei, H. *et al.* Differential Rac1 signalling by guanine nucleotide exchange factors implicates FLII in regulating Rac1-driven cell migration. *Nat Commun* **7**, 10664 (2016).
94. Bokoch, G.M. Regulation of the phagocyte respiratory burst by small GTP-binding proteins. *Trends Cell Biol.* **5**, 109-113 (1995).
95. Cotteret, S. & Chernoff, J. The evolutionary history of effectors downstream of Cdc42 and Rac. *Genome Biol.* **3**, REVIEWS0002 (2002).
96. Pick, E. Role of the Rho GTPase Rac in the activation of the phagocyte NADPH oxidase: Outsourcing a key task. *Small GTPases* **5**, e27952 (2014).
97. Dorseuil, O., Reibel, L., Bokoch, G.M., Camonis, J. & Gacon, G. The Rac target NADPH oxidase p67phox interacts preferentially with Rac2 rather than Rac1. *J. Biol. Chem.* **271**, 83-88 (1996).
98. Katoh, H. & Negishi, M. RhoG activates Rac1 by direct interaction with the Dock180-binding protein Elmo. *Nature* **424**, 461-464 (2003).

99. Patel, M., Pelletier, A. & Cote, J.F. Opening up on ELMO regulation: New insights into the control of Rac signaling by the DOCK180/ELMO complex. *Small GTPases* **2**, 268-275 (2011).
100. Patel, M. *et al.* An evolutionarily conserved autoinhibitory molecular switch in ELMO proteins regulates Rac signaling. *Curr. Biol.* **20**, 2021-2027 (2010).
101. Woehlke, G. & Schliwa, M. Directional motility of kinesin motor proteins. *Biochim. Biophys. Acta* **1496**, 117-127 (2000).
102. Vignal, E., Blangy, A., Martin, M., Gauthier-Rouviere, C. & Fort, P. Kinectin is a key effector of RhoG microtubule-dependent cellular activity. *Mol. Cell. Biol.* **21**, 8022-8034 (2001).
103. Abe, T., Kato, M., Miki, H., Takenawa, T. & Endo, T. Small GTPase Tc10 and its homologue RhoT induce N-WASP-mediated long process formation and neurite outgrowth. *J. Cell Sci.* **116**, 155-168 (2003).
104. Wilson, E. *et al.* RhoJ interacts with the GIT–PIX complex and regulates focal adhesion disassembly. *J. Cell Sci.* **127**, 3039 (2014).
105. Shi, T.T., Li, G. & Xiao, H.T. The Role of RhoJ in Endothelial Cell Biology and Tumor Pathology. *Biomed Res Int* **2016**, 6386412 (2016).
106. Nobes, C.D. & Hall, A. Rho, rac, and cdc42 GTPases regulate the assembly of multimolecular focal complexes associated with actin stress fibers, lamellipodia, and filopodia. *Cell* **81**, 53-62 (1995).
107. Carlier, M.-F., Ducruix, A. & Pantaloni, D. Signalling to actin: the Cdc42-N-WASP-Arp2/3 connection. *Chem. Biol.* **6**, R235-R240 (1999).
108. Higgs, H.N. & Pollard, T.D. Activation by Cdc42 and Pip(2) of Wiskott-Aldrich Syndrome Protein (Wasp) Stimulates Actin Nucleation by Arp2/3 Complex. *The Journal of Cell Biology* **150**, 1311-1320 (2000).
109. Papayannopoulos, V. *et al.* A Polybasic Motif Allows N-WASP to Act as a Sensor of PIP2 Density. *Mol. Cell* **17**, 181-191 (2005).
110. Martinez-Quiles, N. *et al.* WIP regulates N-WASP-mediated actin polymerization and filopodium formation. *Nat. Cell Biol.* **3**, 484 (2001).
111. Yamaguchi, H. *et al.* Molecular mechanisms of invadopodium formation: the role of the N-WASP-Arp2/3 complex pathway and cofilin. *J. Cell Biol.* **168**, 441-452 (2005).
112. Razidlo, G.L., Schroeder, B., Chen, J., Billadeau, D.D. & McNiven, M.A. Vav1 as a central regulator of invadopodia assembly. *Curr. Biol.* **24**, 86-93 (2014).
113. Kühn, S. & Geyer, M. Formins as effector proteins of Rho GTPases. *Small GTPases* **5**, e29513 (2014).
114. Swart-Mataraza, J.M., Li, Z. & Sacks, D.B. IQGAP1 is a component of Cdc42 signaling to the cytoskeleton. *J. Biol. Chem.* **277**, 24753-24763 (2002).
115. LeCour, L., Jr. *et al.* The Structural Basis for Cdc42-Induced Dimerization of IQGAPs. *Structure* **24**, 1499-1508 (2016).
116. Kaur, S. *et al.* RhoJ/TCL regulates endothelial motility and tube formation and modulates actomyosin contractility and focal adhesion numbers. *Arterioscler. Thromb. Vasc. Biol.* **31**, 657-664 (2011).
117. Hou, A. *et al.* Rho GTPases and regulation of cell migration and polarization in human corneal epithelial cells. *PLoS One* **8**, e77107 (2013).
118. Paterson, H.F. *et al.* Microinjection of recombinant p21rho induces rapid changes in cell morphology. *J. Cell Biol.* **111**, 1001-1007 (1990).

119. Ridley, A.J. & Hall, A. The small GTP-binding protein rho regulates the assembly of focal adhesions and actin stress fibers in response to growth factors. *Cell* **70**, 389-399 (1992).
120. Narumiya, S. & Thumkeo, D. Rho signaling research: history, current status and future directions. *FEBS Lett.* **592**, 1763-1776 (2018).
121. Mohan, S. *et al.* Structure of a Highly Conserved Domain of Rock1 Required for Shroom-Mediated Regulation of Cell Morphology. *PLoS One* **8**, e81075 (2013).
122. Li, F. & Higgs, H.N. The mouse Formin mDia1 is a potent actin nucleation factor regulated by autoinhibition. *Curr. Biol.* **13**, 1335-1340 (2003).
123. Narumiya, S., Tanji, M. & Ishizaki, T. Rho signaling, ROCK and mDia1, in transformation, metastasis and invasion. *Cancer Metastasis Rev.* **28**, 65-76 (2009).
124. Higashida, C. *et al.* G-actin regulates rapid induction of actin nucleation by mDia1 to restore cellular actin polymers. *J. Cell Sci.* **121**, 3403-3412 (2008).
125. Bartolini, F. *et al.* The formin mDia2 stabilizes microtubules independently of its actin nucleation activity. *The Journal of Cell Biology* **181**, 523-536 (2008).
126. Pertz, O., Hodgson, L., Klemke, R.L. & Hahn, K.M. Spatiotemporal dynamics of RhoA activity in migrating cells. *Nature* **440**, 1069-1072 (2006).
127. Machacek, M. *et al.* Coordination of Rho GTPase activities during cell protrusion. *Nature* **461**, 99-103 (2009).
128. Kitzing, T.M., Wang, Y., Pertz, O., Copeland, J.W. & Grosse, R. Formin-like 2 drives amoeboid invasive cell motility downstream of RhoC. *Oncogene* **29**, 2441 (2010).
129. Hakem, A. *et al.* RhoC is dispensable for embryogenesis and tumor initiation but essential for metastasis. *Genes Dev.* **19**, 1974-1979 (2005).
130. Jaiswal, M., Fansa, E.K., Dvorsky, R. & Ahmadian, M.R. New insight into the molecular switch mechanism of human Rho family proteins: shifting a paradigm. *Biol. Chem.* **394**, 89-95 (2013).
131. Murphy, C. *et al.* Endosome dynamics regulated by a Rho protein. *Nature* **384**, 427 (1996).
132. Tsubakimoto, K. *et al.* Small GTPase RhoD suppresses cell migration and cytokinesis. *Oncogene* **18**, 2431-2440 (1999).
133. Gad, A.K., Nehru, V., Ruusala, A. & Aspenstrom, P. RhoD regulates cytoskeletal dynamics via the actin nucleation-promoting factor WASp homologue associated with actin Golgi membranes and microtubules. *Mol. Biol. Cell* **23**, 4807-4819 (2012).
134. Pellegrin, S. & Mellor, H. The Rho family GTPase Rif induces filopodia through mDia2. *Curr. Biol.* **15**, 129-133 (2005).
135. Goh, W.I. *et al.* mDia1 and WAVE2 proteins interact directly with IRSp53 in filopodia and are involved in filopodium formation. *J. Biol. Chem.* **287**, 4702-4714 (2012).
136. Fan, L., Pellegrin, S., Scott, A. & Mellor, H. The small GTPase Rif is an alternative trigger for the formation of actin stress fibers in epithelial cells. *J. Cell Sci.* **123**, 1247 (2010).
137. Riou, P., Villalonga, P. & Ridley, A.J. Rnd proteins: multifunctional regulators of the cytoskeleton and cell cycle progression. *Bioessays* **32**, 986-992 (2010).
138. Oinuma, I., Kawada, K., Tsukagoshi, K. & Negishi, M. Rnd1 and Rnd3 targeting to lipid raft is required for p190 RhoGAP activation. *Mol. Biol. Cell* **23**, 1593-1604 (2012).
139. Tanaka, H., Katoh, H. & Negishi, M. Pragmin, a novel effector of Rnd2 GTPase, stimulates RhoA activity. *J. Biol. Chem.* **281**, 10355-10364 (2006).

140. Ji, W. & Rivero, F. Atypical Rho GTPases of the RhoBTB Subfamily: Roles in Vesicle Trafficking and Tumorigenesis. *Cells* **5** (2016).
141. Manjarrez, J.R., Sun, L., Prince, T. & Matts, R.L. Hsp90-dependent assembly of the DBC2/RhoBTB2-Cullin3 E3-ligase complex. *PLoS One* **9**, e90054 (2014).
142. Hamaguchi, M. *et al.* DBC2, a candidate for a tumor suppressor gene involved in breast cancer. *Proc. Natl. Acad. Sci. U. S. A.* **99**, 13647-13652 (2002).
143. Beder, L.B. *et al.* Identification of a candidate tumor suppressor gene RHOBTB1 located at a novel allelic loss region 10q21 in head and neck cancer. *J. Cancer Res. Clin. Oncol.* **132**, 19-27 (2006).
144. Berthold, J., Schenkova, K. & Rivero, F. Rho GTPases of the RhoBTB subfamily and tumorigenesis. *Acta Pharmacol. Sin.* **29**, 285-295 (2008).
145. Mao, H. *et al.* RhoBTB2 (DBC2) functions as tumor suppressor via inhibiting proliferation, preventing colony formation and inducing apoptosis in breast cancer cells. *Gene* **486**, 74-80 (2011).
146. Jin, Z., Han, Y.X. & Han, X.R. Downregulated RhoBTB2 expression contributes to poor outcome in osteosarcoma patients. *Cancer Biother. Radiopharm.* **28**, 709-716 (2013).
147. Yoshihara, T., Collado, D. & Hamaguchi, M. Cyclin D1 down-regulation is essential for DBC2's tumor suppressor function. *Biochem. Biophys. Res. Commun.* **358**, 1076-1079 (2007).
148. Stump, M., Mukohda, M., Hu, C. & Sigmund, C.D. PPARgamma Regulation in Hypertension and Metabolic Syndrome. *Curr. Hypertens. Rep.* **17**, 89 (2015).
149. Pelham, C.J. *et al.* Cullin-3 regulates vascular smooth muscle function and arterial blood pressure via PPARgamma and RhoA/Rho-kinase. *Cell Metab.* **16**, 462-472 (2012).
150. Saras, J., Wollberg, P. & Aspenstrom, P. Wrch1 is a GTPase-deficient Cdc42-like protein with unusual binding characteristics and cellular effects. *Exp. Cell Res.* **299**, 356-369 (2004).
151. Shutes, A., Berzat, A.C., Cox, A.D. & Der, C.J. Atypical mechanism of regulation of the Wrch-1 Rho family small GTPase. *Curr. Biol.* **14**, 2052-2056 (2004).
152. Tao, W., Pennica, D., Xu, L., Kalejta, R.F. & Levine, A.J. Wrch-1, a novel member of the Rho gene family that is regulated by Wnt-1. *Genes Dev.* **15**, 1796-1807 (2001).
153. Aronheim, A. *et al.* Chp, a homologue of the GTPase Cdc42Hs, activates the JNK pathway and is implicated in reorganizing the actin cytoskeleton. *Curr. Biol.* **8**, 1125-1128 (1998).
154. Shepelev, M.V. & Korobko, I.V. Pak6 protein kinase is a novel effector of an atypical Rho family GTPase Chp/RhoV. *Biochemistry (Mosc.)* **77**, 26-32 (2012).
155. Dart, A.E. *et al.* PAK4 promotes kinase-independent stabilization of RhoU to modulate cell adhesion. *J. Cell Biol.* **211**, 863-879 (2015).
156. Ruusala, A. & Aspenstrom, P. The atypical Rho GTPase Wrch1 collaborates with the nonreceptor tyrosine kinases Pyk2 and Src in regulating cytoskeletal dynamics. *Mol. Cell. Biol.* **28**, 1802-1814 (2008).
157. Chuang, Y.Y., Valster, A., Coniglio, S.J., Backer, J.M. & Symons, M. The atypical Rho family GTPase Wrch-1 regulates focal adhesion formation and cell migration. *J. Cell Sci.* **120**, 1927-1934 (2007).
158. Loebel, D.A. *et al.* Rhou maintains the epithelial architecture and facilitates differentiation of the foregut endoderm. *Development* **138**, 4511-4522 (2011).

159. Loebel, D.A. & Tam, P.P. Rho GTPases in endoderm development and differentiation. *Small GTPases* **3**, 40-44 (2012).
160. Guemar, L. *et al.* The small GTPase RhoV is an essential regulator of neural crest induction in Xenopus. *Dev. Biol.* **310**, 113-128 (2007).
161. Gu, Y. *et al.* RhoH GTPase recruits and activates Zap70 required for T cell receptor signaling and thymocyte development. *Nat. Immunol.* **7**, 1182-1190 (2006).
162. Li, X. *et al.* The hematopoiesis-specific GTP-binding protein RhoH is GTPase deficient and modulates activities of other Rho GTPases by an inhibitory function. *Mol. Cell. Biol.* **22**, 1158-1171 (2002).
163. Chae, H.D., Lee, K.E., Williams, D.A. & Gu, Y. Cross-talk between RhoH and Rac1 in regulation of actin cytoskeleton and chemotaxis of hematopoietic progenitor cells. *Blood* **111**, 2597-2605 (2008).
164. Rao, V.S., Srinivas, K., Sujini, G.N. & Kumar, G.N. Protein-protein interaction detection: methods and analysis. *Int J Proteomics* **2014**, 147648 (2014).
165. Fields, S. & Song, O. A novel genetic system to detect protein-protein interactions. *Nature* **340**, 245-246 (1989).
166. Luker, K.E. & Piwnica-Worms, D. Optimizing Luciferase Protein Fragment Complementation for Bioluminescent Imaging of Protein–Protein Interactions in Live Cells and Animals, in *Methods in Enzymology*, Vol. 385 349-360 (Academic Press, 2004).
167. Brückner, A., Polge, C., Lentze, N., Auerbach, D. & Schlattner, U. Yeast Two-Hybrid, a Powerful Tool for Systems Biology. *International journal of molecular sciences* **10**, 2763-2788 (2009).
168. Nealon, J.O., Philomina, L.S. & McGuffin, L.J. Predictive and Experimental Approaches for Elucidating Protein-Protein Interactions and Quaternary Structures. *International journal of molecular sciences* **18** (2017).
169. Dunham, W.H., Mullin, M. & Gingras, A.C. Affinity-purification coupled to mass spectrometry: basic principles and strategies. *Proteomics* **12**, 1576-1590 (2012).
170. Blikstad, C. & Ivarsson, Y. High-throughput methods for identification of protein-protein interactions involving short linear motifs. *Cell communication and signaling : CCS* **13**, 38 (2015).
171. Jones, R.B., Gordus, A., Krall, J.A. & MacBeath, G. A quantitative protein interaction network for the ErbB receptors using protein microarrays. *Nature* **439**, 168-174 (2006).
172. Kaushansky, A. *et al.* Quantifying protein–protein interactions in high throughput using protein domain microarrays. *Nat. Protoc.* **5**, 773 (2010).
173. Sundell, G.N. & Ivarsson, Y. Interaction analysis through proteomic phage display. *Biomed Res Int* **2014**, 176172 (2014).
174. Sidhu, S.S., Fairbrother, W.J. & Deshayes, K. Exploring protein-protein interactions with phage display. *ChemBioChem* **4**, 14-25 (2003).
175. Sidhu, S.S. & Koide, S. Phage display for engineering and analyzing protein interaction interfaces. *Curr. Opin. Struct. Biol.* **17**, 481-487 (2007).
176. Luck, K. & Trave, G. Phage display can select over-hydrophobic sequences that may impair prediction of natural domain-peptide interactions. *Bioinformatics* **27**, 899-902 (2011).
177. Xie, Q., Soutto, M., Xu, X., Zhang, Y. & Johnson, C.H. Bioluminescence Resonance Energy Transfer (BRET) Imaging in Plant Seedlings and Mammalian Cells. *Methods in*

molecular biology (Clifton, N.J.) **680**, 3-28 (2011).
178. Xu, Y., Piston, D.W. & Johnson, C.H. A bioluminescence resonance energy transfer (BRET) system: Application to interacting circadian clock proteins. *Proc. Natl. Acad. Sci. U. S. A.* **96**, 151-156 (1999).
179. Wiens, M.D. & Campbell, R.E. Surveying the landscape of optogenetic methods for detection of protein-protein interactions. *Wiley interdisciplinary reviews. Systems biology and medicine* **10**, e1415 (2018).
180. Lan, T.H., Liu, Q., Li, C., Wu, G. & Lambert, N.A. Sensitive and high resolution localization and tracking of membrane proteins in live cells with BRET. *Traffic* **13**, 1450-1456 (2012).
181. Buntru, A., Zimmermann, T. & Hauck, C.R. Fluorescence resonance energy transfer (FRET)-based subcellular visualization of pathogen-induced host receptor signaling. *BMC Biol.* **7**, 81 (2009).
182. Goyet, E., Bouquier, N., Ollendorff, V. & Perroy, J. Fast and high resolution single-cell BRET imaging. *Scientific Reports* **6**, 28231 (2016).
183. Borroto-Escuela, D.O., Flajolet, M., Agnati, L.F., Greengard, P. & Fuxe, K. BIOLUMINISCENCE RESONANCE ENERGY TRANSFER (BRET) METHODS TO STUDY G PROTEIN-COUPLED RECEPTOR - RECEPTOR TYROSINE KINASE HETERORECEPTOR COMPLEXES. *Methods Cell Biol.* **117**, 141-164 (2013).
184. Bauer, A. & Kuster, B. Affinity purification-mass spectrometry. Powerful tools for the characterization of protein complexes. *Eur. J. Biochem.* **270**, 570-578 (2003).
185. Nguyen, T.N. & Goodrich, J.A. Protein-protein interaction assays: eliminating false positive interactions. *Nat. Methods* **3**, 135-139 (2006).
186. Picknett, T.M. & Brenner, S. X-Ray Crystallography, in *Encyclopedia of Genetics*. (eds. S. Brenner & J.H. Miller) 2154 (Academic Press, New York; 2001).
187. Acharya, K.R. & Lloyd, M.D. The advantages and limitations of protein crystal structures. *Trends Pharmacol. Sci.* **26**, 10-14 (2005).
188. Carpenter, E.P., Beis, K., Cameron, A.D. & Iwata, S. Overcoming the challenges of membrane protein crystallography. *Curr. Opin. Struct. Biol.* **18**, 581-586 (2008).
189. Gao, G., Williams, J.G. & Campbell, S.L. Protein-protein interaction analysis by nuclear magnetic resonance spectroscopy. *Methods Mol. Biol.* **261**, 79-92 (2004).
190. Thompson, P.M., Beck, M.R. & Campbell, S.L. Protein-protein interaction analysis by nuclear magnetic resonance spectroscopy. *Methods Mol. Biol.* **1278**, 267-279 (2015).
191. Michnick, S.W., Ear, P.H., Landry, C., Malleshaiah, M.K. & Messier, V. Protein-fragment complementation assays for large-scale analysis, functional dissection and dynamic studies of protein-protein interactions in living cells. *Methods Mol. Biol.* **756**, 395-425 (2011).
192. Roux, K.J., Kim, D.I., Raida, M. & Burke, B. A promiscuous biotin ligase fusion protein identifies proximal and interacting proteins in mammalian cells. *J. Cell Biol.* **196**, 801-810 (2012).
193. Chapman-Smith, A. & Cronan, J.E., Jr. Molecular biology of biotin attachment to proteins. *J. Nutr.* **129**, 477S-484S (1999).
194. Kwon, K. & Beckett, D. Function of a conserved sequence motif in biotin holoenzyme synthetases. *Protein Sci.* **9**, 1530-1539 (2000).
195. Choi-Rhee, E., Schulman, H. & Cronan, J.E. Promiscuous protein biotinylation by Escherichia coli biotin protein ligase. *Protein Sci.* **13**, 3043-3050 (2004).

196. Streaker, E.D. & Beckett, D. Nonenzymatic biotinylation of a biotin carboxyl carrier protein: unusual reactivity of the physiological target lysine. *Protein Sci.* **15**, 1928-1935 (2006).
197. Cronan, J.E. Targeted and proximity-dependent promiscuous protein biotinylation by a mutant Escherichia coli biotin protein ligase. *J. Nutr. Biochem.* **16**, 416-418 (2005).
198. Roux, K.J., Kim, D.I. & Burke, B. BioID: a screen for protein-protein interactions. *Current protocols in protein science / editorial board, John E. Coligan ... [et al.]* **74**, Unit 19 23 (2013).
199. Kim, D.I. *et al.* Probing nuclear pore complex architecture with proximity-dependent biotinylation. *Proc. Natl. Acad. Sci. U. S. A.* **111**, E2453-2461 (2014).
200. Firat-Karalar, E.N. & Stearns, T. Probing mammalian centrosome structure using BioID proximity-dependent biotinylation. *Methods Cell Biol.* **129**, 153-170 (2015).
201. Lambert, J.P., Tucholska, M., Go, C., Knight, J.D. & Gingras, A.C. Proximity biotinylation and affinity purification are complementary approaches for the interactome mapping of chromatin-associated protein complexes. *J Proteomics* (2014).
202. Lambert, J.-P., Tucholska, M., Pawson, T. & Gingras, A.-C. Incorporating DNA shearing in standard affinity purification allows simultaneous identification of both soluble and chromatin-bound interaction partners. *Journal of Proteomics* **100**, 55-59 (2014).
203. Li, P., Li, J., Wang, L. & Di, L.J. Proximity Labeling of Interacting Proteins: Application of BioID as a Discovery Tool. *Proteomics* **17** (2017).
204. Rees, J.S., Li, X.-W., Perrett, S., Lilley, K.S. & Jackson, A.P. Protein Neighbors and Proximity Proteomics. *Molecular & Cellular Proteomics : MCP* **14**, 2848-2856 (2015).
205. Varnaitė, R. & MacNeill, S.A. Meet the neighbors: Mapping local protein interactomes by proximity-dependent labeling with BioID. *Proteomics* **16**, 2503-2518 (2016).
206. Youn, J.Y. *et al.* High-Density Proximity Mapping Reveals the Subcellular Organization of mRNA-Associated Granules and Bodies. *Mol. Cell* **69**, 517-532 e511 (2018).
207. Coyaud, E. *et al.* BioID-based identification of SCF beta-TrCP1/2 E3 ligase substrates. *Mol. Cell. Proteomics* (2015).
208. Gupta, G.D. *et al.* A Dynamic Protein Interaction Landscape of the Human Centrosome-Cilium Interface. *Cell* **163**, 1484-1499 (2015).
209. Methot, S.P. *et al.* A licensing step links AID to transcription elongation for mutagenesis in B cells. *Nat Commun* **9**, 1248 (2018).
210. Comartin, D. *et al.* CEP120 and SPICE1 cooperate with CPAP in centriole elongation. *Curr. Biol.* **23**, 1360-1366 (2013).
211. Firat-Karalar, E.N., Rauniyar, N., Yates, J.R., 3rd & Stearns, T. Proximity interactions among centrosome components identify regulators of centriole duplication. *Curr. Biol.* **24**, 664-670 (2014).
212. Fredriksson, K. *et al.* Proteomic analysis of proteins surrounding occludin and claudin-4 reveals their proximity to signaling and trafficking networks. *PLoS One* **10**, e0117074 (2015).
213. Van Itallie, C.M. *et al.* Biotin ligase tagging identifies proteins proximal to E-cadherin, including lipoma preferred partner, a regulator of epithelial cell-cell and cell-substrate adhesion. *J. Cell Sci.* **127**, 885-895 (2014).
214. Van Itallie, C.M. *et al.* The N and C termini of ZO-1 are surrounded by distinct proteins and functional protein networks. *J. Biol. Chem.* **288**, 13775-13788 (2013).
215. Ueda, S., Blee, A.M., Macway, K.G., Renner, D.J. & Yamada, S. Force dependent

biotinylation of myosin IIA by alpha-catenin tagged with a promiscuous biotin ligase. *PLoS One* **10**, e0122886 (2015).
216. Steed, E. *et al.* MarvelD3 couples tight junctions to the MEKK1-JNK pathway to regulate cell behavior and survival. *J. Cell Biol.* **204**, 821-838 (2014).
217. Lamb, C.A. *et al.* TBC1D14 regulates autophagy via the TRAPP complex and ATG9 traffic. *EMBO J.* **35**, 281-301 (2016).
218. Couzens, A.L. *et al.* Protein interaction network of the mammalian Hippo pathway reveals mechanisms of kinase-phosphatase interactions. *Science signaling* **6**, rs15 (2013).
219. Schweingruber, C., Soffientini, P., Ruepp, M.D., Bachi, A. & Muhlemann, O. Identification of Interactions in the NMD Complex Using Proximity-Dependent Biotinylation (BioID). *PLoS One* **11**, e0150239 (2016).
220. Jahan, A.S. *et al.* Usp12 stabilizes the T-cell receptor complex at the cell surface during signaling. *Proc. Natl. Acad. Sci. U. S. A.* **113**, E705-714 (2016).
221. Cole, A. *et al.* Inhibition of the Mitochondrial Protease ClpP as a Therapeutic Strategy for Human Acute Myeloid Leukemia. *Cancer Cell* **27**, 864-876 (2015).
222. Elzi, D.J., Song, M., Hakala, K., Weintraub, S.T. & Shiio, Y. Proteomic Analysis of the EWS-Fli-1 Interactome Reveals the Role of the Lysosome in EWS-Fli-1 Turnover. *J. Proteome Res.* (2014).
223. Dingar, D. *et al.* BioID identifies novel c-MYC interacting partners in cultured cells and xenograft tumors. *J Proteomics* (2014).
224. Kim, D.I. *et al.* An improved smaller biotin ligase for BioID proximity labeling. *Mol. Biol. Cell* (2016).
225. Schopp, I.M. *et al.* Split-BioID a conditional proteomics approach to monitor the composition of spatiotemporally defined protein complexes. *Nature Communications* **8**, 15690 (2017).
226. Branon, T.C. *et al.* Efficient proximity labeling in living cells and organisms with TurboID. *Nat. Biotechnol.* (2018).
227. Jaberi, A. *et al.* Identification of Tpr and α-actinin-4 as two novel SLK-interacting proteins. *Biochim. Biophys. Acta* **1853**, 2539-2552 (2015).
228. Quizi, J.L. *et al.* SLK-mediated phosphorylation of paxillin is required for focal adhesion turnover and cell migration. *Oncogene* **32**, 4656 (2012).
229. Patel, M., Chiang, T.C., Tran, V., Lee, F.J. & Cote, J.F. The Arf family GTPase Arl4A complexes with ELMO proteins to promote actin cytoskeleton remodeling and reveals a versatile Ras-binding domain in the ELMO proteins family. *J. Biol. Chem.* **286**, 38969-38979 (2011).
230. Tighe, A., Johnson, V.L. & Taylor, S.S. Truncating APC mutations have dominant effects on proliferation, spindle checkpoint control, survival and chromosome stability. *J. Cell Sci.* **117**, 6339-6353 (2004).
231. Ran, F.A. *et al.* Genome engineering using the CRISPR-Cas9 system. *Nat. Protoc.* **8**, 2281-2308 (2013).
232. Kean, M.J., Couzens, A.L. & Gingras, A.C. Mass spectrometry approaches to study mammalian kinase and phosphatase associated proteins. *Methods* **57**, 400-408 (2012).
233. Liu, G. *et al.* ProHits: integrated software for mass spectrometry-based interaction proteomics. *Nat. Biotechnol.* **28**, 1015-1017 (2010).
234. Kessner, D., Chambers, M., Burke, R., Agus, D. & Mallick, P. ProteoWizard: open

source software for rapid proteomics tools development. *Bioinformatics* **24**, 2534-2536 (2008).
235. Eng, J.K., Jahan, T.A. & Hoopmann, M.R. Comet: an open-source MS/MS sequence database search tool. *Proteomics* **13**, 22-24 (2013).
236. Shteynberg, D. *et al.* iProphet: multi-level integrative analysis of shotgun proteomic data improves peptide and protein identification rates and error estimates. *Mol. Cell. Proteomics* **10**, M111 007690 (2011).
237. Shannon, P. *et al.* Cytoscape: a software environment for integrated models of biomolecular interaction networks. *Genome Res.* **13**, 2498-2504 (2003).
238. Morris, J.H. *et al.* Affinity purification-mass spectrometry and network analysis to understand protein-protein interactions. *Nat. Protoc.* **9**, 2539-2554 (2014).
239. Hermjakob, H. *et al.* IntAct: an open source molecular interaction database. *Nucleic Acids Res* **32**, D452-455 (2004).
240. van Dongen, S. & Abreu-Goodger, C. Using MCL to extract clusters from networks. *Methods Mol. Biol.* **804**, 281-295 (2012).
241. Knight, J.D.R. *et al.* ProHits-viz: a suite of web tools for visualizing interaction proteomics data. *Nat. Methods* **14**, 645-646 (2017).
242. Baryshnikova, A. Systematic Functional Annotation and Visualization of Biological Networks. *Cell Syst* **2**, 412-421 (2016).
243. Abu-Thuraia, A. *et al.* Axl phosphorylates Elmo scaffold proteins to promote Rac activation and cell invasion. *Mol. Cell. Biol.* **35**, 76-87 (2015).
244. Goyette, M.-A. *et al.* The Receptor Tyrosine Kinase AXL Is Required at Multiple Steps of the Metastatic Cascade during HER2-Positive Breast Cancer Progression. *Cell Reports* **23**, 1476-1490 (2018).
245. Meller, J., Vidali, L. & Schwartz, M.A. Endogenous RhoG is dispensable for integrin-mediated cell spreading but contributes to Rac-independent migration. *J. Cell Sci.* **121**, 1981-1989 (2008).
246. Barry, D.J., Durkin, C.H., Abella, J.V. & Way, M. Open source software for quantification of cell migration, protrusions, and fluorescence intensities. *J. Cell Biol.* **209**, 163-180 (2015).
247. Capala, M.E. *et al.* Mitochondrial Dysfunction in Human Leukemic Stem/Progenitor Cells upon Loss of RAC2. *PLoS One* **10**, e0128585 (2015).
248. Fueller, F. & Kubatzky, K.F. The small GTPase RhoH is an atypical regulator of haematopoietic cells. *Cell communication and signaling : CCS* **6**, 6 (2008).
249. Steinbuck, M.P. & Winandy, S. A Review of Notch Processing With New Insights Into Ligand-Independent Notch Signaling in T-Cells. *Frontiers in Immunology* **9** (2018).
250. Tang, Y. *et al.* Rnd3 regulates lung cancer cell proliferation through notch signaling. *PLoS One* **9**, e111897 (2014).
251. Watabe-Uchida, M., John, K.A., Janas, J.A., Newey, S.E. & Van Aelst, L. The Rac Activator DOCK7 Regulates Neuronal Polarity through Local Phosphorylation of Stathmin/Op18. *Neuron* **51**, 727-739 (2006).
252. Zhou, Y., Johnson, J.L., Cerione, R.A. & Erickson, J.W. Prenylation and membrane localization of Cdc42 are essential for activation by DOCK7. *Biochemistry* **52**, 4354-4363 (2013).
253. Bos, J.L., Rehmann, H. & Wittinghofer, A. GEFs and GAPs: critical elements in the control of small G proteins. *Cell* **129**, 865-877 (2007).

254. Stanley, R.J. & Thomas, G.M.H. Activation of G Proteins by Guanine Nucleotide Exchange Factors Relies on GTPase Activity. *PLoS One* **11**, e0151861 (2016).
255. Feng, Q., Baird, D. & Cerione, R.A. Novel regulatory mechanisms for the Dbl family guanine nucleotide exchange factor Cool-2/alpha-Pix. *EMBO J.* **23**, 3492-3504 (2004).
256. Cote, J.F. & Vuori, K. GEF what? Dock180 and related proteins help Rac to polarize cells in new ways. *Trends Cell Biol.* **17**, 383-393 (2007).
257. Abiko, H. *et al.* Rho-guanine nucleotide exchange factors involved in cyclic stretch-induced reorientation of vascular endothelial cells. *J. Cell Sci.* (2015).
258. Sun, Y.-J. *et al.* Solo/Trio8, a Membrane-Associated Short Isoform of Trio, Modulates Endosome Dynamics and Neurite Elongation. *Mol. Cell. Biol.* **26**, 6923-6935 (2006).
259. Himmel, K.L. *et al.* Activation of clg, a novel dbl family guanine nucleotide exchange factor gene, by proviral insertion at evi24, a common integration site in B cell and myeloid leukemias. *J. Biol. Chem.* **277**, 13463-13472 (2002).
260. Nguyen, T.T. *et al.* PLEKHG3 enhances polarized cell migration by activating actin filaments at the cell front. *Proc. Natl. Acad. Sci. U. S. A.* **113**, 10091-10096 (2016).
261. Gupta, M. *et al.* Plekhg4 is a novel Dbl family guanine nucleotide exchange factor protein for rho family GTPases. *J. Biol. Chem.* **288**, 14522-14530 (2013).
262. Bruurs, L.J.M., Zwakenberg, S., van der Net, M.C., Zwartkruis, F.J. & Bos, J.L. A Two-Tiered Mechanism Enables Localized Cdc42 Signaling during Enterocyte Polarization. *Mol. Cell. Biol.* **37**, e00547-00516 (2017).
263. Kepner, E.M. *et al.* Cool-1/betaPIX functions as a guanine nucleotide exchange factor in the cycling of Cdc42 to regulate insulin secretion. *Am. J. Physiol. Endocrinol. Metab.* **301**, E1072-1080 (2011).
264. Abe, K. *et al.* Vav2 is an activator of Cdc42, Rac1, and RhoA. *J. Biol. Chem.* **275**, 10141-10149 (2000).
265. Rossman, K.L. *et al.* A crystallographic view of interactions between Dbs and Cdc42: PH domain-assisted guanine nucleotide exchange. *EMBO J.* **21**, 1315-1326 (2002).
266. Oliver, A.W. *et al.* The HPV16 E6 binding protein Tip-1 interacts with ARHGEF16, which activates Cdc42. *Br. J. Cancer* **104**, 324-331 (2011).
267. Steenblock, C. *et al.* The Cdc42 Guanine Nucleotide Exchange Factor FGD6 Coordinates Cell Polarity and Endosomal Membrane Recycling in Osteoclasts. *The Journal of Biological Chemistry* **289**, 18347-18359 (2014).
268. Ellerbroek, S.M. *et al.* SGEF, a RhoG Guanine Nucleotide Exchange Factor that Stimulates Macropinocytosis. *Mol. Biol. Cell* **15**, 3309-3319 (2004).
269. Ford-Speelman, D.L., Roche, J.A., Bowman, A.L. & Bloch, R.J. The rho-guanine nucleotide exchange factor domain of obscurin activates rhoA signaling in skeletal muscle. *Mol. Biol. Cell* **20**, 3905-3917 (2009).
270. Medley, Q.G. *et al.* The trio guanine nucleotide exchange factor is a RhoA target. Binding of RhoA to the trio immunoglobulin-like domain. *J. Biol. Chem.* **275**, 36116-36123 (2000).
271. Shamah, S.M. *et al.* EphA Receptors Regulate Growth Cone Dynamics through the Novel Guanine Nucleotide Exchange Factor Ephexin. *Cell* **105**, 233-244 (2001).
272. Yohe, M.E. *et al.* Auto-inhibition of the Dbl family protein Tim by an N-terminal helical motif. *J. Biol. Chem.* **282**, 13813-13823 (2007).
273. Guilluy, C. *et al.* The Rho GEFs LARG and GEF-H1 regulate the mechanical response to force on integrins. *Nat. Cell Biol.* **13**, 722 (2011).

274. Rumenapp, U. *et al.* Rho-specific binding and guanine nucleotide exchange catalysis by KIAA0380, a dbl family member. *FEBS Lett.* **459**, 313-318 (1999).
275. Dubash, A.D. *et al.* A novel role for Lsc/p115 RhoGEF and LARG in regulating RhoA activity downstream of adhesion to fibronectin. *J. Cell Sci.* **120**, 3989-3998 (2007).
276. Ren, Y., Li, R., Zheng, Y. & Busch, H. Cloning and characterization of GEF-H1, a microtubule-associated guanine nucleotide exchange factor for Rac and Rho GTPases. *J. Biol. Chem.* **273**, 34954-34960 (1998).
277. Reuther, G.W. *et al.* Leukemia-associated Rho guanine nucleotide exchange factor, a Dbl family protein found mutated in leukemia, causes transformation by activation of RhoA. *J. Biol. Chem.* **276**, 27145-27151 (2001).
278. Rümenapp, U., Freichel-Blomquist, A., Wittinghofer, B., Jakobs, K.H. & Wieland, T. A mammalian Rho-specific guanine-nucleotide exchange factor (p164-RhoGEF) without a pleckstrin homology domain. *Biochem. J.* **366**, 721-728 (2002).
279. Blomquist, A. *et al.* Identification and characterization of a novel Rho-specific guanine nucleotide exchange factor. *Biochem. J.* **352 Pt 2**, 319-325 (2000).
280. Diviani, D., Soderling, J. & Scott, J.D. AKAP-Lbc anchors protein kinase A and nucleates Galpha 12-selective Rho-mediated stress fiber formation. *J. Biol. Chem.* **276**, 44247-44257 (2001).
281. Tatsumoto, T., Xie, X., Blumenthal, R., Okamoto, I. & Miki, T. Human ECT2 is an exchange factor for Rho GTPases, phosphorylated in G2/M phases, and involved in cytokinesis. *J. Cell Biol.* **147**, 921-928 (1999).
282. Nakamura, T. *et al.* Grit, a GTPase-activating protein for the Rho family, regulates neurite extension through association with the TrkA receptor and N-Shc and CrkL/Crk adapter molecules. *Mol. Cell. Biol.* **22**, 8721-8734 (2002).
283. Bai, Y., Xiang, X., Liang, C. & Shi, L. Regulating Rac in the Nervous System: Molecular Function and Disease Implication of Rac GEFs and GAPs. *Biomed Res Int* **2015**, 632450 (2015).
284. Billuart, P. *et al.* Oligophrenin-1 encodes a rhoGAP protein involved in X-linked mental retardation. *Nature* **392**, 923 (1998).
285. Richnau, N. & Aspenstrom, P. Rich, a rho GTPase-activating protein domain-containing protein involved in signaling by Cdc42 and Rac1. *J. Biol. Chem.* **276**, 35060-35070 (2001).
286. Bai, X. *et al.* The smooth muscle-selective RhoGAP GRAF3 is a critical regulator of vascular tone and hypertension. *Nature Communications* **4**, 2910 (2013).
287. Tomino, T. *et al.* DOCK1 inhibition suppresses cancer cell invasion and macropinocytosis induced by self-activating Rac1(P29S) mutation. *Biochem. Biophys. Res. Commun.* **497**, 298-304 (2018).
288. Barrio-Real, L. *et al.* Subtype-specific overexpression of the Rac-GEF P-REX1 in breast cancer is associated with promoter hypomethylation. *Breast Cancer Res.* **16**, 441 (2014).
289. Sosa, M.S. *et al.* IDENTIFICATION OF THE Rac-GEF P-REX1 AS AN ESSENTIAL MEDIATOR OF ErbB SIGNALING IN BREAST CANCER. *Mol. Cell* **40**, 877-892 (2010).
290. Yang, J. *et al.* PREX2 promotes the proliferation, invasion and migration of pancreatic cancer cells by modulating the PI3K signaling pathway. *Oncology Letters* **12**, 1139-1143 (2016).
291. Cullis, J. *et al.* The RhoGEF GEF-H1 is required for oncogenic RAS signaling via KSR-

1. *Cancer Cell* **25**, 181-195 (2014).
292. Yang, X.-Y. *et al.* p120Ras-GAP binds the DLC1 Rho-GAP tumor suppressor protein and inhibits its RhoA GTPase and growth suppressing activities. *Oncogene* **28**, 1401-1409 (2009).
293. He, Y. *et al.* The Cdc42/Rac1 regulator CdGAP is a novel E-cadherin transcriptional co-repressor with Zeb2 in breast cancer. *Oncogene* **36**, 3490-3503 (2017).
294. Al-Zahrani, K.N., Baron, K.D. & Sabourin, L.A. Ste20-like kinase SLK, at the crossroads: a matter of life and death. *Cell adhesion & migration* **7**, 1-10 (2013).
295. Wagner, S.M. & Sabourin, L.A. A novel role for the Ste20 kinase SLK in adhesion signaling and cell migration. *Cell adhesion & migration* **3**, 182-184 (2009).
296. Machicoane, M. *et al.* SLK-dependent activation of ERMs controls LGN-NuMA localization and spindle orientation. *J. Cell Biol.* **205**, 791-799 (2014).
297. Viswanatha, R., Ohouo, P.Y., Smolka, M.B. & Bretscher, A. Local phosphocycling mediated by LOK/SLK restricts ezrin function to the apical aspect of epithelial cells. *J. Cell Biol.* **199**, 969-984 (2012).
298. Hipfner, D.R., Keller, N. & Cohen, S.M. Slik Sterile-20 kinase regulates Moesin activity to promote epithelial integrity during tissue growth. *Genes Dev.* **18**, 2243-2248 (2004).
299. Cybulsky, A.V., Guillemette, J., Papillon, J. & Abouelazm, N.T. Regulation of Ste20-like kinase, SLK, activity: Dimerization and activation segment phosphorylation. *PLoS One* **12**, e0177226 (2017).
300. Knight, J.D. *et al.* A web-tool for visualizing quantitative protein-protein interaction data. *Proteomics* (2014).
301. Matsui, T., Yonemura, S., Tsukita, S. & Tsukita, S. Activation of ERM proteins in vivo by Rho involves phosphatidyl-inositol 4-phosphate 5-kinase and not ROCK kinases. *Curr. Biol.* **9**, 1259-1262 (1999).
302. Fievet, B.T. *et al.* Phosphoinositide binding and phosphorylation act sequentially in the activation mechanism of ezrin. *J. Cell Biol.* **164**, 653-659 (2004).
303. Kunda, P., Pelling, A.E., Liu, T. & Baum, B. Moesin Controls Cortical Rigidity, Cell Rounding, and Spindle Morphogenesis during Mitosis. *Curr. Biol.* **18**, 91-101 (2008).
304. Carreno, S. *et al.* Moesin and its activating kinase Slik are required for cortical stability and microtubule organization in mitotic cells. *J. Cell Biol.* **180**, 739-746 (2008).
305. Belkina, N.V., Liu, Y., Hao, J.J., Karasuyama, H. & Shaw, S. LOK is a major ERM kinase in resting lymphocytes and regulates cytoskeletal rearrangement through ERM phosphorylation. *Proc. Natl. Acad. Sci. U. S. A.* **106**, 4707-4712 (2009).
306. Oshiro, N., Fukata, Y. & Kaibuchi, K. Phosphorylation of moesin by rho-associated kinase (Rho-kinase) plays a crucial role in the formation of microvilli-like structures. *J. Biol. Chem.* **273**, 34663-34666 (1998).
307. Luhovy, A.Y., Jaberi, A., Papillon, J., Guillemette, J. & Cybulsky, A.V. Regulation of the Ste20-like kinase, SLK: involvement of activation segment phosphorylation. *J. Biol. Chem.* **287**, 5446-5458 (2012).
308. Ponuwei, G.A. A glimpse of the ERM proteins. *J. Biomed. Sci.* **23**, 35 (2016).
309. Guilluy, C. *et al.* Ste20-related kinase SLK phosphorylates Ser188 of RhoA to induce vasodilation in response to angiotensin II Type 2 receptor activation. *Circ. Res.* **102**, 1265-1274 (2008).